The Journal of Antibiotics (2016) 69, 220–252

www.nature.com/ja

REVIEW ARTICLE

# Synthesis of the phorboxazoles—potent, architecturally novel marine natural products

Zachary Shultz[1] and James W Leahy[1,2,3]

**The phorboxazoles have attracted the attention of synthetic chemists around the globe due to their potent biological activity and novel structure. A review of the recent synthetic efforts as well as new phorboxazole analogs is discussed.**
*The Journal of Antibiotics* (2016) **69,** 220–252; doi:10.1038/ja.2016.8; published online 9 March 2016

## INTRODUCTION

In 1995, Searle and Molinski reported the isolation of a pair of novel natural products from the Indian Ocean marine sponge *Phorbas* sp. collected off the Muiron Islands that demonstrated potent antifungal and cytostatic activity.[1] The subsequent structural elucidation of these two macrolides,[2–4] phorboxazoles A (**1**, Figure 1) and B (**2**), has inspired considerable attention and synthetic creativity over the succeeding two decades that has resulted in 10 total syntheses as well as a number of additional synthetic approaches, the discovery of new members of the phorboxazole family, the creation of biological probes and the generation of analogs to uncover hints about their bioactivity. Some of the highlights of these efforts are reviewed here.

More recently, Capon *et al.*[5] isolated both **1** and **2** from a *Raspailia* sp. sponge collected along the Australian Northern Rottnest Shelf while searching for nematocidal agents. This second isolation from such a taxonomically distinct source suggests a potential microbial biosynthetic origin or at least contribution that has yet to be uncovered, leaving synthesis as the primary source for further consideration of the natural products.

It is not surprising that the distinctive structural features of the phorboxazoles, which includes the presence of four unique pyran rings and two oxazoles, attracted the interest of a number of synthetic groups. In fact, the first synthetic approach to the molecule was reported before the final structure elucidation was published![6] Seitz and Hoffmann have previously examined some of the earliest syntheses of the phorboxazoles,[7,8] and therefore we will primarily focus on the efforts that were not previously highlighted.

With a target as structurally diverse as the phorboxazoles, there is an array of potential approaches to be considered. However, the need to form a macrolide left a limited number of options for the cyclization. The most commonly exploited approach was to close the ring via an olefination of the α,β-unsaturated macrolactone—a strategy that has proven to be quite effective in this regard. Notably, the Evans total synthesis[9] and the Paterson synthetic approach[10] utilized a Yamaguchi macrolactonization as an alternative. The other common disconnection was about the C16–C18 oxazole or the C19–C20 olefin to join the two macrolide fragments. As the two natural products differ only about the stereochemical disposition of the hydroxyl substituent at the C13 position, the phorboxazoles serve as an excellent vehicle for the study of the various approaches to solve the synthetic challenges posed. In this review, we will first evaluate the completed syntheses of **1** and **2**, respectively, followed by the approaches of other groups in this regard and the efforts reported to date on the discovery of other members of the phorboxazole family, biological probes and additional analogs.

## DISCUSSION

### Total syntheses

*Earliest syntheses.* As the earlier reviews covered the first generation syntheses of **1** by Forsyth and Smith as well as the syntheses of **1** by Pattenden and Williams and the synthesis of **2** by Evans, we will only point out a few of the salient highlights from these seminal works. Forsyth, who was the first to complete the synthesis of either natural product (Figure 2),[11] established the Michael cyclization to the pentasubstituted pyran and developed a biomimetic route to the oxazoles. He observed the same lack of diastereoselectivity in the formation of the C38 center observed by Molinski and Leahy,[2] ascertained the viability of the hetero-Diels–Alder approach to the pyrans and established the feasibility of the Still–Gennari macrocyclization. Before 2006, Evans had achieved the only synthesis of **2**,[9] which featured a macrolactonization strategy of an acetylene to enable a selective reduction to the Z C2–C3 olefin (Figure 3). In addition, Evans' lithiation of the oxazole methyl, optimization of the C19–C20 Wittig and use of β-ketoesters enabled many of the efforts that followed. Smith's pioneering use of the Petasis–Ferrier rearrangement serves as a hallmark of his synthesis of **1** (Figure 4),[12] and he implemented a Stille protocol for introduction of the exocyclic oxazole, allowing it to serve as a linchpin for the two complex

[1]Department of Chemistry, University of South Florida, Tampa, FL, USA; [2]Department of Molecular Medicine, Morsani College of Medicine, University of South Florida, Tampa, FL, USA and [3]Florida Center of Excellence for Drug Discovery and Innovation, University of South Florida, Tampa, FL, USA
Correspondence: Professor JW Leahy, Department of Chemistry, University of South Florida, 4202 E. Fowler Avenue, CHE 205, Tampa, FL 33620, USA.
E-mail: jwleahy@usf.edu
Dedicated to Professor Amos B Smith, III - an outstanding chemist, mentor and friend.
Received 11 December 2015; revised 14 January 2016; accepted 19 January 2016; published online 9 March 2016

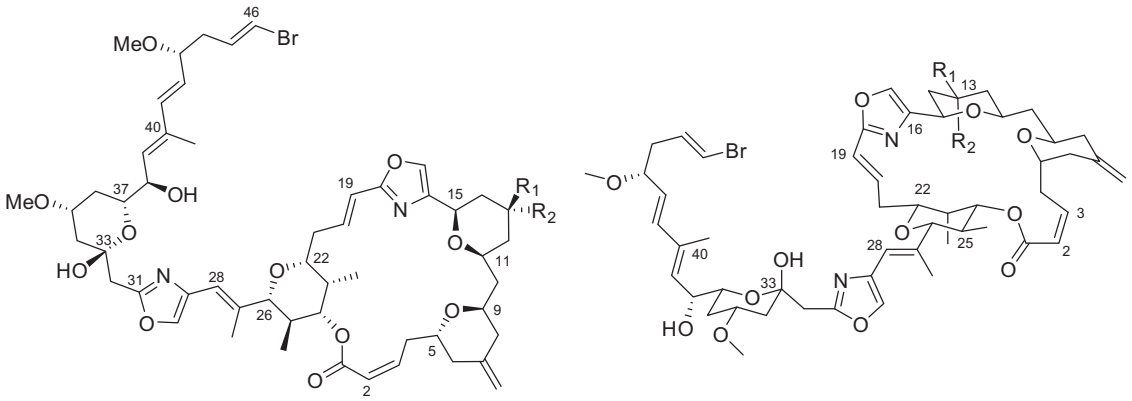

Phorboxazole A (**1**, $R_1$ = H, $R_2$ = OH)
Phorboxazole B (**2**, $R_1$ = OH, $R_2$ = H)

**Figure 1** Structures of phorboxazoles A and B.

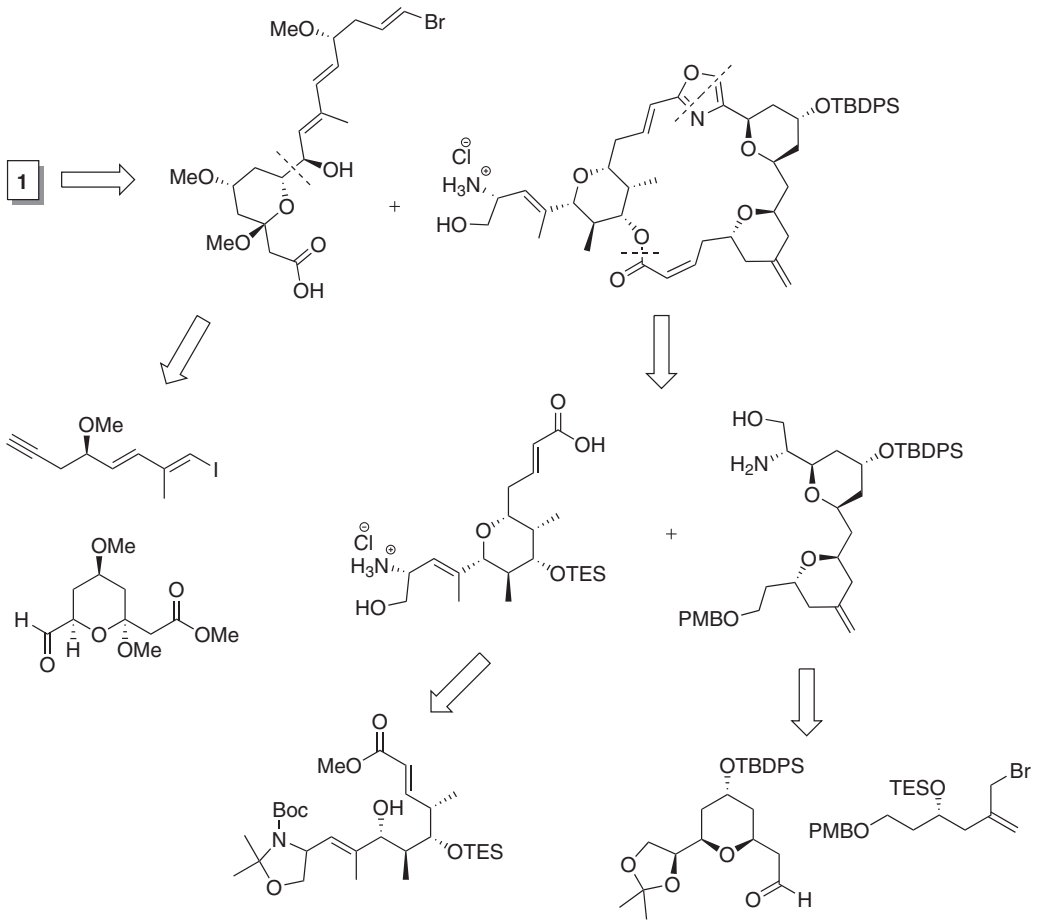

**Figure 2** Retrosynthetic analysis of Craig Fosyth's first-generation total synthesis of phorboxazole A.

fragments. Pattenden was the first to use a carbohydrate starting material (D-xylose) in his synthesis of **1**,[13] and his utilization of the Julia olefination for the introduction of the polyene side chain was adopted by several subsequent synthetic approaches (Figure 5). In addition to using a Horner–Wadsworth–Emmons approach to C19–C20 and C27–C28, Williams was able to take advantage of his *in situ* asymmetric transmetallation/allylation protocol in his synthesis of **1** (Figure 6).[14]

## Recent syntheses

*Second generation synthesis of **1** by Amos B Smith, III.* In the years since those syntheses were completed, five additional total syntheses

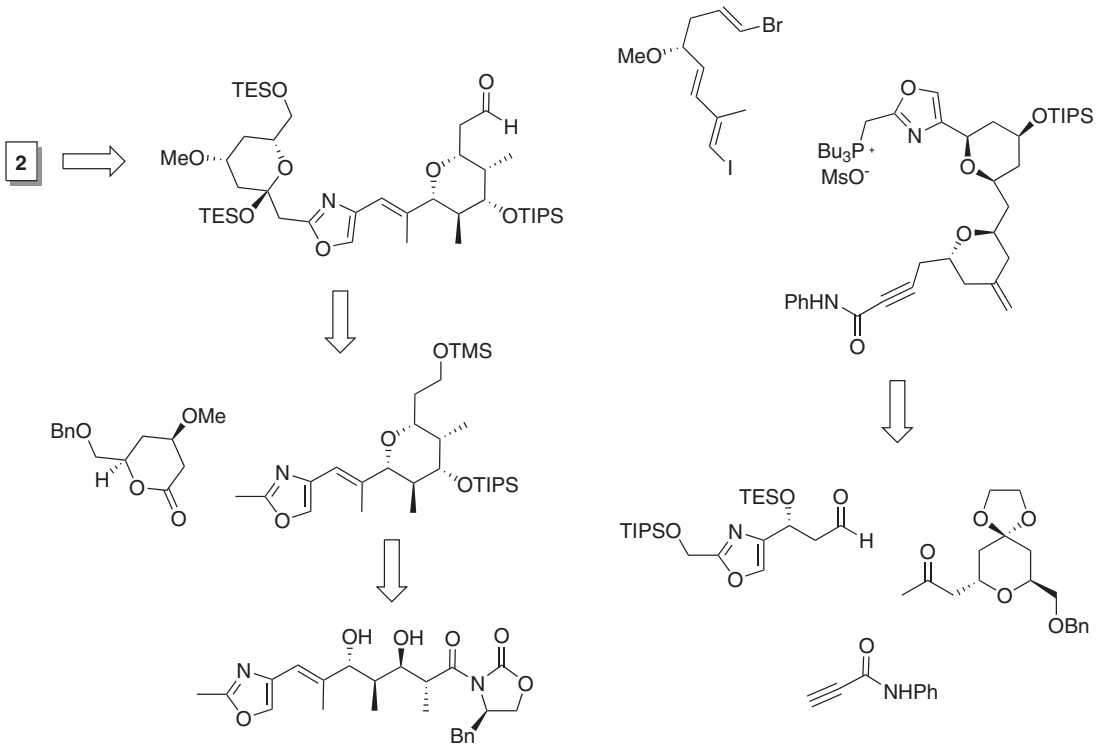


**Figure 3** Retrosynthetic analysis of Dave Evans' total synthesis of phorboxazole B.

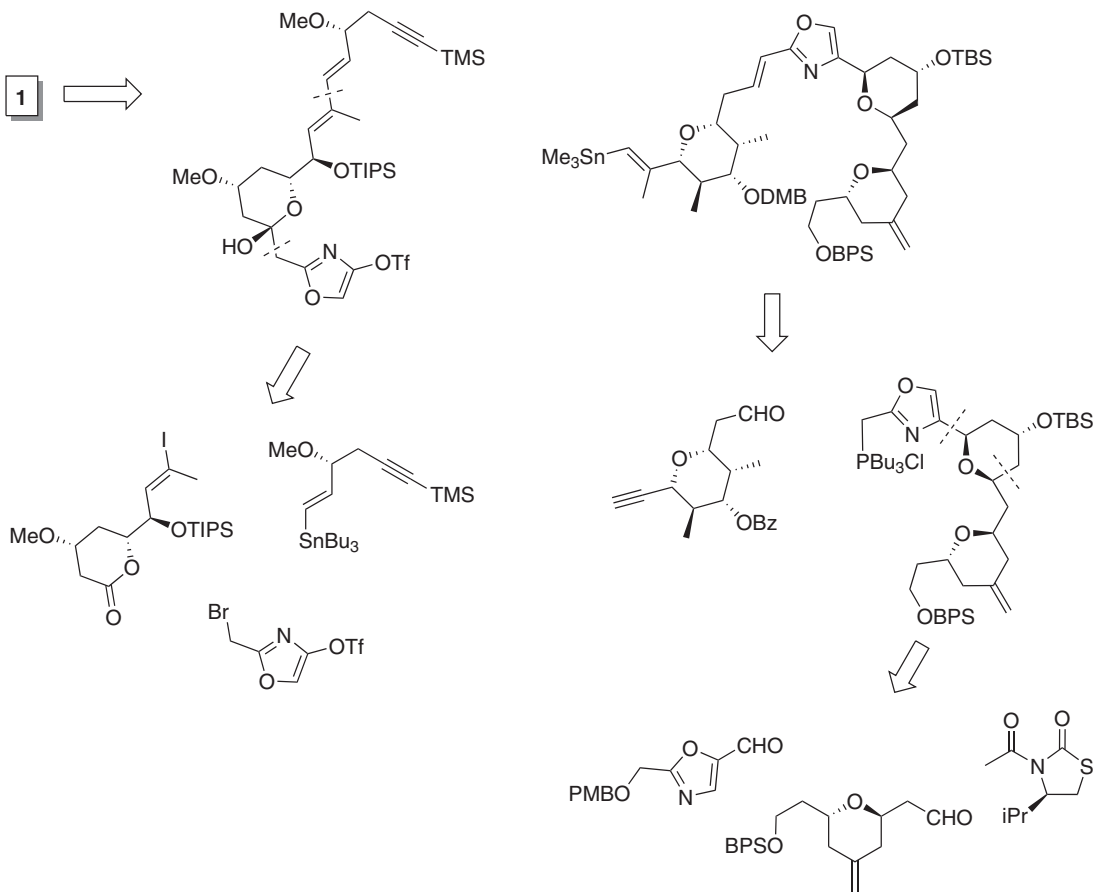


**Figure 4** Retrosynthetic analysis of Amos Smith's first-generation total synthesis of phorboxazole A.

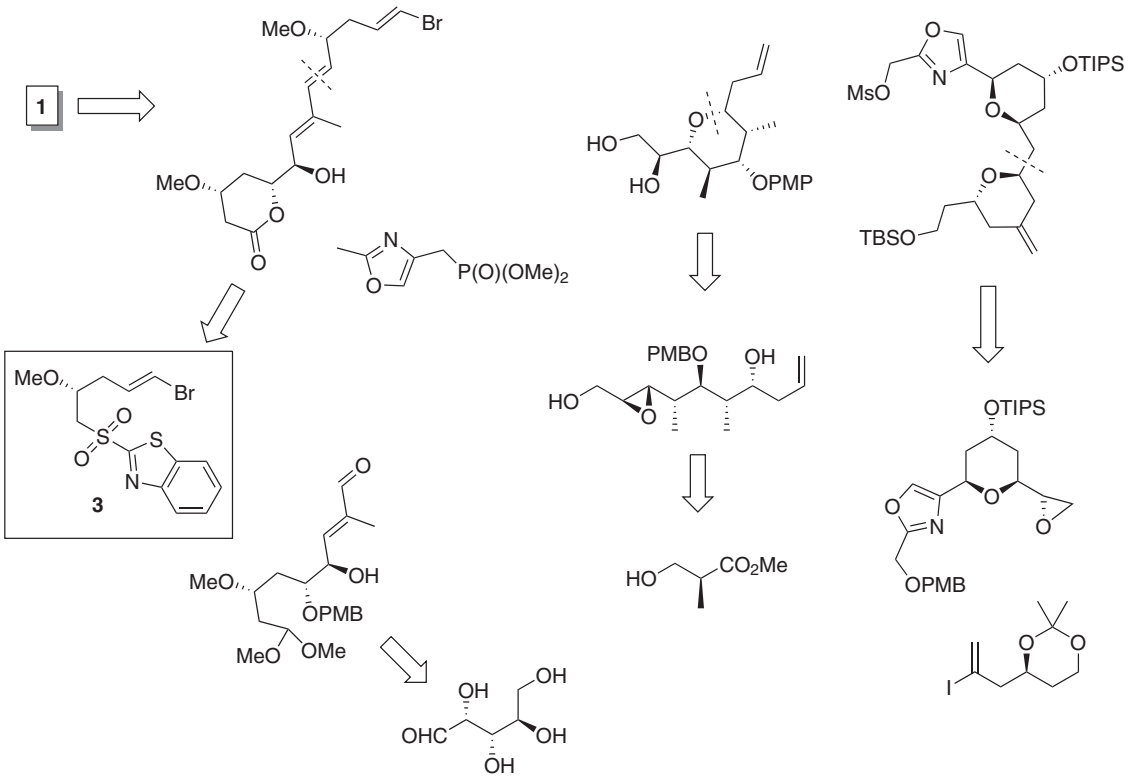


**Figure 5** Retrosynthetic analysis of Gerald Pattenden's total synthesis of phorboxazole A.

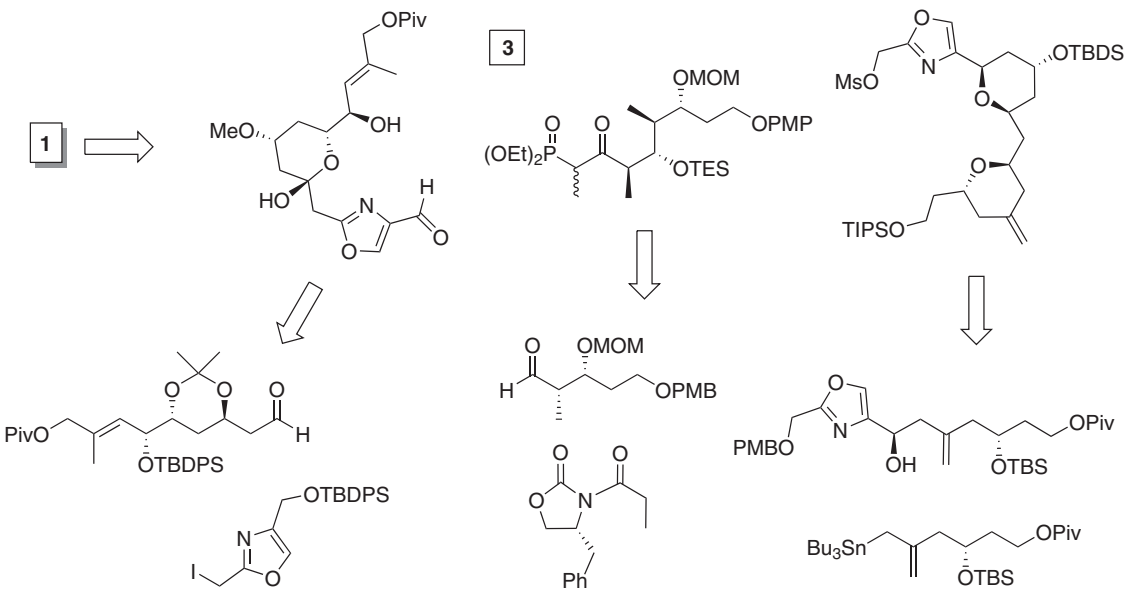


**Figure 6** Retrosynthetic analysis of David Williams' total synthesis of phorboxazole A.

have been reported. The first of these was a second generation approach to **1** by Smith,[15] who has shown an admirable commitment to developing scalable syntheses of scarce natural products in order to facilitate their biological investigation.[16,17] His retrosynthesis, which is a bit more convergent than his first generation approach but uses many of the same disconnections, is shown in Figure 7. Asymmetric hetero-Diels–Alder cyclization of **14** with Danishefsky's diene (**15**) gave **17** in 95% ee using Jacobsen's catalyst (**16**) on a >70-g scale (Scheme 1). Michael addition of an acetate provided excellent trans selectivity, which allowed for the completion of the initial pyran **18**. An acetate aldol set the stage for the formation of acetal **21**, which then underwent the Petasis–Ferrier rearrangement to bis-pyran **22**. Once the ketone was reduced to the axial alcohol, the C3–C19 fragment (**9**) was completed as expected. Smith also used **14** as his

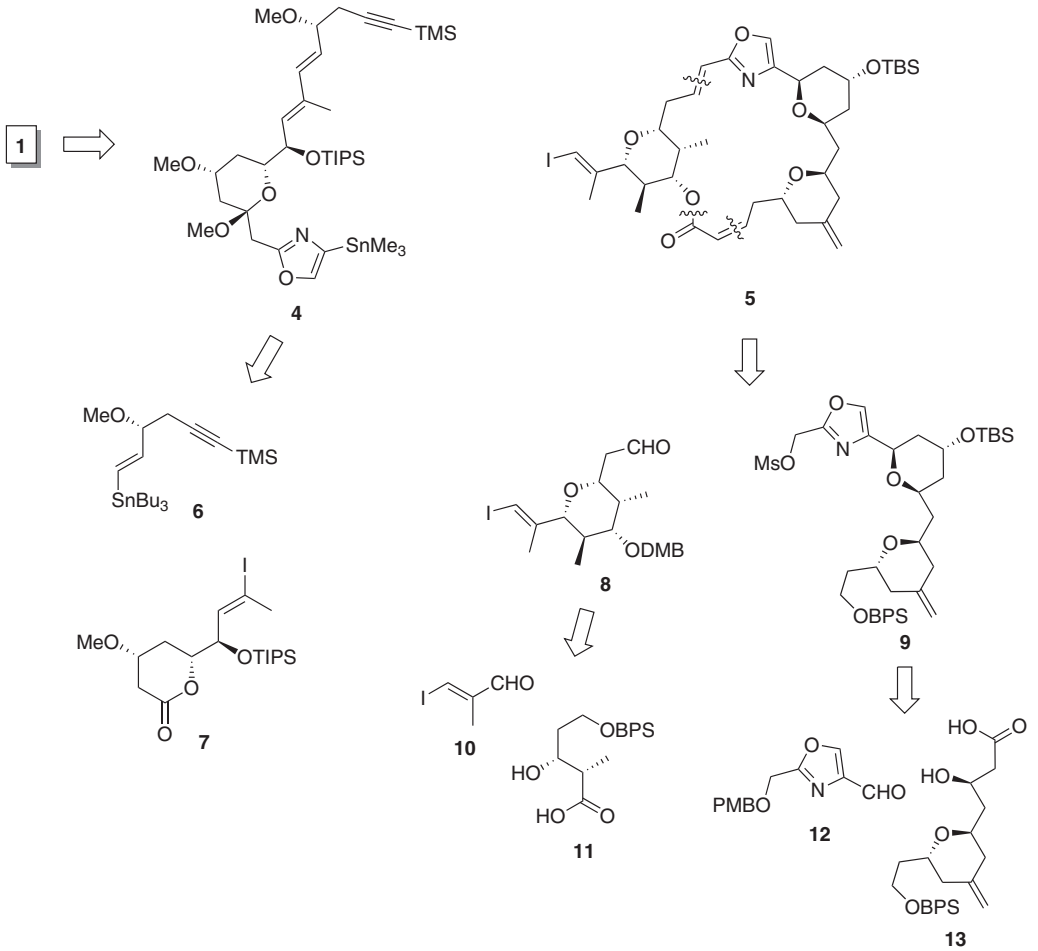


**Figure 7** Retrosynthetic analysis of Amos Smith's second generation total synthesis of phorboxazole A.

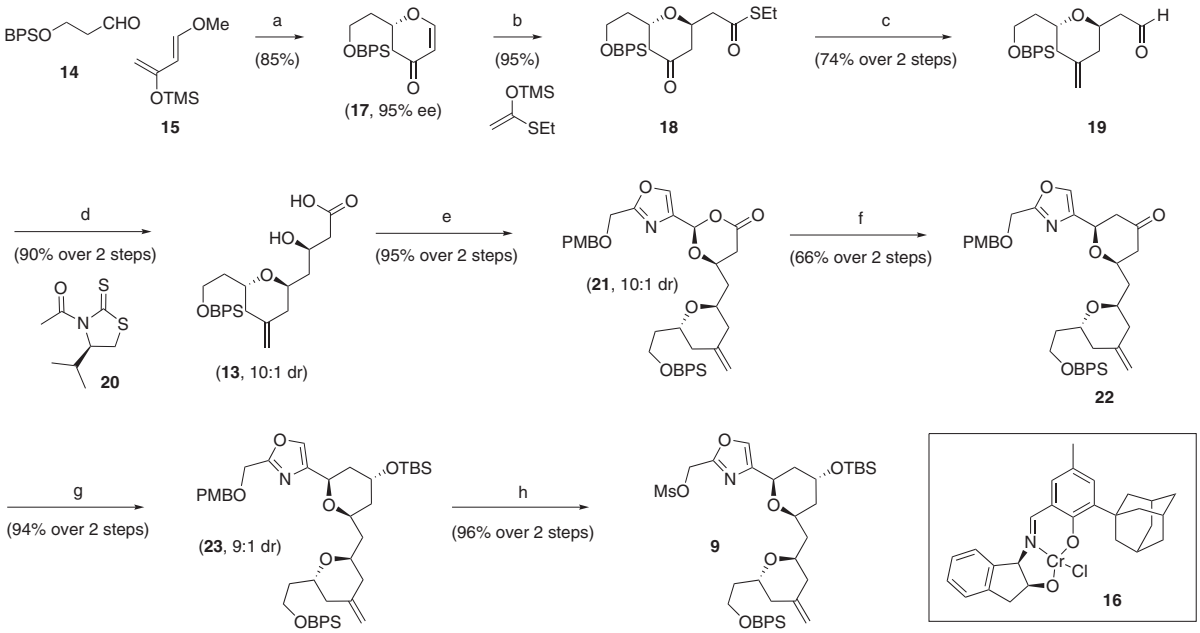


**Scheme 1** (a) **16**, 4 Å MS, $Me_2O$, RT; (b) TFA, 0 °C; (c) (1) $Cp_2TiMe_2$, ethyl pivalate, THF, 55 °C; (2) $HSiEt_3$, 10% Pd-C, $CH_2Cl_2$, RT; (d) (1) **20**, $Sn(OTf)_2$, *N*-ethylpiperidine, −55 to −78 °C; (2) LiOH, $H_2O_2$, THF, 0 °C; (e) (1) HMDS, $CH_2Cl_2$, RT; (2) **12**, TMSOTf, −78 to −30 °C; (f) (1) $Cp_2TiMe_2$, ethyl pivalate, THF, 53 °C; (2) $Me_2AlCl$, $Cs_2CO_3$, $CH_2Cl_2$, RT; (g) (1) K-selectride, THF, −78 °C; (2) TBSOTf, 2-6-lutidine, $CH_2Cl_2$, −78 °C; (h) DDQ, $H_2O$, $CH_2Cl_2$, RT; (2) MsCl, DIPEA, $CH_2Cl_2$, 0 °C.

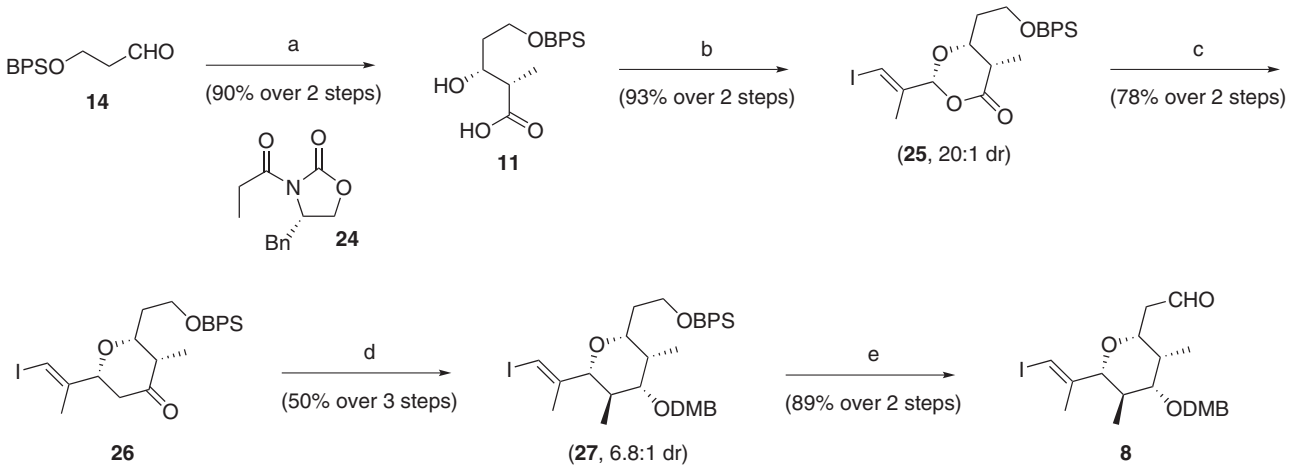


**Scheme 2** (a) (1) **24**, $Bu_2BOTf$, DIPEA; (2) LiOH, $H_2O_2$, 0 °C; (b) (1) HMDS, $CH_2Cl_2$; (2) **10**, TMSOTf, TfOH, 2-6-DTBMP; (c) (1) $Cp_2TiMe_2$, THF, 55 °C, (2) $Me_2AlCl$, $CH_2Cl_2$, −78 °C; (d) (1) LiHMDS, MeI, HMPA, −78 °C; (2) $NaBH_4$, EtOH, −10 °C; (3) KH, DMBCl, 15-c-5; (e) (1) TBAF, THF, RT; (2) $SO_3$ pyr, $Et_3N$, DMSO, $CH_2Cl_2$, RT.

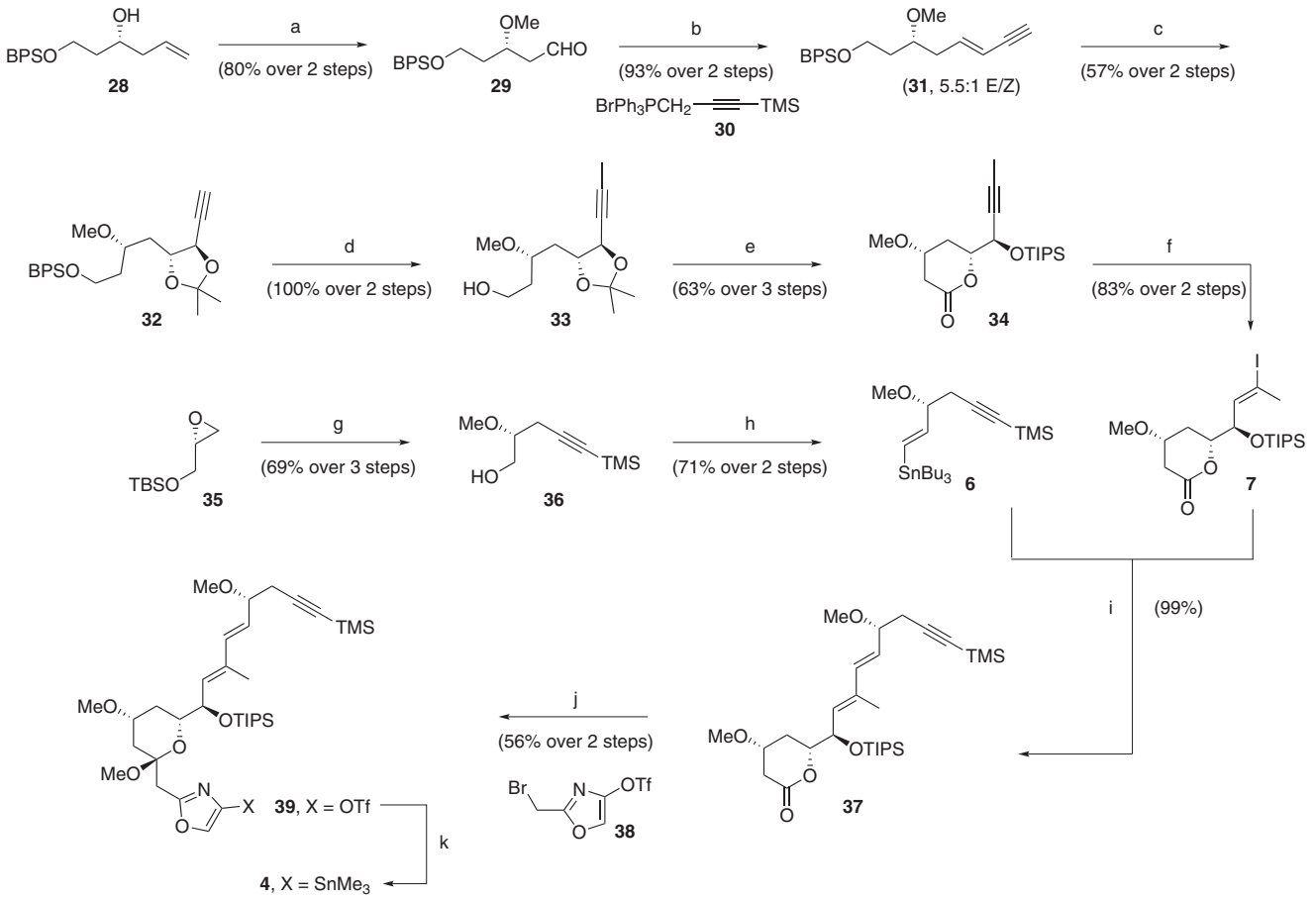


**Scheme 3** (a) (1) DTBMP, MeOTf, 4 d; (2) $O_3$, $PPh_3$; (b) (1) **30**, *n*-BuLi, THF; (2) $K_2CO_3$, MeOH; (c) (1) AD Mix β, 0 °C, 5 d; (2) $Me_2C(OMe)_2$, PPTS; (d) (1) *t*-BuLi, MeI; (2) TBAF; (e) (1) TEMPO, MeCN, pH 6.7 buffer, NaOCl, $NaClO_2$; (2) $FeCl_3$-$6H_2O$; (3) TIPSCl, imidazole; (f) (1) $Bu_3SnH$, $PdCl_2(PPh_3)_2$; (2) $I_2$; (g) (1) TMS-acetylene, *t*-BuLi, $BF_3$-$Et_2O$; (2) MeOTf, DTBMP; (3) HCl (cat.), MeOH; (h) (1) $SO_3$, pyr, DMSO; (2) $CrCl_2$, $Bu_3SnCHBr_2$, LiI, THF/DMF; (i) $Pd_2(dba)_3$—$CHCl_3$, DMF, RT, 4 h, $Ph_2PO_2NBu_4$; (j) (1) **38**, iPrMgCl, −78 °C; (2) PTSA, MeOH; (k) $Pd(PPh_3)_4$, $(Me_3Sn)_2$, LiCl, Dioxane, 90 °C.

entry point to the pentasubstituted pyran. Evans aldol addition followed by acetalization with **10** led to dioxanone **25**, which underwent the two-step Tebbe olefination/Petasis–Ferrier rearrangement without incident (Scheme 2). α-Methylation and elaboration to aldehyde **8** yielded the Wittig coupling partner. The synthesis of Smith's final pyran was achieved using an intermediate from his first

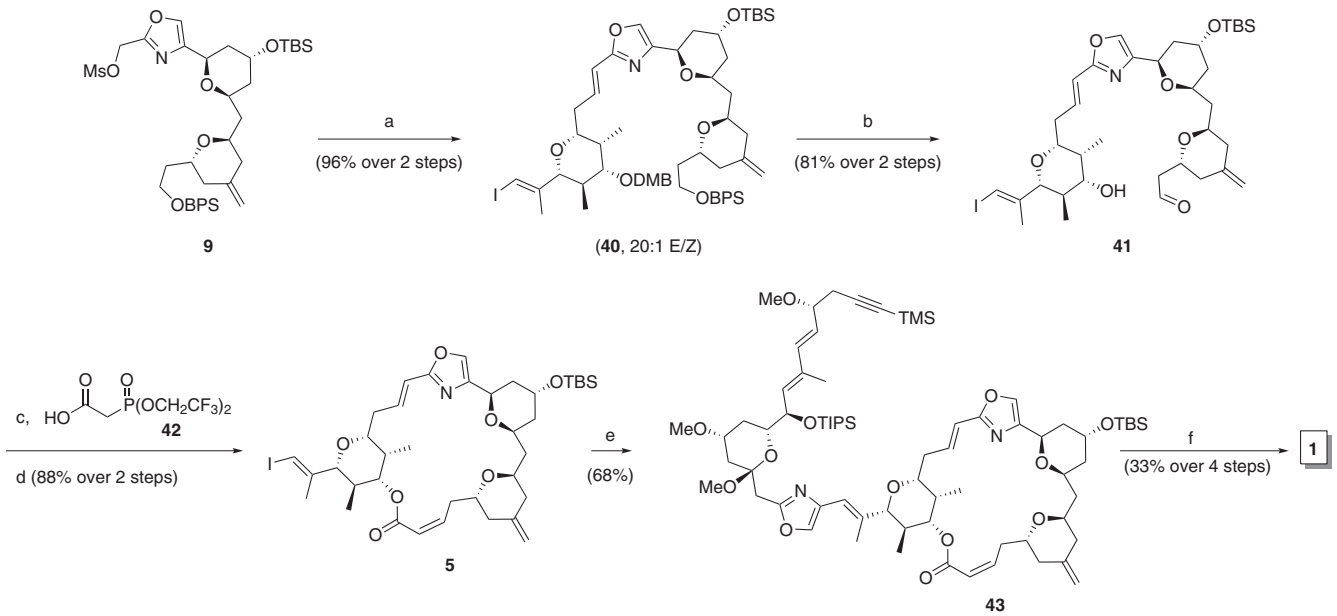


**Scheme 4** (a) (1) $PBu_3$, DMF, RT; (2) **8**, DBU, DMF, RT; (b) (1) KOH, 18-c-6, THF, 4% $H_2O$; (2) Dess–Martin, $NaHCO_3$, $CH_2Cl_2$, 0 °C; (3) DDQ, pH 7 buffer, $CH_2Cl_2$; (c) (1) EDCI-MeI, HOBT, **42**, $CH_2Cl_2$; (d) $K_2CO_3$, 18-c-6, toluene, RT; (e) $Pd_2(dba)_3$, $CHCl_3$, **4**, $AsPh_3$, DIPEA, $Ph_2PO_2NBu_4$, DMF, RT; (f) (1) $AgNO_3$, NBS, acetone; (2) $PdCl_2(PPh_3)_2$, $HSnBu_3$, THF (6:1, ext:int); (3) NBS, MeCN, 0 °C; (4) 6% HCl, THF, RT.

generation synthesis (which could also be prepared from aldehyde **14**, meaning all of the fragments emanate from the same starting material), and features an asymmetric Sharpless dihydroxylation to set the C37 and C38 stereocenters, a Stille coupling of **6** and **7** to install the diene and the introduction of the linchpin oxazole (Scheme 3). With all of the intermediates in hand, Wittig coupling of **8** and **9** proceeded with outstanding selectivity (Scheme 4). Macrocyclization was achieved using the Still–Gennari conditions to give the Z-olefin with 2.5:1 selectivity. The two fragments were united via a Stille coupling, and the peripheral vinyl bromide was installed followed by global deprotection to give **1**.

*Total synthesis of **1** by James White.* In their synthetic approach to **1**, the White group installed the elaborated polyene before introducing the bis-pyran portion of the macrolide (Figure 8).[18,19] Asymmetric allylation of tartrate-derived **52** leads to **53**, which was oxidized and acetalized (Scheme 5). Protection of the secondary alcohol allows for the Wittig homologation to **58**, which facilitated the generation of lactone **60**. Asymmetric crotylation of **62** installed the C25 and C26 stereocenters with 92% ee (Scheme 6), which was further elaborated via a second asymmetric crotylation with good diastereocontrol. A palladium-mediated alkoxycarbonylation then created the pentasubstituted pyran **66**, which was converted to **47** in anticipation of coupling to **46**, which was achieved via deprotonation of the oxazole methyl (Scheme 7). Formation of enal **68** and Julia olefination provided the C20–C46 fragment. It should be noted that the vinyl bromide had to be installed after the introduction of the oxazole, as it promoted elimination to the undesired terminal alkyne.

White prepared the bis pyran from the asymmetric allylation of **14** (Scheme 8). Seyferth–Gilbert homologation to the alkyne preceded bromoboration and extension to allylsilane **49**. Asymmetric allylation of **74** proceeded with outstanding enantiocontrol (Scheme 9), which was extended to **77** via a second asymmetric allylboration. The *cis* pyran was again formed via a carbonylative process, which was then coupled with **49** to complete the C3–C19 fragments. The undesired diastereomer at C9 was able to be converted to **45** using an oxidation/reduction protocol. The final assembly of **1** was achieved via the Wittig union of the fragments, which selectively gave the trans product (Scheme 10). The *trans*-pyran was then closed and the macrolide formed via intramolecular Horner–Wadsworth–Emmons olefination with 4:1 selectivity. Global deprotection yielded **1**.

*Second generation syntheses of **1** by Craig Forsyth.* Forsyth has also recently disclosed an extensive study that culminated in a second-generation synthesis of **1**, expanding on his *de novo* oxazole approach (Figure 9).[20,21] Hetero–Diels–Alder cyclization with Garner's aldehyde (**84**) gave an excellent yield of exclusively **86**, which is initially the *trans*-pyran (Scheme 11). Manta has also reported the synthesis of **86** using this methodology. Upon elaboration to aldehyde **88**, this could be equilibrated to the desired *cis* product (**89**). A second hetero-Diels–Alder cyclization with diene **85** then provided bis-pyran **90**. β-Ketoimide aldol addition to **91** and directed reduction gave the stereotetrad of the pentasubstituted pyran, which was extended to α,β-unsaturated ester **96** and closed via the Michael protocol (Scheme 12) to render primarily the *trans*-pyran. Equilibration via a retro-Michael/Michael process then afforded the desired stereochemistry, and the ester was extended and saponified to **82**.

Forsyth's approach to the exoxyclic pyran ultimately emanated from D-xylose derived **100** (Scheme 13). Silylketene acetal addition gave >4:1 selectivity for **102**, which was converted to the aldehyde and extended to **106**. Julia addition of the terminus gave **108**, which could be ketalized and advanced to vinyl bromide **81**.

Forsyth explored an impressive array of approaches to optimize the final formation of **1**, including a ring closing metathesis that dramatically improved the C2–C3 Z:E selectivity and a tandem *de novo* oxazole formation of both rings. The most direct synthesis is shown in Scheme 14. Ultimately, his second-generation synthesis achieves **1** in an overall yield of 6% with a longest linear sequence of 19 steps from **84**.

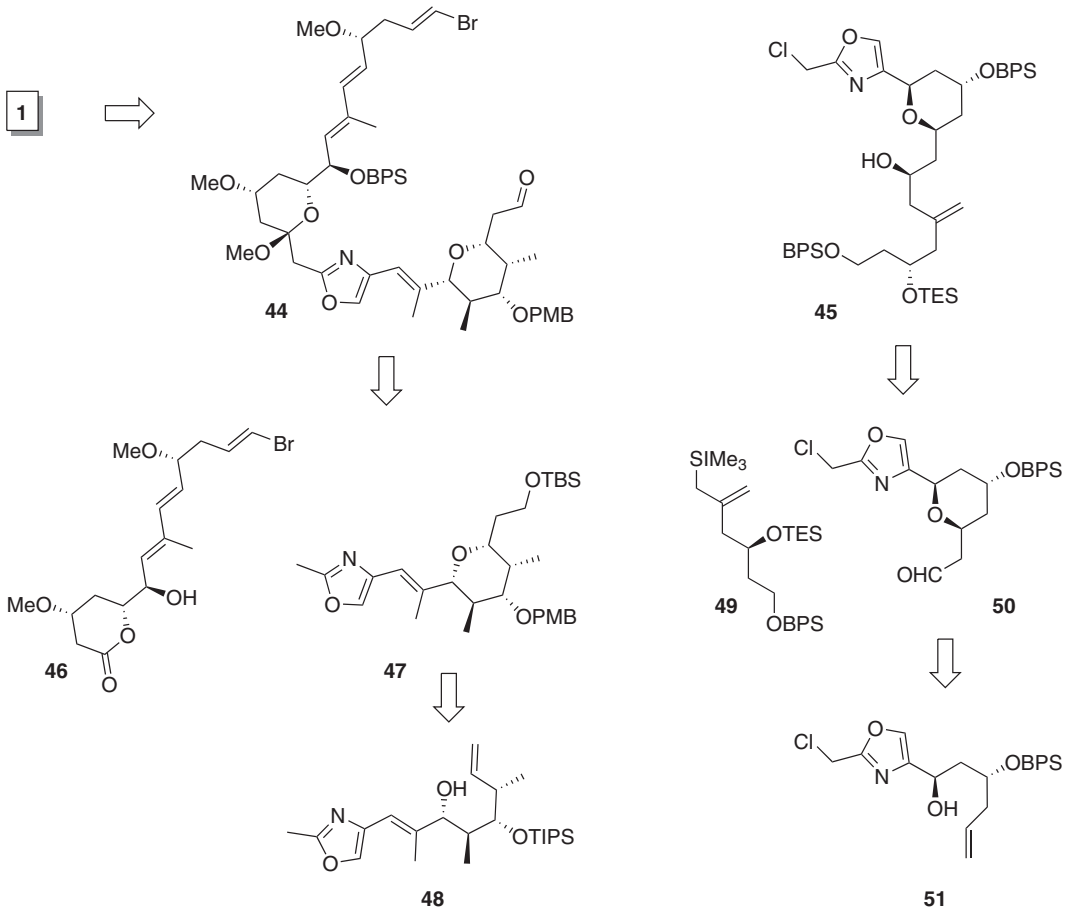


**Figure 8** Retrosynthetic analysis of James White's total synthesis of phorboxazole A.

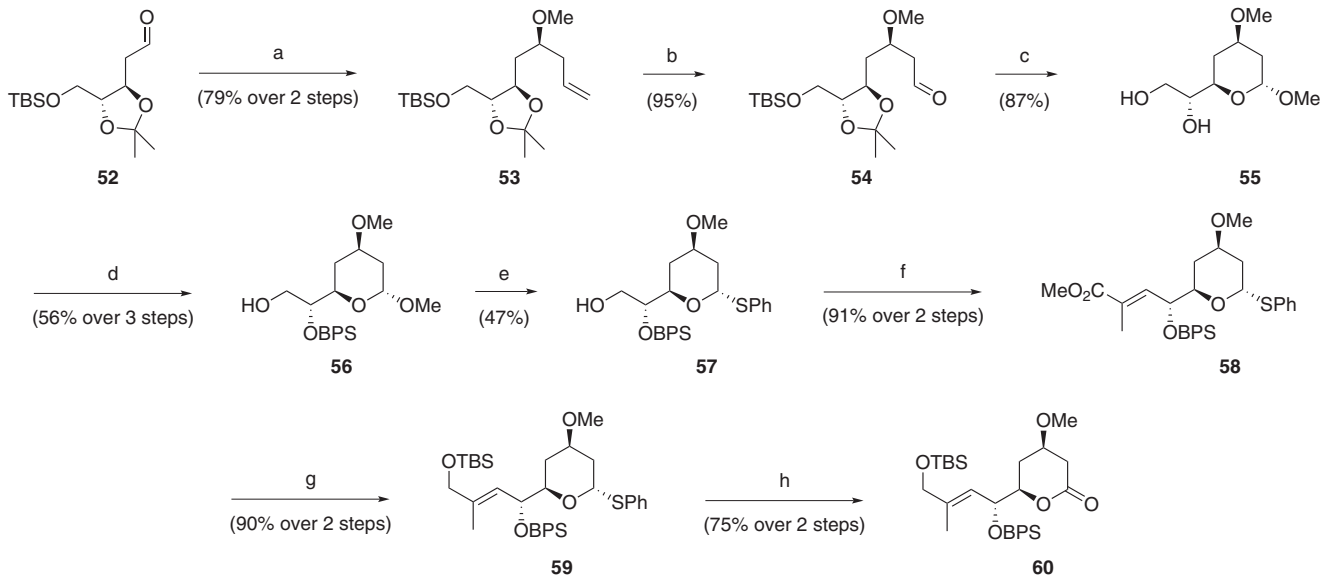


**Scheme 5** (a) $H_2C=CHCH_2MgBr$, (−)-$(Ipc)_2BOMe$, $Et_2O$, −100 °C; (2) NaH, MeI, THF, heat; (b) $O_3$, $CH_2Cl_2$, $PPh_3$, −78 °C; (c) MeOH, PPTS (cat.); (d) (1) TBSCl, imidazole, DMF, −78 °C; (2) TBDPSOTf, 2,6-lutidine, $CH_2Cl_2$; (3) MeOH, PPTS (cat.); (e) $PhSSiMe_3$, $ZnI_2$, EDC; (f) (1) $(COCl)_2$, DMSO, $Et_3N$; (2) $Ph_3P=C(CH_3)CO_2Me$, toluene, heat; (g) (1) DIBAL-H, toluene, −78 °C; (2) TBSCl, DIPEA, $CH_2Cl_2$; (h) (1) $AgNO_3$, 2,6-lutidine; (2) TPAP, NMO, $CH_2Cl_2$.

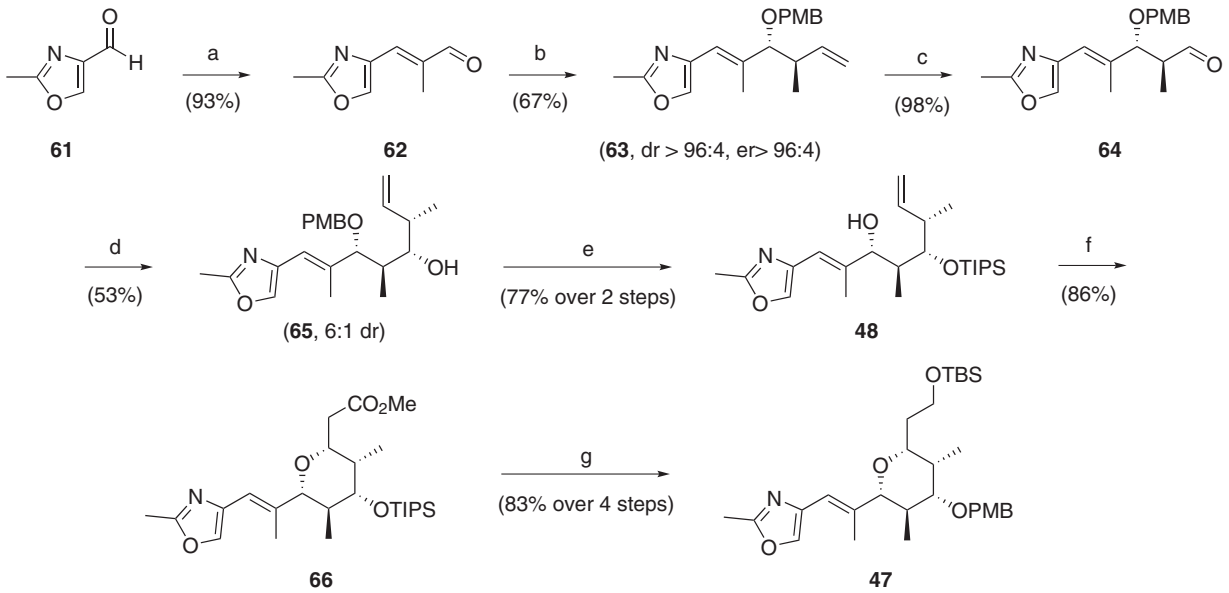


**Scheme 6** (a) $Ph_3P{=}CC(CH_3)CHO$, benzene, heat, 20 h; (b) *trans*-$CH_3CH{=}CHCH_3$, *t*-BuOK, *n*-BuLi, THF, then (+)-$(Ipc)_2BOMe$, THF, −70 °C, 6 h; $H_2O_2$, $NaHCO_3$, RT, 15 h; (2) NaH, THF, heat, 40 min, then PMBCl, *n*-$Bu_4NI$, heat, 6 h, 89%; (c) (1) $OsO_4$ (cat.), NMO, THF-$H_2O$, RT, 10 h, 84%; (2) $NaIO_4$, $H_2O$-THF, RT, 30 min, 98%; (d) *trans*-$CH_3CH{=}CHCH_3$, *t*-BuOK, *n*-BuLi, THF, then (−)-$(Ipc)_2BOMe$; $HOCH_2CH_2NH_2$, MeOH, RT, 3 h, 53%; (e) (1) TIPSOTf, 2,6-lutidine, $CH_2Cl_2$, RT, 2 h, 99%; (2) $AlCl_3$, EtSH, $CH_2Cl_2$, −20 to −4 °C, 3.5 h, 78%; (f) $Pd(OAc)_2$ (3 eq.), CO, MeOH–MeCN, 70 h; (g) (1) $LiAlH_4$, $Et_2O$, 0 °C; (2) TBAF, THF, 0 °C; (3) TBSCl, DIPEA, DMAP, $CH_2Cl_2$, (4) NaH, PMBCl, TBAI, THF.

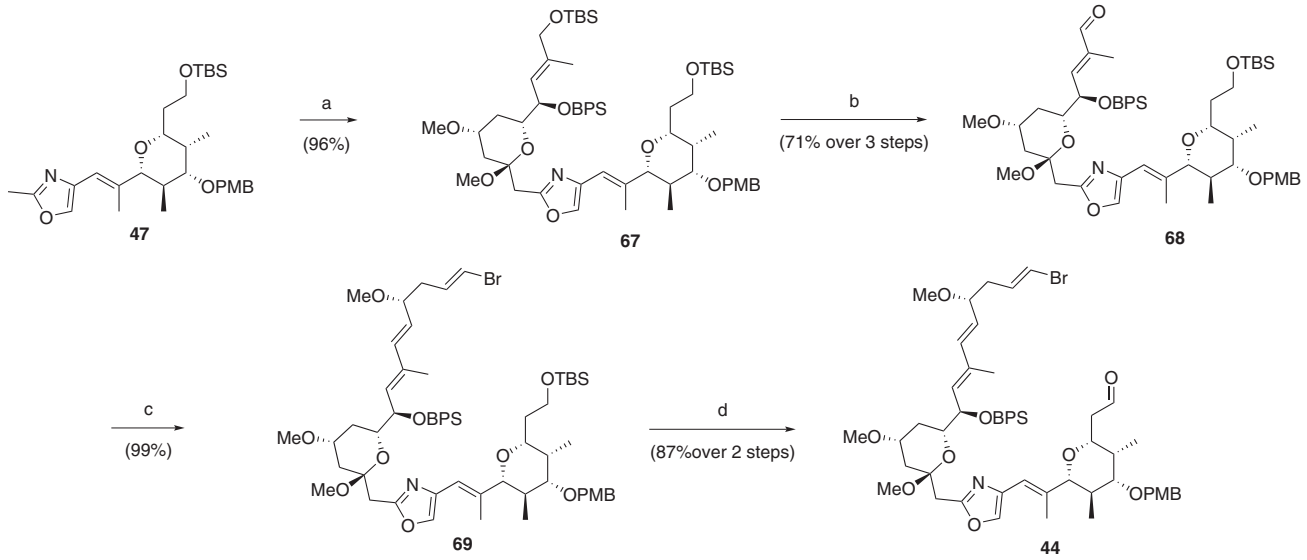


**Scheme 7** (a) $Et_2NH$, *n*-BuLi, THF, −78 °C then **60**; (b) (1) MeOH, PTSA; (2) $MnO_2$, $CH_2Cl_2$; (3) TBSCl, imidazole, $CH_2Cl_2$; (c) **3**, NaHMDS, THF, −78 °C; (d) (1) MeOH, PTSA; (2) Dess–Martin.

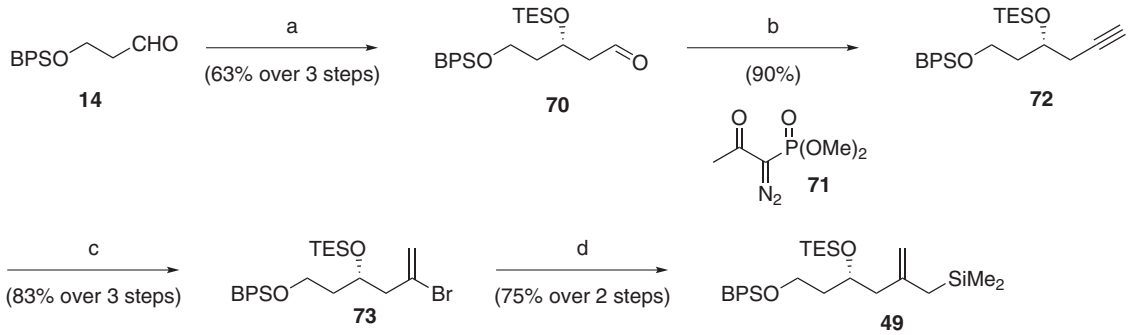


**Scheme 8** (a) (1) $H_2C{=}CHCH_2MgBr$, (+)-$(Ipc)_2BOMe$, $Et_2O$, −100 °C; (2) TESOTf, 2,6-lutidine, $CH_2Cl_2$; (3) $O_3$, $CH_2Cl_2$-MeOH, $PPh_3$, −78 °C; (b) **71**, NaOMe, MeOH-THF; (c) (1) PPTS, MeOH; (2) B-Br-9-BBN, $CH_2Cl_2$; (3) TESOTf, 2,6-lutidine, $CH_2Cl_2$; (d) $Me_3SiCH_2MgCl$, $NiCl_2$(dppp).

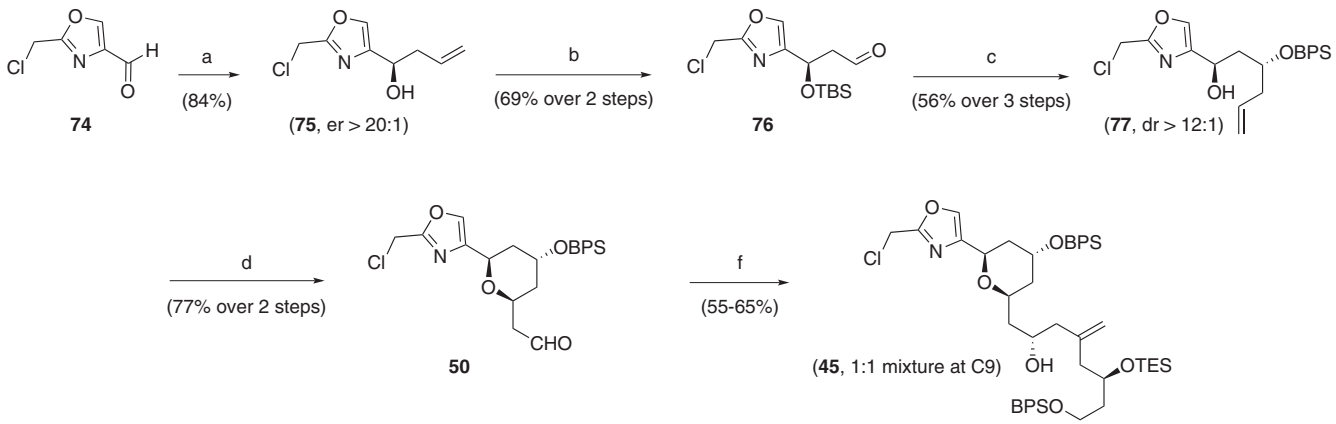


**Scheme 9** (a) (+)-(Ipc)$_2$BOMe, $CH_2=CHCH_2MgBr$, $Et_2O$, −100 °C; (b) (1) TBSOTf, 2,6-lutidine, $CH_2Cl_2$, RT; (2) $OsO_4$(cat.), $NaIO_4$, $H_2O$-THF; (c) (1) (+)-(Ipc)$_2$BOMe, $CH_2=CHCH_2MgBr$, $Et_2O$, −100 °C; (2) TBDPSOTf, 2,6-lutidine, $CH_2Cl_2$, RT; (3) HCl (3N), THF–$H_2O$; (d) (1) $PdCl_2(MeCN)_2$, (10 mol%), CO (1 atm), MeOH, *p*-benzoquinone; (2) DIBAL-H, $CH_2Cl_2$, −78 °C; (f) **49**, $SnCl_4$, $CH_2Cl_2$, −78 °C (inverted unwanted diastereomer by [O]/[H] process).

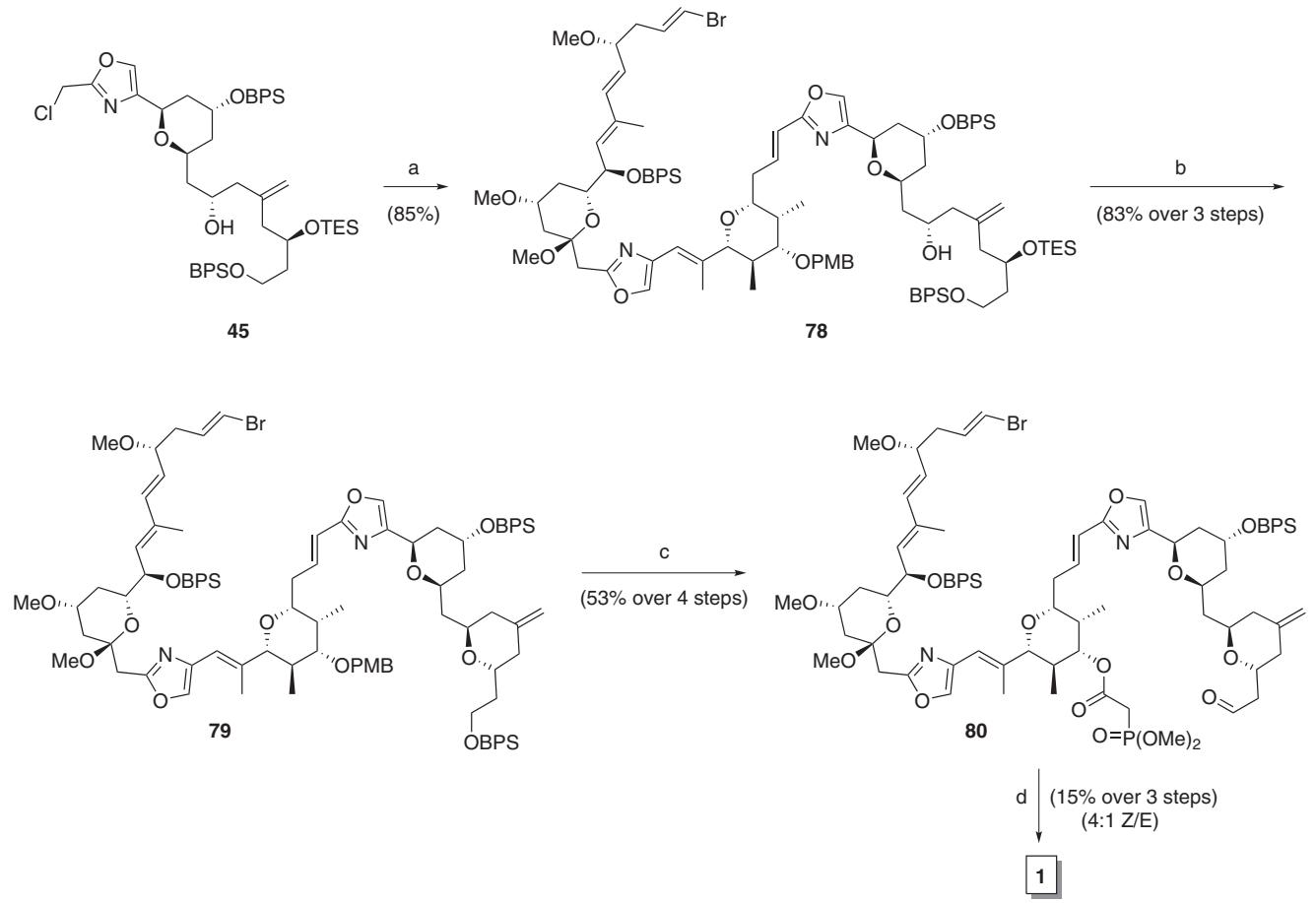


**Scheme 10** (a) $Bu_3P$, DMF, DBU, then **44**; (b) (1) MsCl, $Et_3N$; (2) MeOH, PPTS, $CH_2Cl_2$; (3) $Et_3N$, MeCN; (c) (1) DDQ, $CH_2Cl_2$;(2) $(MeO)_2P(O)CH_2CO_2H$, DCC, $Ch_2Cl_2$; (3) $NH_4F$ (excess), MeOH, 50°C; (4) Dess–Martin, $CH_2Cl_2$; (d) $K_2CO_3$, 18-c-6, toluene, −78 °C to RT; (2) TBAF, THF; HCl (6%), THF.

*Total synthesis of **2** by Guo-Qiang Lin and Wei-Shan Zhou.* Two total syntheses of **2** have also been achieved in the last decade. The first of these came from the labs of Lin and Zhou (Figure 10).[22] Asymmetric allylation and Wacker oxidation of the protected product gave an 87% ee of ketone **126** (Scheme 15). Aldol addition and oxidation led to diketone **128**, which was closed to pyranone **129**. Hydrogenation simultaneously set the C13 and C15 stereocenters, leading to aldehyde **122**. Aldol addition of **123** (derived as the opposite antipode to **126**,

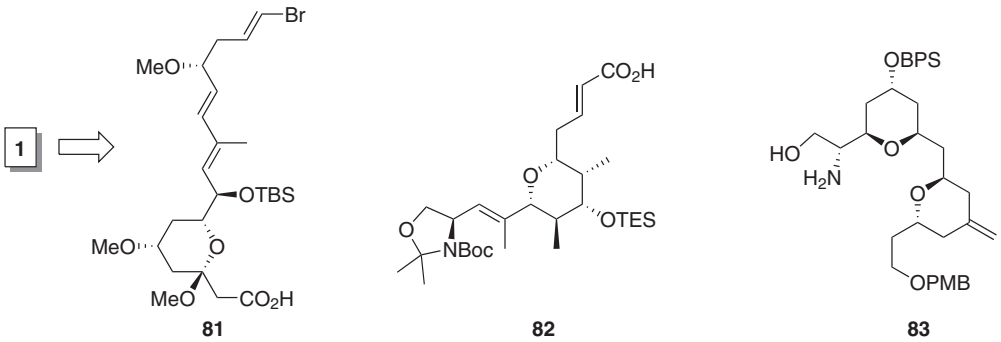


**Figure 9** Retrosynthetic analysis of Craig Forsyth's second-generation total synthesis of phorboxazole A.

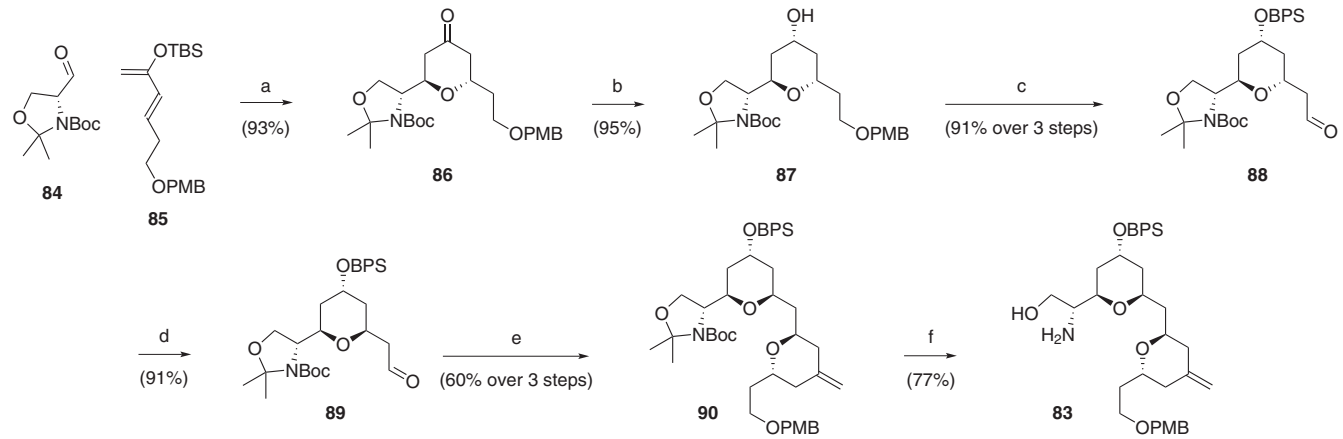


**Scheme 11** (a) $ZnCl_2$, $CH_2Cl_2$, 0 °C, then TBAF; (b) K-selectride, THF, −78 °C; (c) (1) TBDPSCl, imidazole, DMAP, $CH_2Cl_2$; (2) DDQ, pH 7 buffer, $CH_2Cl_2$, *t*-BuOH; (3) $(COCl)_2$, DMSO, $iPr_2NEt$, $CH_2Cl_2$; (d) DBU, benzene, reflux; (e) (1) **85**, $ZnCl_2$, $CH_2Cl_2$, 0 °C; (2) TBAF; (3) $Ph_3PCH_3Br$, *n*-BuLi, THF, 0 °C; (f) AcCl, MeOH, 0 °C.

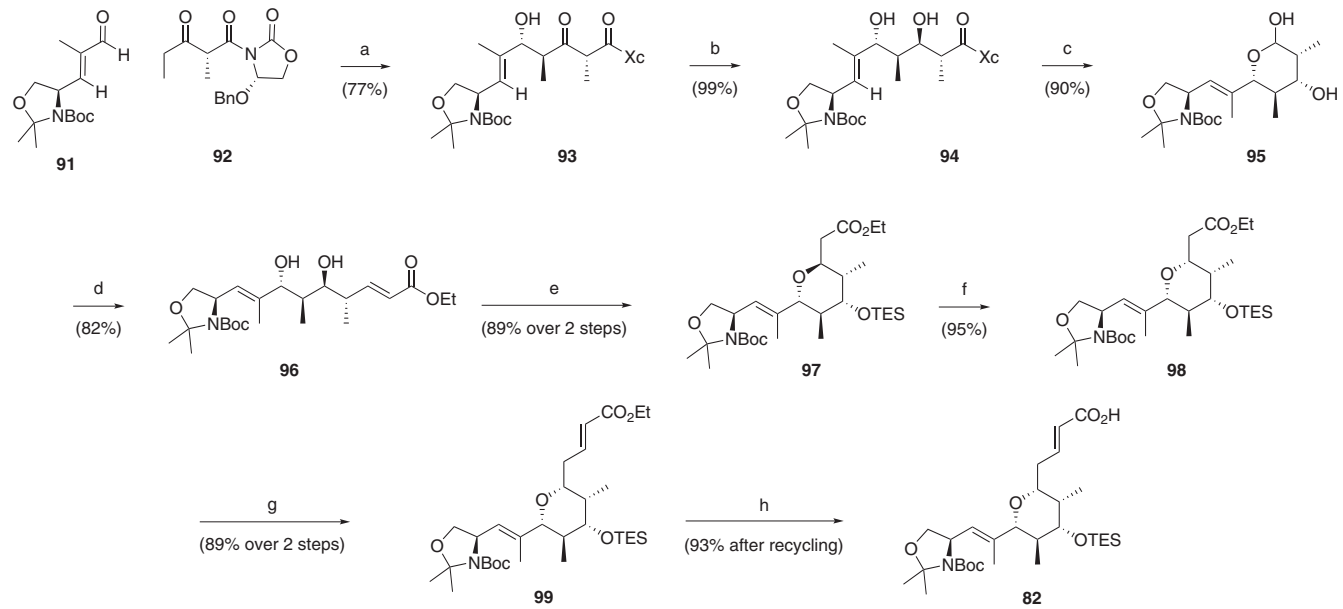


**Scheme 12** (a) $(c\text{-hexyl})_2BCl$, $Et_3N$, $Et_2O$, 0 °C, then **91**, −78 °C; (b) $Me_4NBH(OAc)_3$, HOAc, MeCN, −20 °C; (c) DBU, $CH_2Cl_2$, then DIBAL-H, −78 °C; (d) $Ph_3PCHCO_2Et$, benzene, reflux; (e) (1) KOtBu, THF, −50 °C; (2) TESCl. $Et_3N$, DMAP, $CH_2Cl_2$; (f) KH, THF, methyl pivolate, 0 °C to RT; (g) (1) DIBAL-H, $CH_2Cl_2$, −78 °C; (2) $Ph_3PCHCO_2Me$, MeCN, 65 °C; (h) LiOH, THF, $H_2O$ (recycled deprotected alcohol: TESCl, $Et_3N$, DMAP, then aq $NH_4Cl$).

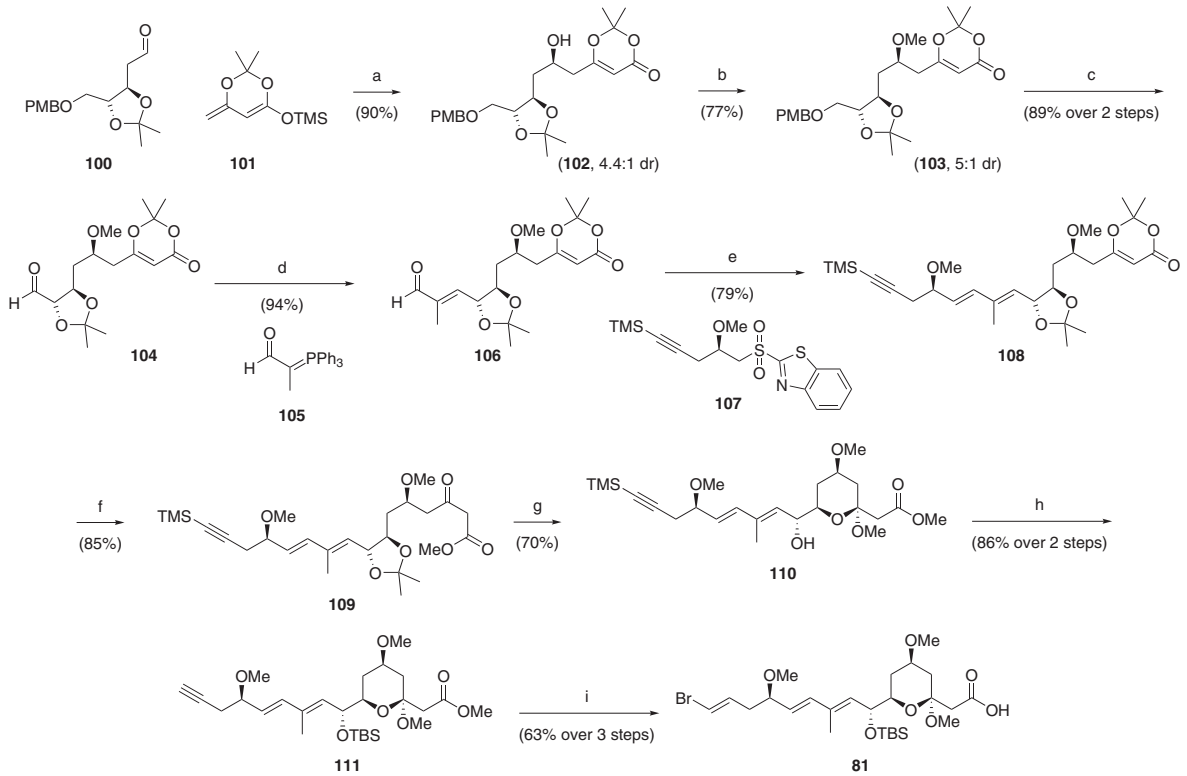


**Scheme 13** (a) **101**, $Ti(OiPr)_2Cl_2$ (1.2 eq.), toluene; (b) $Me_3O^+BF_4^-$, proton sponge, $CH_2Cl_2$, 3 A sieves; (c) (1) DDQ, $CH_2Cl_2$; (2) $SO_3$-Pyr, DMSO, $iPr_2NEt$, $CH_2Cl_2$; (d) **105**, toluene, 60 °C; (e) **107**, NaHMDS, THF, −78 °C; (f) MeOH (16 eq.), toluene, reflux; (g) TsOH, MeOH; (h) (1) TBAF, THF, 0 °C; (2) TBSCl, imidazole, DMAP, $CH_2Cl_2$; (i) (1) $Bu_3SnH$, $Et_3B$, benzene; (2) NBS, MeCN; (2) $Ba(OH)_2$, MeOH, $H_2O$.

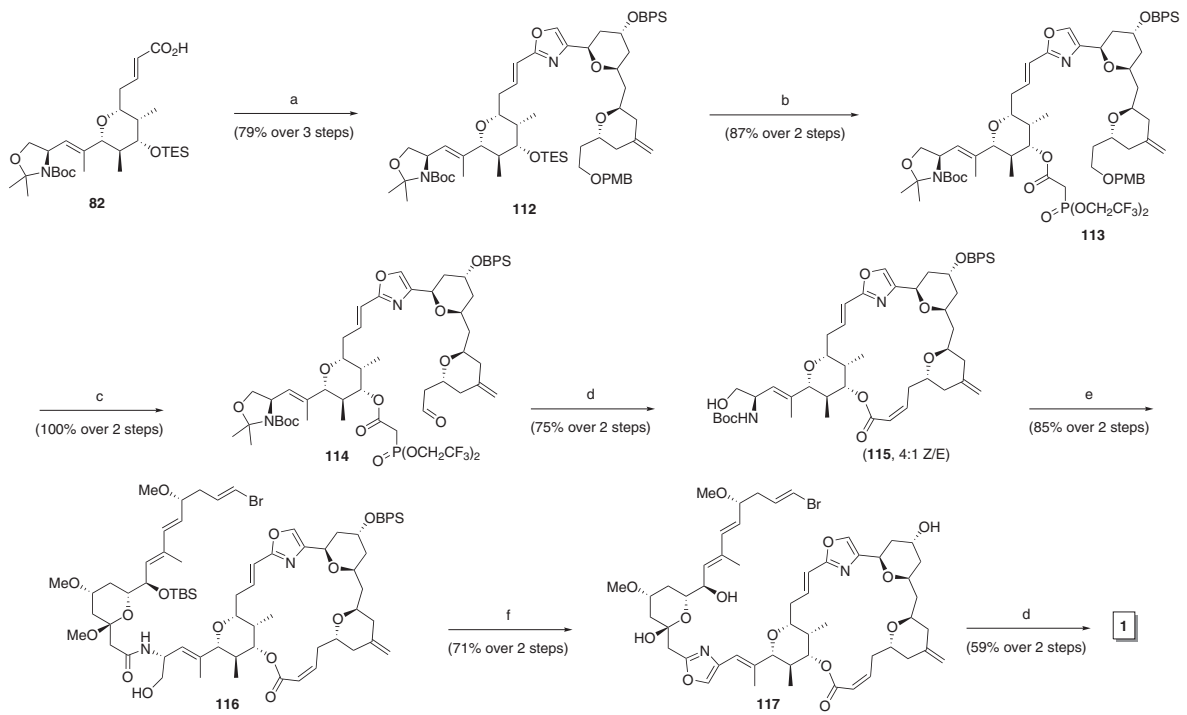


**Scheme 14** (a) (1) **83**, EDCI-MeI, HOBt, $CH_2Cl_2$; (2) Dess–Martin, $NaHCO_3$, *t*-BuOH, $CH_2Cl_2$; (3) $(CCl_2Br)_2$, $PPh_3$, DIPEA, $CH_2Cl_2$, RT; (b) (1) TBAF, THF; (2) **42**, EDCI-MeI, HOBt, $CH_2Cl_2$; (c) (1) DDQ, pH 7 buffer, *t*-BuOH, $CH_2Cl_2$; (2) Dess–Martin, $NaHCO_3$, *t*-BuOH, $CH_2Cl_2$; (d) (1) $K_2CO_3$, toluene, 18-**c**-6, RT, 3 h; (2) PTSA, MeOH; (e) TFA, $CH_2Cl_2$, then pH 7.4 buffer; (2) **81**, PyAOP, i-$Pr_2NEt$, $CH_2Cl_2$; (f) (1) Dess–Martin, $NaHCO_3$, *t*-BuOH, $CH_2Cl_2$; (2) $(CCl_2Br)_2$, $PPh_3$, i-$Pr_2NEt$, $CH_2Cl_2$; (g) TBAF, EtOAc, THF; (2) aq HCl, THF.

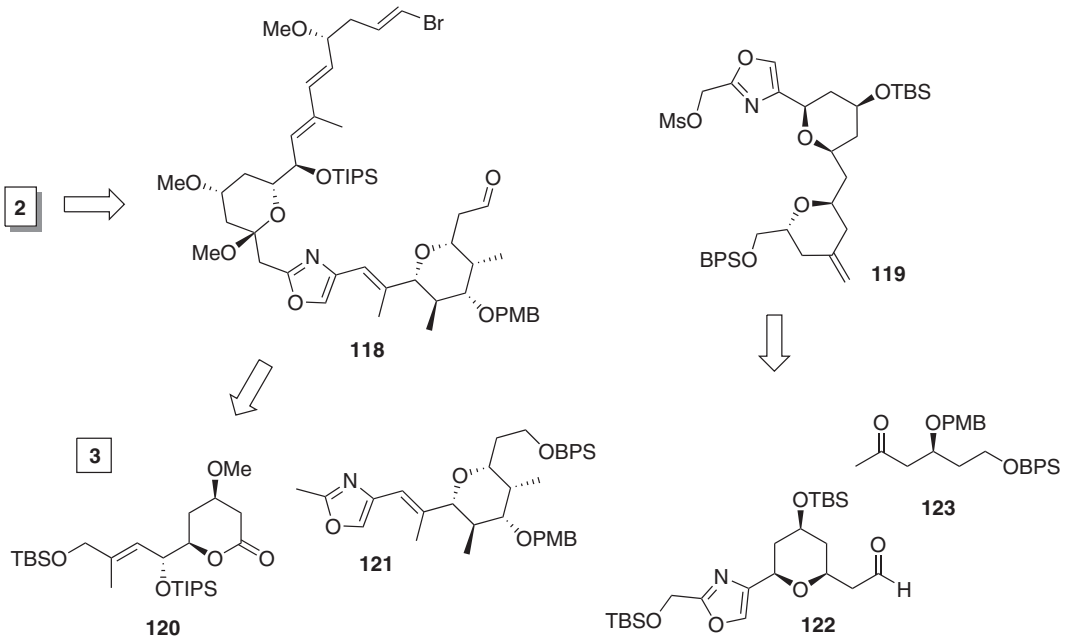


**Figure 10** Retrosynthetic analysis of Gua-Lin Qiang and Wei-Shan Zhou's total synthesis of phorboxazole B.

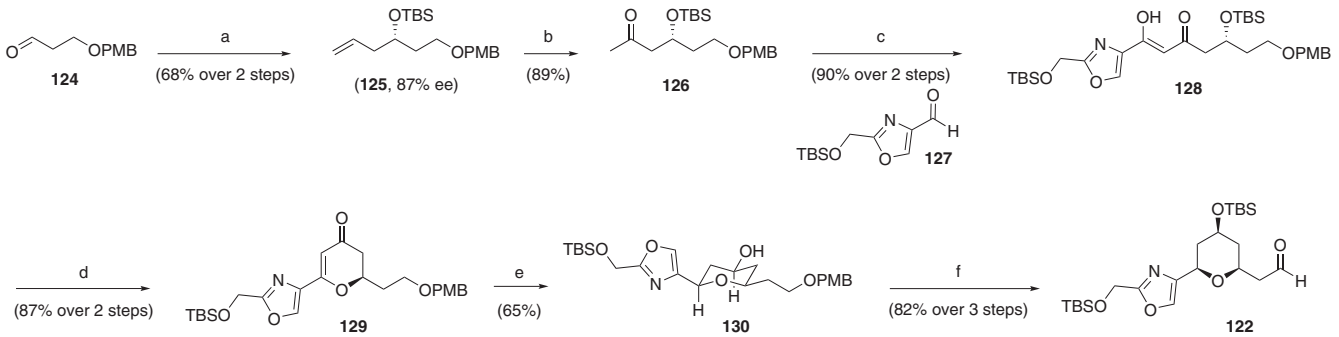


**Scheme 15** (a) (1) (−)-Ipc$_2$BAllyl, Et$_2$O, −78 °C; (2) TBSCl, imidazole, DMF; (b) PdCl$_2$ (cat.), CuCl, O$_2$, DMF/H$_2$O, RT, 6 h; (c) (1) LDA, **127**, THF, −78 °C; (2) Dess–Martin, CH$_2$Cl$_2$, RT; (d) (1) HF in CH$_3$CN, RT, 12 h; (2) TBSCl, imidazole, DMF, RT; (e) H$_2$, 10% Pd/C, EtOAc (saturated with 0.1N HCl), 8 h (f) (1) TBSCl, imidazole, DMF; (2) DDQ, CH$_2$Cl$_2$, H$_2$O; (3) Dess–Martin, CH$_2$Cl$_2$, RT.

Scheme 16) gave a nearly 8:1 diastereomeric ratio of **132**. Nysted olefination and cyclization resulted in bis-pyran **135**, which was then prepped for the Wittig coupling. Sequential asymmetric crotylation of glyceraldehyde **136** using Roush's tartrate-derived methodology produced **140** (Scheme 17), which was closed to the *cis* pyran using an intramolecular oxymercuration cyclization with good stereocontrol. Once the resultant iodide was transformed into a protected silyl ether, removal of the acetonide and periodate cleavage yielded ketone **144**, which was adorned with the oxazole to complete the C20–C32 piece.

The exocyclic pyran was generated from the Sharpless asymmetric dihydroxylation of enoate **147** (Scheme 18). Upon extension to the allylic acetate, the primary TBS ether was converted to the corresponding aldehyde and subjected to a titanium silylketene acetal addition with 4:1 selectivity at C35. Deprotection allowed selective δ-lactone cyclization, which led to **154**. Methyl deprotonation and ketalization was used to prepare **155** (Scheme 19), which underwent Julia olefination with **3** to C20–C46 fragment **118**. Although its use in the synthesis of the phorboxazoles was well established by Pattenden, Lin and Zhou prepared **3** via dihydroxylation of bis-allyl ether **157** and Wipf's hydrozirconation protocol (Scheme 20). The synthesis of **2** was completed via Wittig coupling of the C19-C20 olefin and Horner–Wadsworth–Emmons macrocyclization (Scheme 21).

*Total synthesis of 2 by Steven Burke.* The Burke synthesis of **2** (Figure 11) is a beautiful illustration of the use of two-directional synthesis.[23] Readily available diol **171** was ozonolyzed and converted to achiral tetraol **170** (Scheme 22). Palladium-catalyzed desymmetrization with Trost's DPPBA ligand gave the bis-pyran **174** in 98% ee. Selective asymmetric dihydroxylation of the equatorial vinyl group completed the desymmetrization, which was able to be oxidized to carboxylate **177** and cyclized under Mitsunobu conditions to lactone **178**, thus differentiating the two secondary alcohols. Upon reductive opening of the lactone, the exocyclic alkene was installed using the Tebbe reagent to generate **180**. Removal of the acetonide and selective primary protection allowed for the introduction of nitrogen with diphenylphosphoryl azide. Burke was the first to utilize an asymmetric

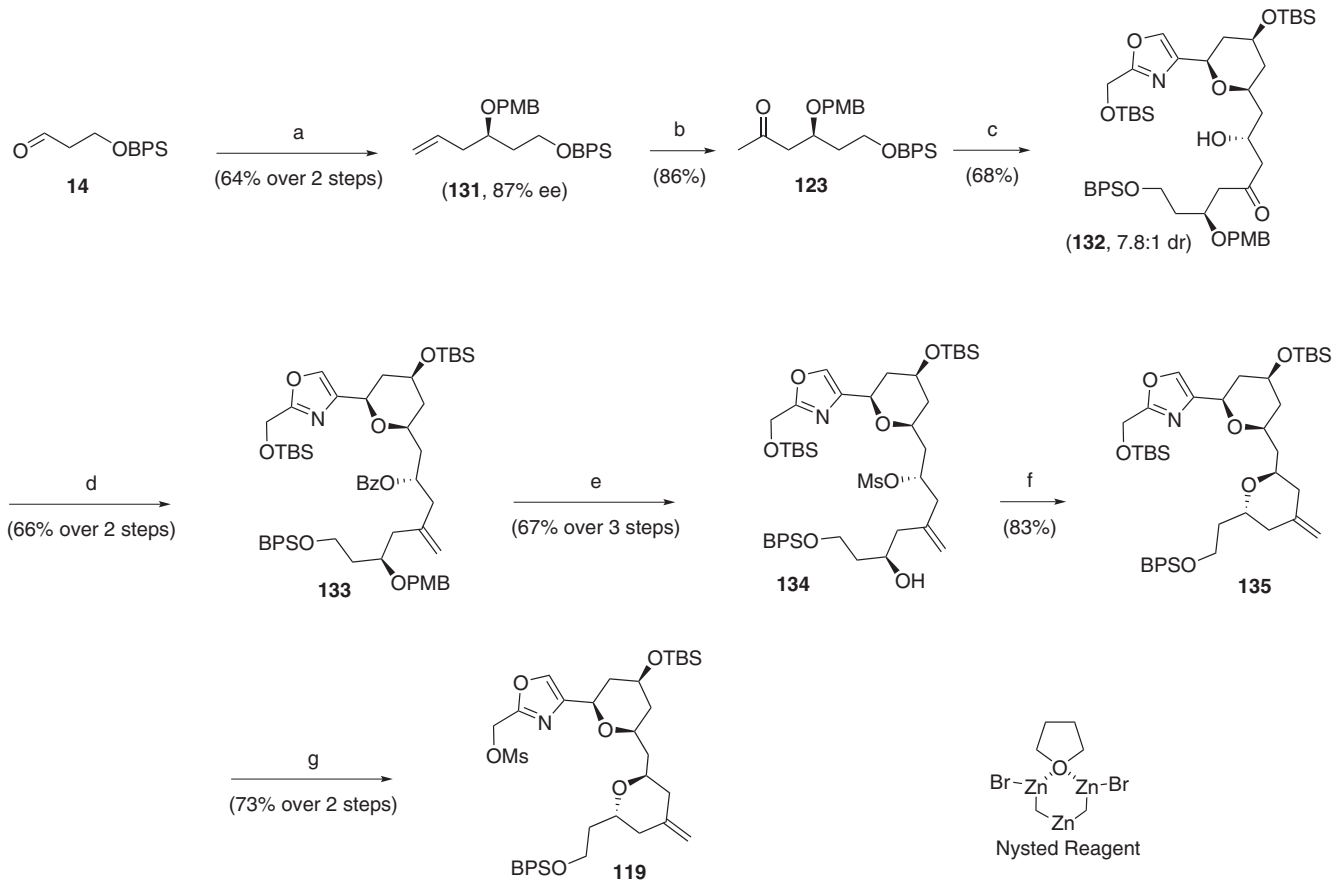


**Scheme 16** (a) (1) (+)-Ipc$_2$BAllyl, $Et_2O$, −78 °C; (2) PMBOC(=NH)$CCl_3$, cyclohexane/$CH_2Cl_2$, $BF_3OEt_2$, 0 °C; (b) $PdCl_2$ (cat.), CuCl, $O_2$, DMF/$H_2O$, RT, 6 h; (c) (1) LiHMDS, TMSCl, THF, −78 °C; (2) **122**, $TiCl_4$, −78 °C; (d) (1) BzCl, pyr, RT; (2) Nysted reagent, $TiCl_4$, RT, 30 min; (e) (1) DIBAL-H, $CH_2Cl_2$, −78 °C; (2) MsCl, $Et_3N$, $CH_2Cl_2$, 0 °C; (3) DDQ, $CH_2Cl_2$/$H_2O$; (f) $Et_3N$, MeCN, reflux; (g) (1) $NH_4F$, MeOH, 50 °C; (2) DIPEA, MsCl.

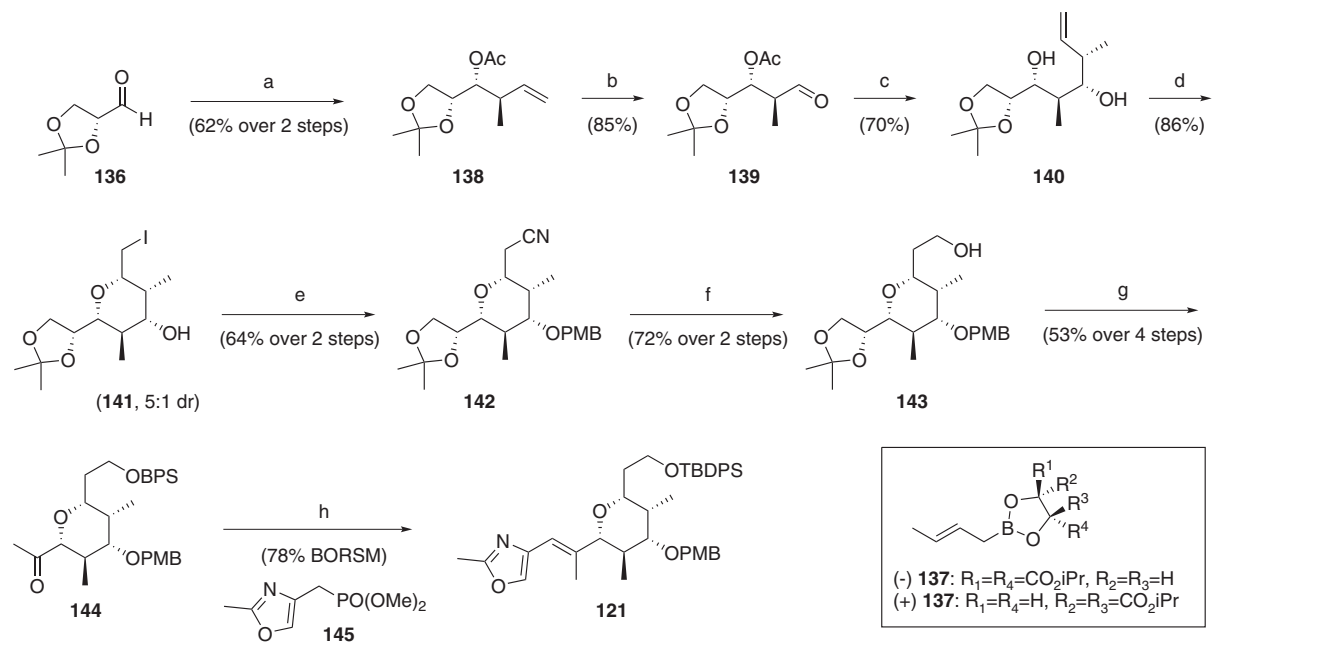


**Scheme 17** (a) (1) (−)-**137**, 4 Å MS, toluene, −78 °C, 7 h; (2) $Ac_2O$, $Et_3N$, DMAP (cat.), $CH_2Cl_2$, RT, overnight; (b) $O_3$, MeOH, −78 °C; then $PPh_3$, RT; (c) (+)-**137**, 4 Å MS, toluene, −78 °C, 6 h; (d) $Hg(OAc)_2$, toluene, 0 °C, $I_2$, 30 °C; (e) (1) PMBOC(=NH)$CCl_3$, $BF_3OEt_2$, 0 °C; (2) NaCN, DMSO, 70 °C; (f) (1) DIBAL-H, $CH_2Cl_2$, 0 °C, then 1N HCl; (2) $NaBH_4$, MeOH; (g) (1) TBDPSCl, $Et_3N$, $CH_2Cl_2$; (2) $HIO_4$, EtOAc; (3) MeLi, THF, −78 °C; (4) Dess–Martin, $CH_2Cl_2$, RT; (h) **145**, LDA, THF, −78 °C.

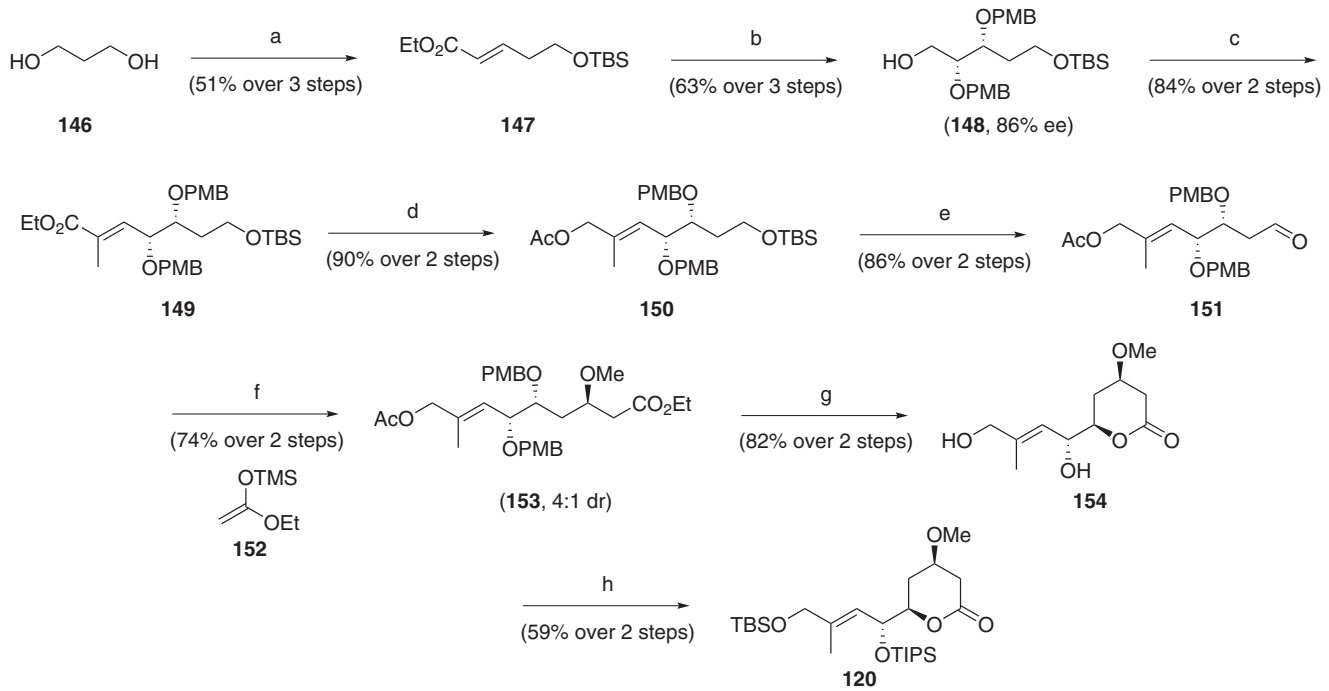


**Scheme 18** (a) (1) NaH, TBSCl, THF, 0 °C; (2) PCC, $CH_2Cl_2$, RT; (3) $Ph_3P{=}CHCO_2Et$, benzene, reflux; (b) (1) AD-mix β, *t*-BuOH/$H_2O$, RT; (2) PMBOC(=NH)$CCl_3$, cyclohexane/$CH_2Cl_2$, $BF_3OEt_2$, 0 °C; (3) $LiAlH_4$, $Et_2O$, RT; (c) (1) $(COCl)_2$, DMSO, $CH_2Cl_2$, −78 °C, then $Et_3N$; (2) $CH_3CH(PPh_3)CO_2Et$, $CH_2Cl_2$, reflux; (d) (1) DIBAL-H, $CH_2Cl_2$, −78 °C; (2) $Ac_2O$, $Et_3N$, $CH_2Cl_2$, RT; (e) (1) $Bu_4NF$, THF, RT; (2) Dess–Martin, $CH_2Cl_2$; (f) (1) $TiCl_2(OiPr)_2$, toluene, −78 °C, then **152**; (2) $Me_3OBF_4$, proton sponge, $CH_2Cl_2$, RT; (g) (1) $K_2CO_3$, EtOH; (2) 10% TFA, $CH_2Cl_2$, then $Et_3N$; (h) (1) TBSCl, $Et_3N$, $CH_2Cl_2$; (2) TIPSCl, $AgNO_3$, pyr.

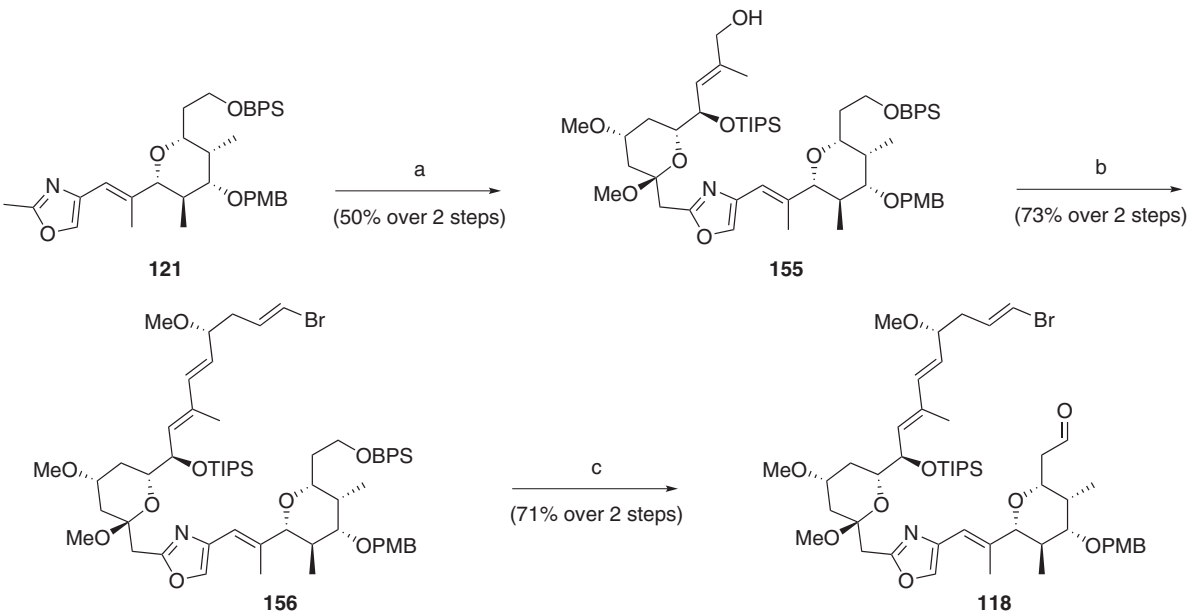


**Scheme 19** (a) (1) $LiNEt_2$, THF, −78 °C, then **120**; (2) PPTS, MeOH, 30 °C; (b) (1) Dess–Martin, $CH_2Cl_2$, pyr, RT; (2) **3**, NaHMDS, THF, −78 °C; (c) (1) $NH_4F$, MeOH, 50 °C; (2) Dess–Martin, $CH_2Cl_2$, pyr, RT.

hetero-Diels–Alder approach to the pentasubstituted pyran, installing four of the centers in a single transformation in good yield and excellent enantioselectivity (Scheme 23). Reduction of ketone **184** gave a solid that could be recrystallized to even higher enantiopurity, and cyanation of the corresponding acetal afforded the axial nitrile, which could be methylated to ketone **187**. Epimerization restored the desired C26 equatorial orientation, and installation of the oxazole resulted in the formation of the desired C20–C32 fragment.

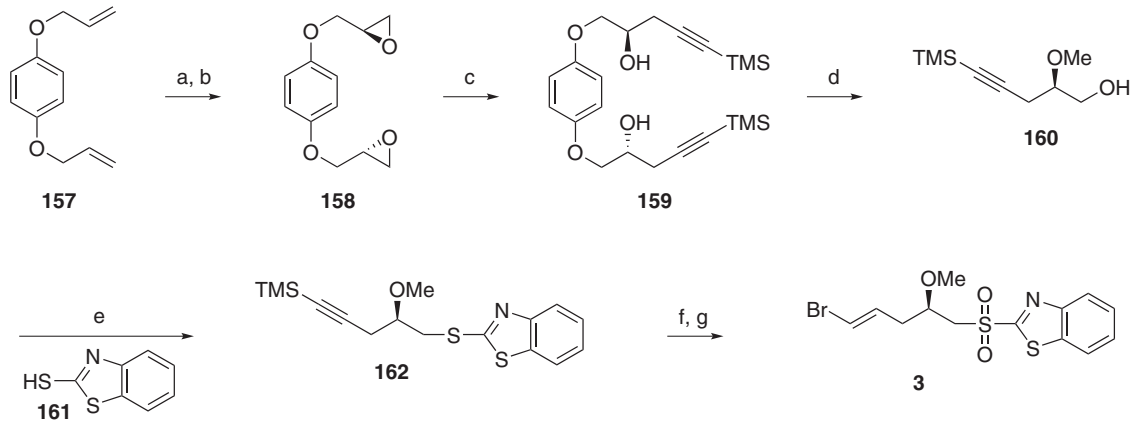


**Scheme 20** (a) AD-mix-α, *t*-BuOH/$H_2O$, RT, 87% ee, 66%; (b) (1) HBr, AcOH; (2) $K_2CO_3$, MeOH, 88%; (c) (1) $TMSC_2H$, BuLi, $BF_3OEt_2$, THF, −78 °C; (2) $Me_3OBF_4$, proton sponge, $CH_2Cl_2$, RT, 70% for two steps; (d) CAN, $CH_3CN/H_2O$, RT, 91%; (e) **161**, $PPh_3$, DEAD, THF, 0 °C, 81%; (f) TBAF, THF, RT, 99%; (g) (1) $Cp_2ZrHCl$, THF; then NBS; (2) $(NH_4)_6Mo_7O_{24}{\cdot}4H_2O$, 30% $H_2O_2$, EtOH, 56% for two steps.

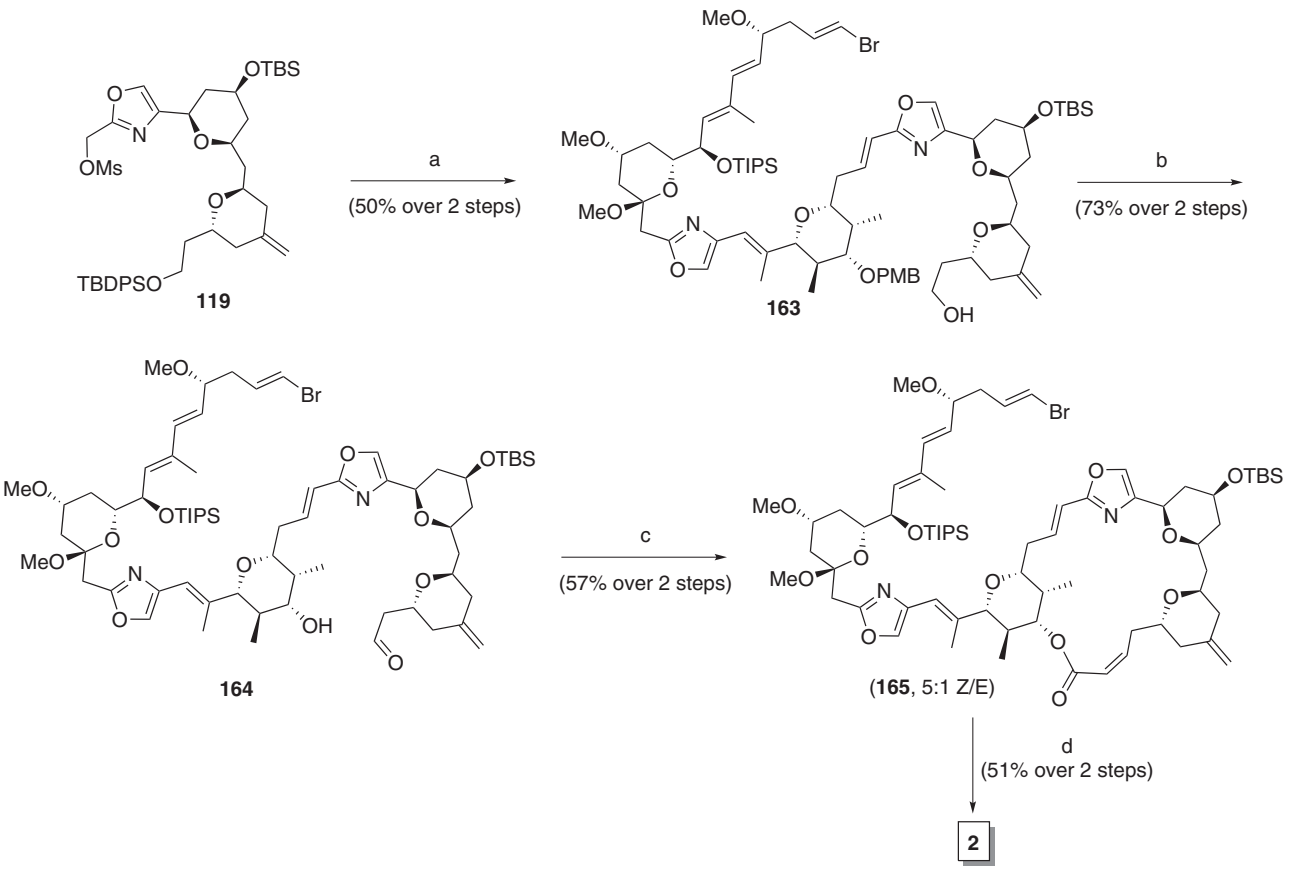


**Scheme 21** (a) (1) $Bu_3P$, DMF, then **118**, DBU, RT; (2) $NH_4F$, MeOH, 50 °C; (b) (1) Dess–Martin, pyr, $CH_2Cl_2$, RT; (2) DDQ, $CH_2Cl_2$, pH 7 buffer; (c) (1) $(EtO)_2P(O)CH_2CO_2H$, DCC, $CH_2Cl_2$; (2) $K_2CO_3$, 18-c-6, toluene, −20 °C; (d) TBAF, THF, RT; (2) 6% HCl, THF.

The exocyclic pyran was also prepared using a hetero-Diels–Alder cyclization which, under europium catalysis, returned **191** as a single diastereomer (Scheme 24). Hydrogenation set the C35 stereocenter and liberated the diol, which could be manipulated to selectively protected **169**. Lithiation of **121** and addition of **169** formed the C32–C33 bond (Scheme 25), and the peripheral triene moiety was realized via the established Wittig/Julia methodology. Selective deprotection of the primary alcohol allowed the Wittig extension to α,β-unsaturated acid **199**, which was coupled to amine **168** to provide the oxazole precursor. Wipf cyclodehydration achieved the oxazole formation, and the macrolide was closed via the Horner–Wadsworth–Emmons olefination (Scheme 26). Desilylation completed the synthesis of **2**.

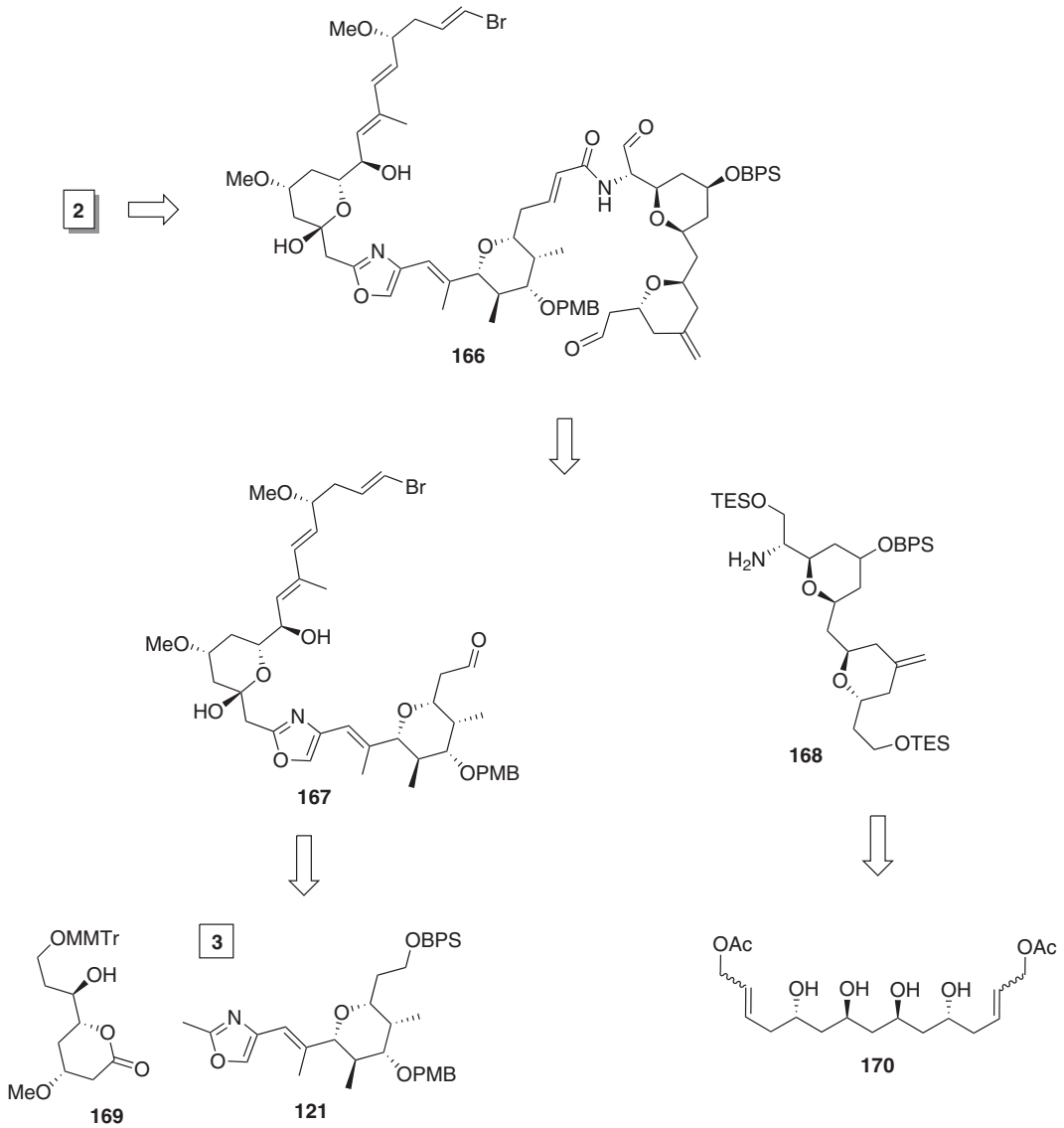


**Figure 11** Retrosynthetic analysis of Steve Burke's total synthesis of phorboxazole B.

**Additional synthetic approaches to the phorboxazoles**

*Phorboxazole macrolide.* Among the reported synthetic approaches to the phorboxazoles, only the Paterson group has published a completed macrolide.[10] The pentasubstituted pyran was assembled using the anti-aldol addition of chiral ketone **204** to aldehyde **62**, intramolecular Tishchenko reduction of the ketone and eventually Michael cyclization to the pyran (Scheme 27). The C5–C9 pyran was prepared via the Michael allylation of enone **17** to set the requisite *trans*-pyran with excellent diastereoselectivity (94% de) using allyl tributylstannane (Scheme 28), and the subsequent aldehyde was converted into the corresponding acetylenic ester **211**. Finally, the C9 side chain was deprotected and converted into siloxydiene **213** to set the stage for a second hetero-Diels–Alder cyclization. Following the Wittig coupling of **214** to **209**, this was achieved to provide a nearly 1:1 mixture of diastereomeric pyrans **217** and **217a** that proved resistant to improved diastereocontrol (Scheme 29). Reduction of ketone **218** followed by generation of the seco acid allowed for the Yamaguchi macrolactonization developed by Evans and synthesis of **220**.

The Hoffmann group recognized that the 8-oxabicyclo[3.2.1]octane ring system mapped well onto the phorboxazole pyrans, and exploited that in their approach.[24] Reduction of meso ketone **221** with L-Selectride and protection set the stage for the asymmetric hydroboration of the olefin with diisopinocampheylborane to give **223** in 96% ee (Scheme 30).[25] Oxidation to the ketone and subsequent Baeyer–Villiger ring expansion provided **225**, which underwent methanolysis to provide pyran acetal **226**. Allylation proceeded with excellent trans selectivity (>99% de), which set the stage for the elaboration to aldehyde **230**. The C11 stereocenter was introduced via asymmetric allylation, which allowed for the remaining elaboration of C3–C13 fragment **233**.

Hoffmann's approach to the pentasubstituted pyran started from the racemic dimethylated bicycle **234** (Scheme 31).[26] DIBAL reduction of the ketone and benzylation gave **235**, which underwent asymmetric hydroboration to a mixture of **236** and **237**. Both components of this mixture proved useful, as **236** was transformed into the C1–C7 portion of discodermolide while **237** was carried on toward the phorboxazoles.[27] Utilizing their PCC/Baeyer–Villiger

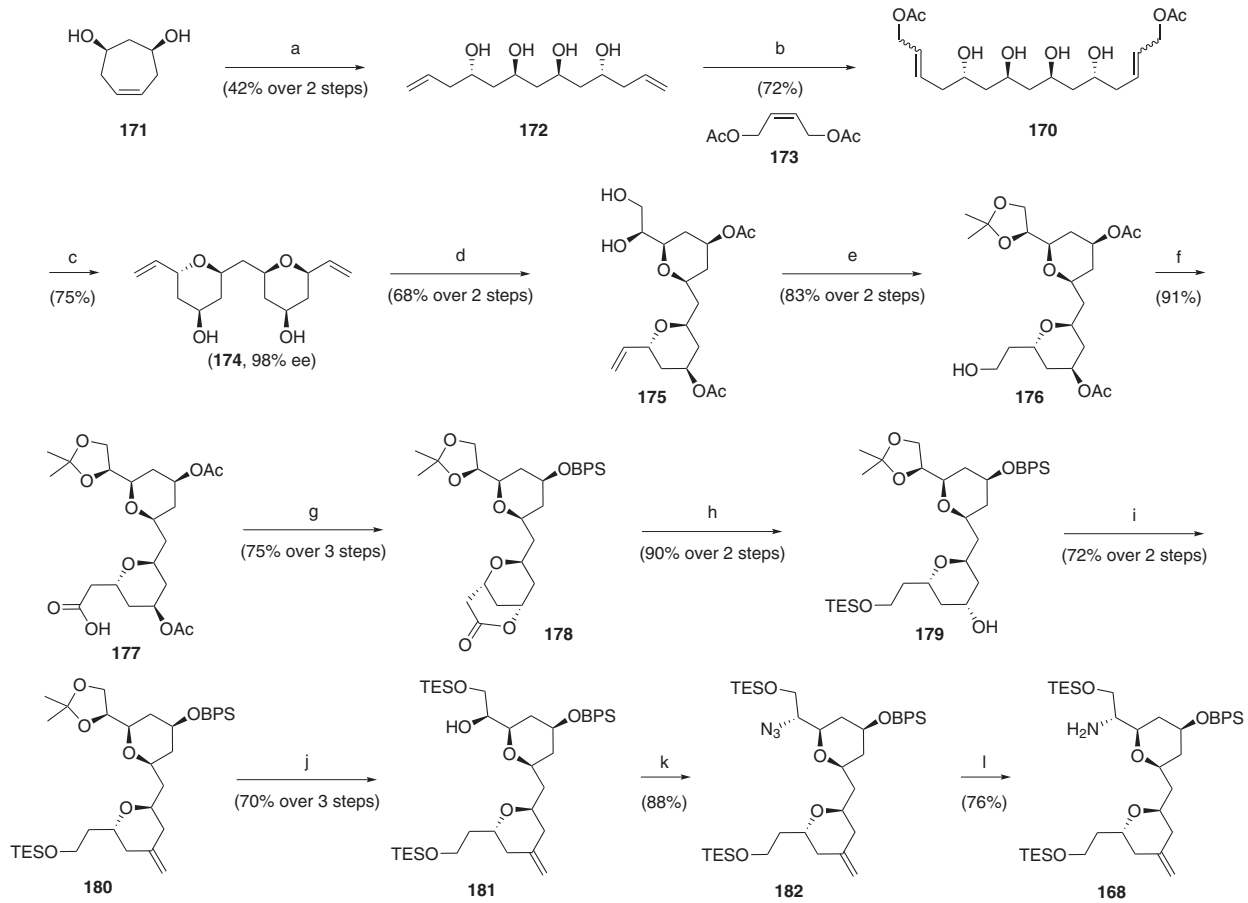


**Scheme 22** (a) (1) $O_3$, DMS, −78 °C to RT; (2) In, allyl bromide, $H_2O$, RT, 24 h; (b) **173**, Grubbs' second-generation, $CH_2Cl_2$:DMF (20:1), RT, 30 min; (c) $Pd_2$dba-$CHCl_3$ (2 mol%), (R,R),DPPBA (6 mol%), $Et_3N$, $CH_2Cl_2$, 0 °C; (d) (1) $Ac_2O$, DMAP, pyr, RT, 1 h; (2) AD-mix β, 0 °C, 3 h, (96% BORSM); (e) (1) 2,2-DMP, PPTS (cat.), 1,2-DCE, 40 °C, 30 min; (2) disiamylborane, RT, 1.5 h, $NaBO_3$, $H_2O$, RT, 1.5 h; (f) $RuCl_3$ (3 mol%), $NaIO_4$, 0 °C, 5 h; (g) (1) NaOH, MeOH, then Dowex CCR-3; (2) DIAD, $PPh_3$, THF, 1 h; (3) TBDPSCl, $Et_3N$, RT (h) (1) $LiBH_4$, THF, 0 °C; (2) TESCl, 2,6-lutidine, $CH_2Cl_2$; (i) (1) Dess–Martin, $CH_2Cl_2$, RT, 4 h; (2) $Cp_2TiMe_2$, THF/toluene, 80 °C; (j) 1) PTSA, MeOH, 40 °C; (2) TESCl, imidazole, −78 °C; (k) DEAD, $PPh_3$, $N_3$-$PO(OMe)_2$; (l) $PPh_3$, $H_2O$, THF, reflux.

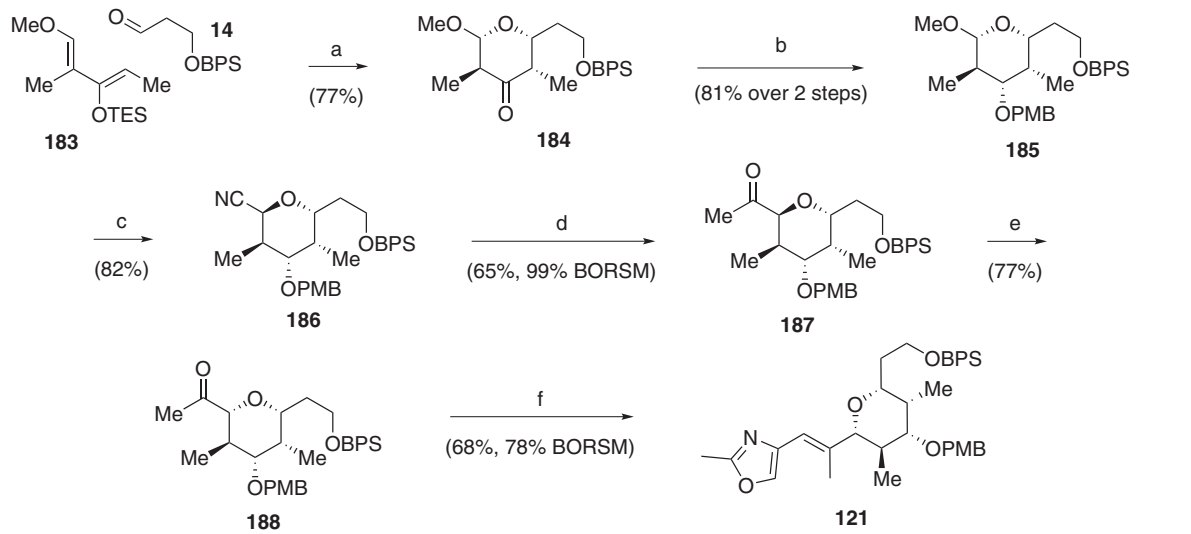


**Scheme 23** (a) **16** (2 mol%), RT, 14 h, then HF/pyr/MeOH, −20 °C, 15 min; (b) (1) $NaBH_4$, EtOH, −10 °C, 15 min (98.5% ee after recrystallization); (2) PMB-Cl, KH, RT, 2 h; (c) 0.5 eq. THM-OTf, TMS-CN, MeCN, 0 °C 2 h; (d) $AlMe_3$ 5% $Ni(acac)_2$, 0 °C, 42 h; (e) KHMDS, LiCl, $PhCH_3$, 55 °C 2 h, 91%; (f) **145**, LDA, THF, −78 °C to RT.

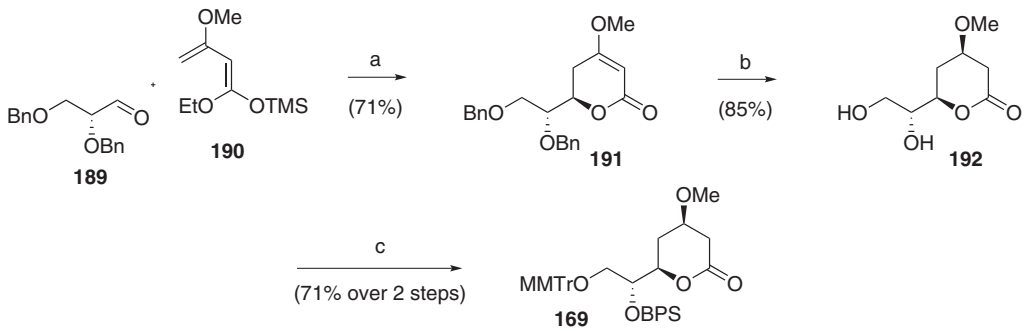


**Scheme 24** (a) [Eu(fod)$_3$], $CH_2Cl_2$, 0 °C; (b) Pd-C, $H_2$, EtOAc; (c) (1) MMTr-Cl, pyr, DMAP; (2) TBDPSCl, $AgNO_3$, pyr, 50 °C.

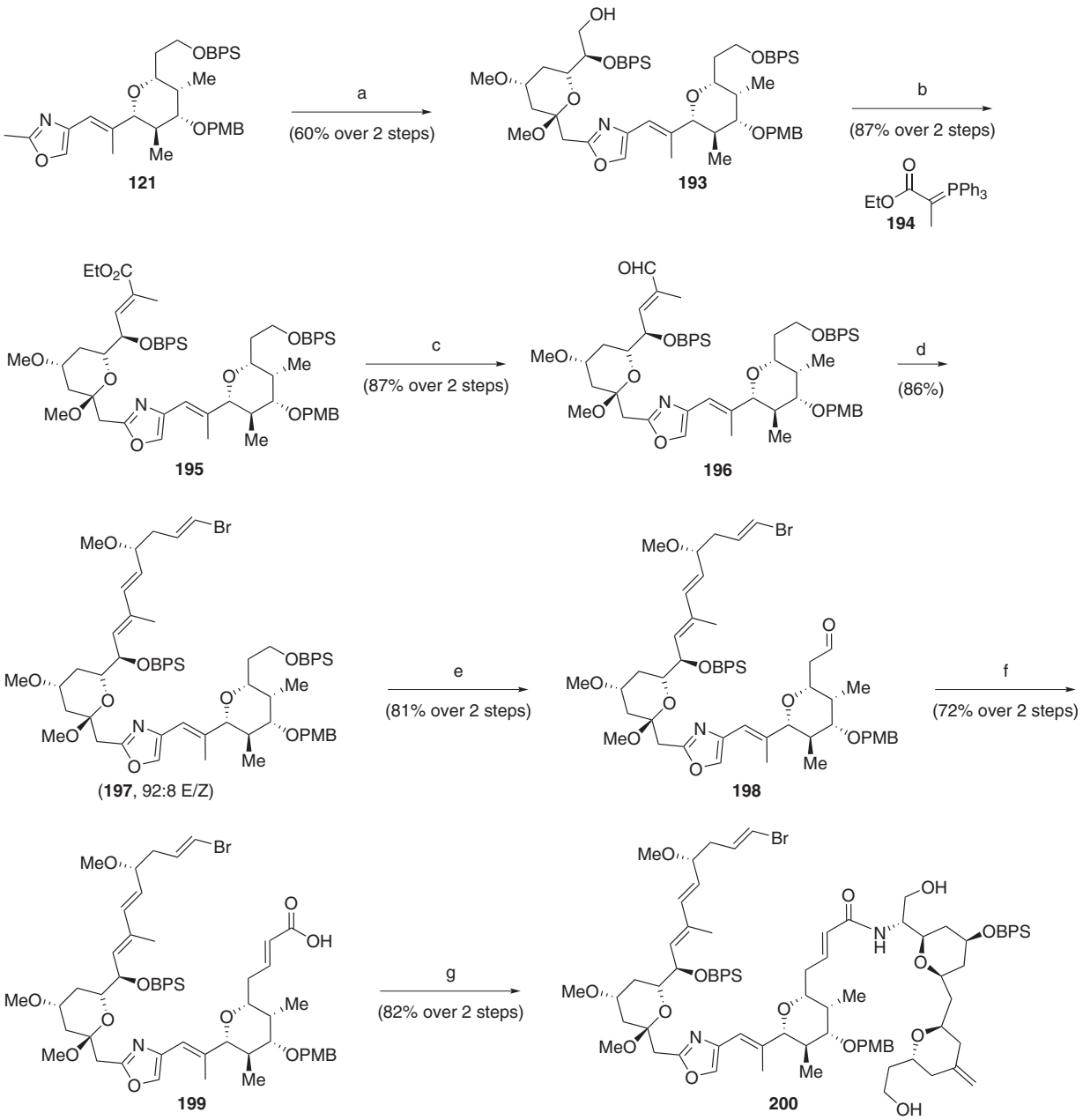


**Scheme 25** (a) (1) $LiNEt_2$, **169**, THF, −78 °C; (2) PPTS, MeOH; (b) (1) Dess–Martin, $CH_2Cl_2$; (2) **194**, toluene, 80 °C; (c) (1) DIBAL-H, $CH_2Cl_2$, −78 °C; (2) Dess–Martin, $CH_2Cl_2$, 2,6-lutidine; (d) **3**, NaHMDS, THF, −78 °C to RT; (e) (1) PTSA, MeOH, MeOH; (2) Dess–Martin, $CH_2Cl_2$; (f) (1) $Ph_3PCHCO_2Et$, toluene, 80 °C; (2) LiOH, THF/MeOH/$H_2O$ (4:1:1); (g) **168**, EDC-MeI, HOBt, $CH_2Cl_2$.

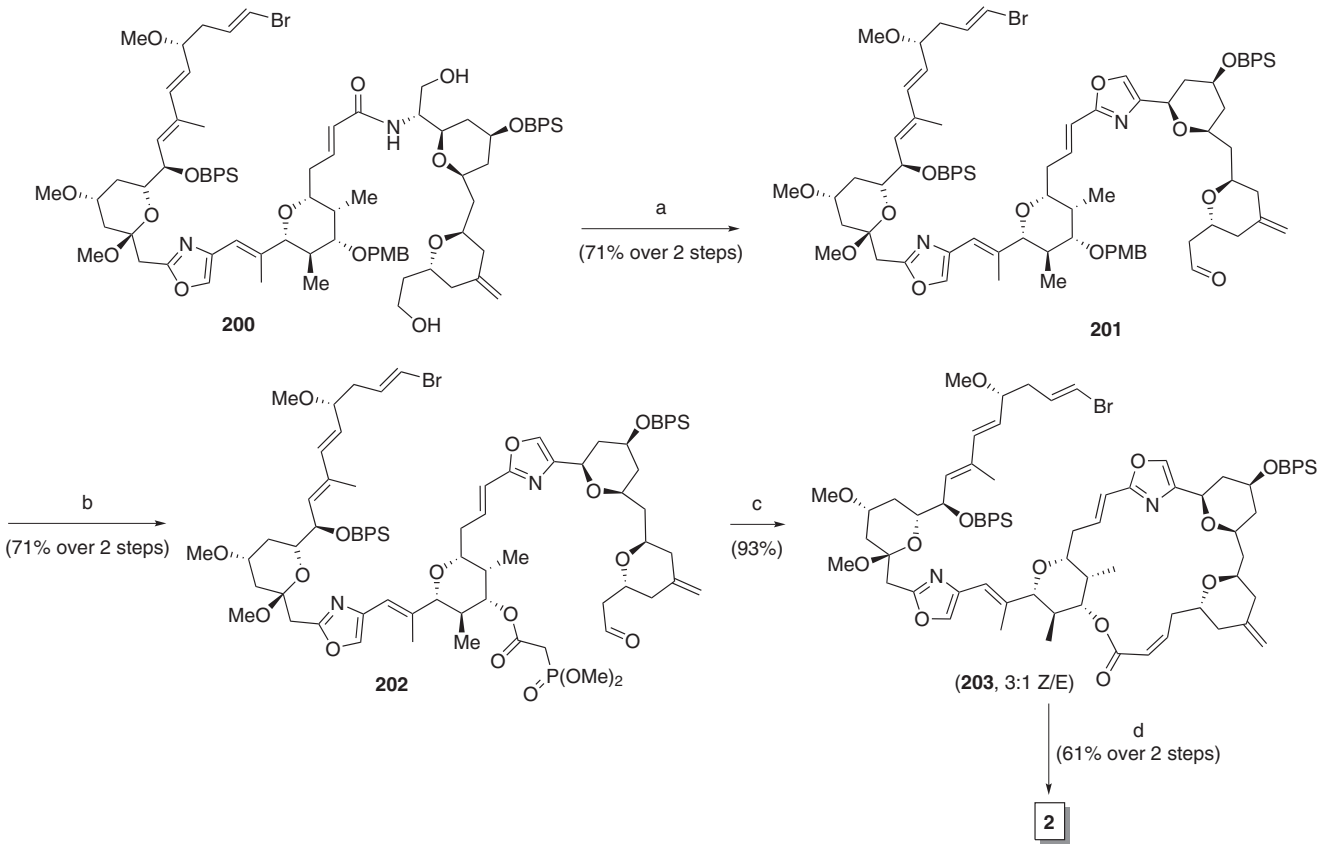


**Scheme 26** (a) (1) Dess–Martin, $CH_2Cl_2$; (2) 2,6-DBMP, $PPh_3$, $(CCl_2Br)_2$, 0 °C, then DBU, MeCN, RT; (b) (1) DDQ, $CH_2Cl_2$, pH 7 buffer; (2) DIC, $(MeO)_2P(O)CH_2CO_2H$, $CH_2Cl_2$; (c) $K_2CO_3$, 18-c-6, toluene, −40 °C to RT; (d) (1) TBAF, THF; (2) 0.72 N HCl, THF RT, 60 h.

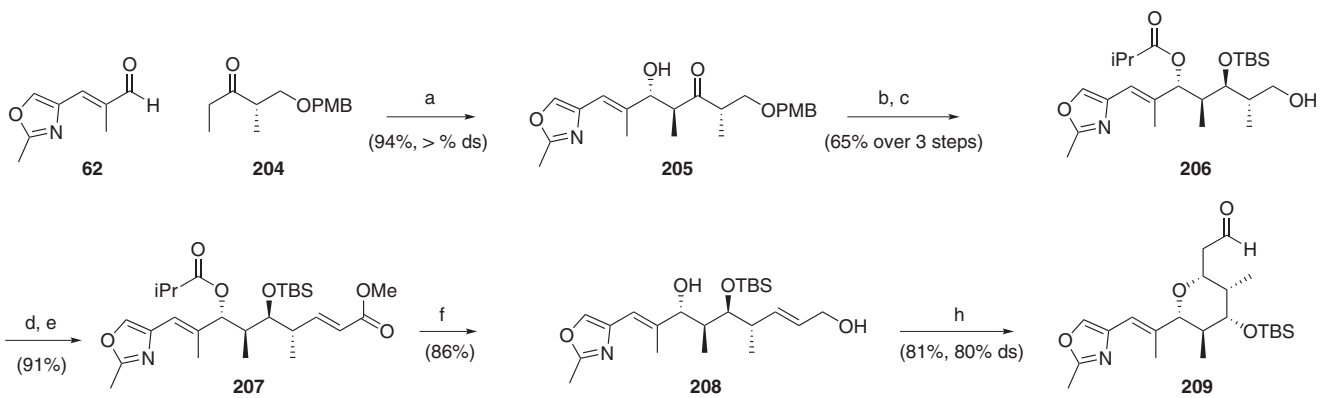


**Scheme 27** (a) $(c\text{-Hex})_2BCl$, $Et_3N$, $Et_2O$, 0 °C, 1 h; **62**, −78 to −20 °C, 18 h; $H_2O_2$, MeOH, pH 7 buffer; (b) $SmI_2$ (30 mol%), iPrCHO, THF, −20 °C; (c) (1) TBSCl, Imidazole, DMAP, DMF, 80 °C, 50 h; (2) DDQ, 20:1 $CH_2Cl_2/H_2O$, 20 °C; (d) $(COCl)_2$, DMSO, −78 °C, 10 min, −78°C, 1 h; $Et_3N$, −78 to −40 °C, 40 min; (e) LiCl, DBU, $(MeO)_2P(O)CH_2CO_2Me$, 4:1 $CH_3CN/CH_2Cl_2$, 20 °C, 2.5 h; (f) DIBAL, $CH_2Cl_2$, −78 °C, 5 h; (h) $SO_3$-pyr, $Et_3N$, 2:1 $CH_2Cl_2$/DMSO, 0 °C, 2 h.

protocol, Hoffmann synthesized **238**, which was elaborated to acrylonitrile **241** and subjected to rhodium catalyzed oxazole cyclization. Finally, LAH reduction simultaneously reduced the oxazole β-methoxy substituent and the ester to provide the C15–C26 fragment.

Yadav initiated his synthetic approach to the macrolide portion from vinyl furan **244**, readily available from D-glucose (Scheme 32),[28] which provided the C13 and C15 stereocenters of phorboxazole A.[29] It is notable that D-galactose would correspond to the phorboxazole B stereochemistry. Upon opening the furan, the olefin was extended via a hydroboration/oxidation/Wittig sequence, and Michael addition of the secondary alcohol of **249** formed *cis*-pyran **250**. Asymmetric allylation followed by acylation with acryloyl chloride gave **252**, which was closed with first-generation Grubbs catalyst to lactone **253**. Reduction to the ethyl acetal and Lewis acid mediated allylation yielded expected *trans*-pyran **255**, which represents the C2–C16 portion of phorboxazole A.

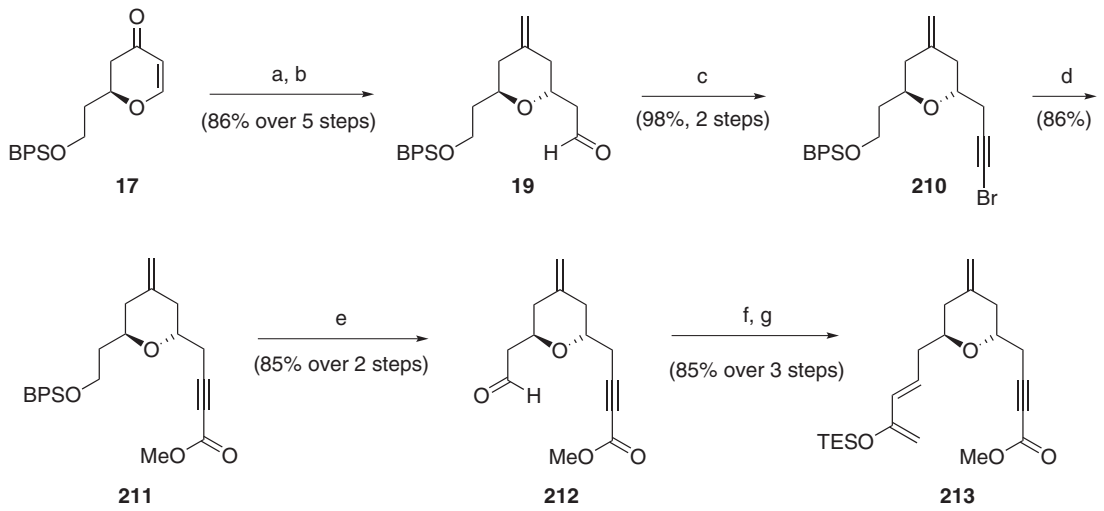


**Scheme 28** (a) (1) $H_2C=CHCH_2SnBu_3$, TMSOTf, $CH_2Cl_2$, −78 to −50 °C; (2) TBAF (1 M THF). AcOH (10:1, v/v), THF, 0 °C; (b) (1) $OsO_4$ (4 mol%), NMO, *t*-BuOH-THF-$H_2O$ (4:4:1); (2) $Ph_3P=CH_2$, THF, −40 to −20 °C; (3) $Pb(OAc)_4$, $Na_2CO_3$, $CH_2Cl_2$, 0 °C to RT; (c) (1) $CBr_4$, $Ph_3P$, $CH_2Cl_2$, −10 °C; (2) NaHMDS, THF, −98 °C; (d) (1) *n*-BuLi, THF, −78 °C, (2) MeOC(O)Cl, HMPA; (e) (1) HF. py, MeCN, 0 °C; (2) DMP, $CH_2Cl_2$; (f) $MeC(O)CH_2P(O)(OMe)_2$, $Ba(OH)_2{\cdot}xH_2O$, THF; (g) TESOTf, $Et_3N$, $Et_2O$, 0 °C.

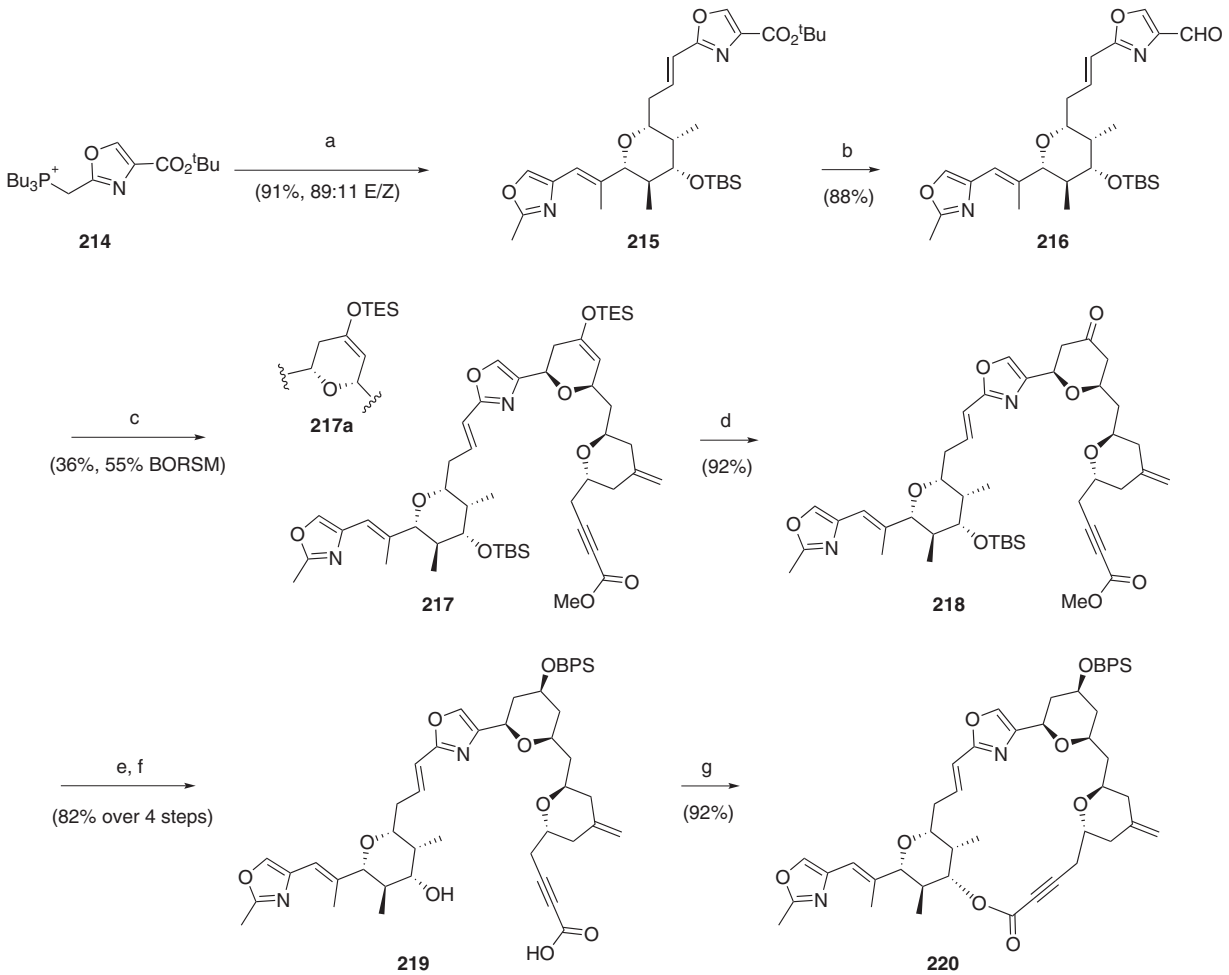


**Scheme 29** (a) LiHMDS, DMF, 0 °C, 30 min, then **209**, DMF, 0 °C, 1 h; (b) DIBAL-H, $CH_2Cl_2$, −78 °C; (c) **213**, HDA cat. (10 mol%), 4 A molecular sieves; (d) TBAF-AcOH (1:2, mol/mol), THF, 0 °C; (e) $LiAl(OtBu)_3H$, THF, −78 to −10 °C (2) BPSCl, imidazole, DMF; (f) conc. HCl (1%), MeOH; (2) LiOH . $H_2O$, THF, $H_2O$; (g) 2,4,6-trichlorobenzoyl chloride, $Et_3N$, THF, (2) DMAP, PhMe.

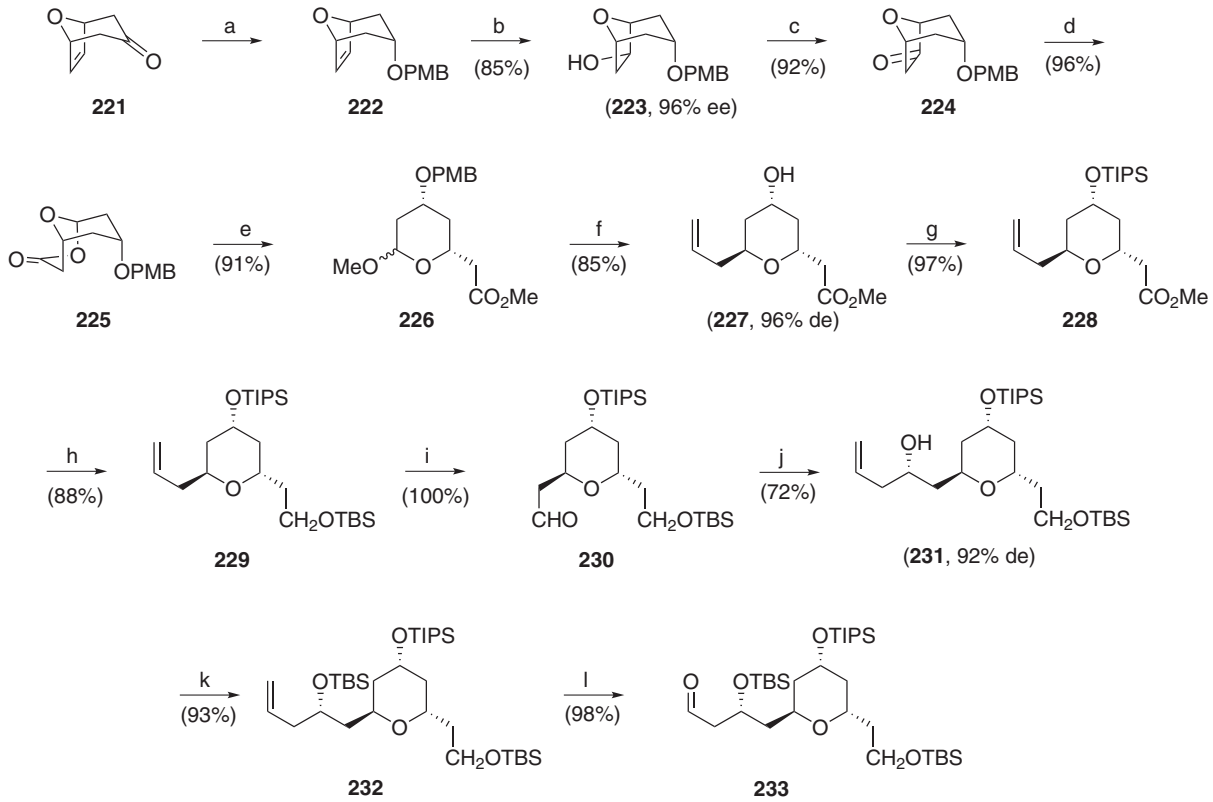


**Scheme 30** (a) (1)[24]; (2) NaH, PMBCl, (n-Bu)$_4$NI, THF, reflux, 6 h; (b) (+)-Ipc$_2$BH, THF, −10 °C, 1 week; (c) PCC, DCM, RT, 5 h; (d) m-CPBA DCM, RT, overnight; (e) MeOH, conc. $H_2SO_4$ (cat.), RT, overnight; (f) allyltrimethylsilane, TMSOTf, MeCN, −20 °C to RT, 1 h; (g) TIPSCl, imidazole, DMF, RT, 16 h; (h) (1) DIBAL-H, −20 °C, THF, 2 h; (2) TBSCl, imidazole, DMF, RT, 16 h; (i) $O_3$, DCM, −78 °C then $PPh_3$ (j) (−)B-allyl-β-diisopinocampheyl-borane, toluene, −78 °C, 5 h then $H_2O_2$, NaOH; (k) TBSOTf, 2,6-lutidine, DCM, 0 °C, 30 min; (l) $O_3$, DCM, −78 °C then $PPh_3$.

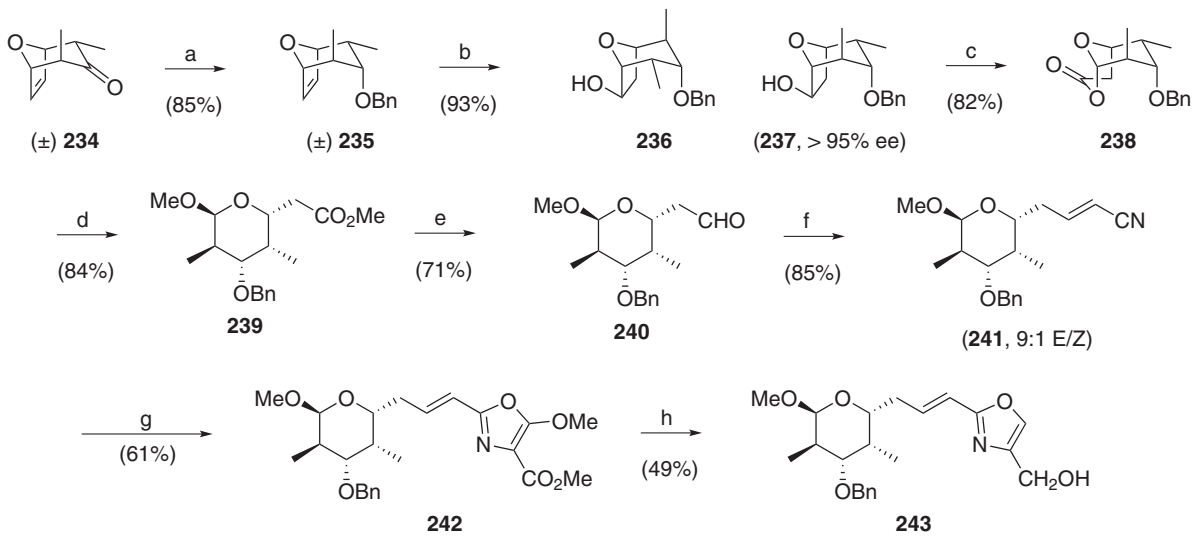


**Scheme 31** (a) (1) DIBAL-H, THF, −78 °C, 11 h; (2) NaH, THF, BnBr, reflux, 16 h; (b) (−)-(Ipc)$_2$BH, THF, −10 °C, 14 d, then NaOH, $H_2O_2$, 3 h; (c) (1) PCC/$SiO_2$, DCM, RT, 15 h; (2) m-CPBA, $NaHCO_3$, DCM, RT, 15 h; (d) $H_2SO_4$ (cat.), MeOH, 16 h; (e) (1) DIBAL-H, THF, 0 °C, 4 h; (2) PCC, DCM, RT, 15 h; (f) $Ph_3PCHCN$, toluene, LiCl, RT, 20 h; (g) $N_2C(CO_2Me)_2$, $Rh_2(OAc)_4$, $CHCl_3$, 15 h, reflux; (h) $LiAlH_4$, THF, −78 °C, 3 h.

Yadav also prepared the pentasubstituted pyran from the 8-oxabicyclo[3.2.1]octane ring system, starting from the asymmetric hydroboration of achiral dimethylated derivative **256** (Scheme 33).[30] Ring opening of Baeyer–Villiger lactone **258** revealed pyran **259** which, upon protection of the C20 Wittig precursor as a benzyl ether, was oxidized to lactone **262.** This allowed for the epimerization of the C25 methyl using DBU with excellent selectivity and conversion. The C27 side chain was then introduced via acetylenation, and hemiketal

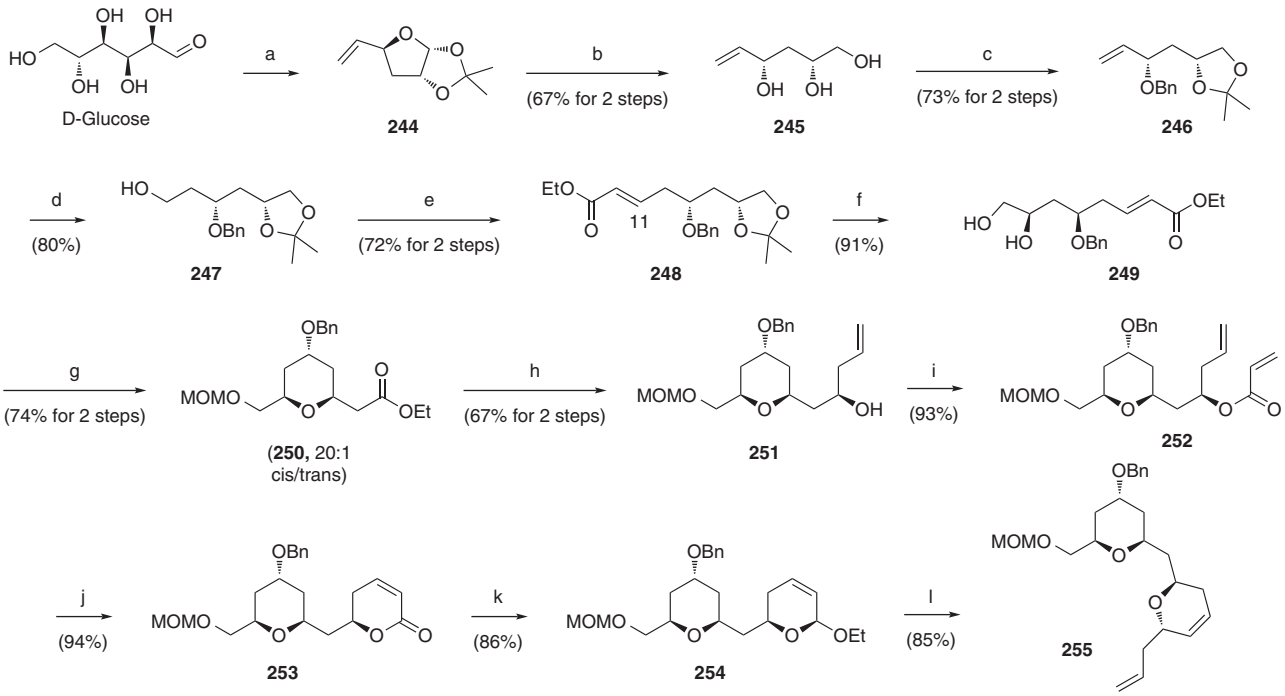


**Scheme 32** (a)[27]; (b) (1) 50% AcOH, $H_2SO_4$ (cat.), 2 h; (2) $NaBH_4$, MeOH, 0 °C to RT, 1 h; (c) (1) PTSA (cat.), acetone, RT, 3 h; (2) NaH, BnBr, THF, reflux, 8 h; (d) $BH_3$-DMS, NaOH, $H_2O_2$, THF, 8 h; (e) (1) IBX, THF, DMSO, RT, 2 h; (2) $Ph_3P{=}CHCO_2Et$, benzene, RT, 12 h; (f) CSA, MeOH, RT, 2 h; (g) (1) NaH, THF, −78 °C, 4 h; (2) $iPr_2NEt$, MOMCl, $CH_2Cl_2$, 0 °C, 6 h. (h) (1) DIBAL-H, $CH_2Cl_2$, −78 °C, 1 h; (2) (+)-allyl diisopinocampheylborane, $Et_3N$, $H_2O_2$, 1 h; (i) $iPr_2NEt$, acryoyl chloride, $CH_2Cl_2$, 0 °C to RT, 4 h; (j) Grubb's 1st gen., $Ti(iOPr)_4$, $CH_2Cl_2$, 60 °C, 6 h; (k) DIBAL-H, $CH_2Cl_2$, −78 °C, 30 min then CSA, EtOH; (l) allyltrimethyl silane. TMSOTf, $CH_2Cl_2$, 0 °C, 1 h.

reduction gave the elaborated pyran as a single isomer. Oxymercuration then gave ketone **265**. The oxazole was introduced via a modified Julia olefination of **265** with sulfone **266** (Scheme 34), giving C20–C32 fragment **267** as a 9:1 mixture of olefin isomers.

The synthesis of the bis pyran was also achieved by the Rychnovsky group using their expertise with the Prins reaction.[31] Epoxide **268** was opened with the lithium anion of **269** to give diol **270**, which was smoothly closed to the pyran and extended to *trans* thioester **273** (Scheme 35). The C11 stereocenter was formed via reduction to the aldehyde and asymmetric allylation. Acylation of the C11 alcohol with oxazole **275** and conversion to the α-acetoxyether generated the Prins precursor, which proceeded as expected to the *cis*-pyran, representing the C3–C19 portion of phorboxazole B. Rychnovsky showed that the Prins cyclization could also be achieved to install the C11 stereocenter, but the yields were diminished presumably due to the proximity of the oxazole nitrogen.

The Prins reaction was also used by Rychnovsky to make the pentasubstituted pyran as well.[32] Asymmetric crotylation of aldehyde **14** with **278** gave **279** in 98% ee (Scheme 36), setting the C22 stereocenter. Acylation with protected lactic acid yielded **281**, which was transformed into Prins precursor **282** in standard fashion. This cyclization proceeded as expected with catalytic $BF_3$ etherate to set the remaining stereocenters of the pyran. Elaboration to ketone **284** was followed by Horner Wadsworth Emmons olefination to afford the C20–C29 fragment as a 3.9:1 mixture of olefin isomers.

The Clarke group also used the macrolide pyrans as a showcase for their work on the asymmetric Maitland–Japp reaction. Toward this end, diketene was able to be coupled to aldehyde **287** (setting the C11 stereocenter) and oxazole aldehyde **61** in a one-pot transformation using Ti(IV) and chiral ligand **295** to prepare pyranone **289** as a mixture of C15 epimers in 73% ee (Scheme 37).[33] The *trans* isomer could be converted to the desired *cis* isomer with $Yb(OTf)_3$. Decarboxylation, reduction and protection thus gave pyran **290**, which was converted to the aldehyde and subjected to a second Maitland–Japp reaction using Chan's diene and Evans' pybox ligand, which established the *trans* pyran ring with excellent stereocontrol and complete enantiomeric enrichment. Once the exocyclic olefin at C7 was introduced, the primary alcohol was liberated and activated for displacement with an acetylenic anion. Radical bromination of the oxazole methyl finally gave C1–C19 fragment **294** functionalized for further elaboration.

Clarke's initial efforts to utilize the Maitland–Japp reaction to generate the pentasubstituted pyran resulted in a C23-epimeric product, so he ultimately initiated his synthesis of the remainder of the macrolide fragment using the anti-aldol addition of **296** to **62** (Scheme 38).[34] Reductive removal of the chiral auxiliary followed silylation of the C26 alcohol, which allowed for outstanding Felkin–Ahn control of the subsequent crotyl addition. Acrylate **300** was added via a metathesis reaction, which set the stage for the Michael cyclization (13:1 selectivity) to the C20–C32 fragment.

Taylor was able to demonstrate that his electrophile-induced ether transfer methodology allowed access to the bis-pyran portion of **1** (Scheme 39).[35] Ether transfer of the BOM-protected analog of **28** with ICl conferred the C5 stereocenter with exquisite control (20:1), and the subsequent sulfone (**303**) could be cyclized and allylated to the *trans* pyran nearly quantitatively. Following elaboration to aldehyde **305**, allylation gave a 1:1 mixture of C11 alcohols that could be separated and completely converted into the desired **306** via

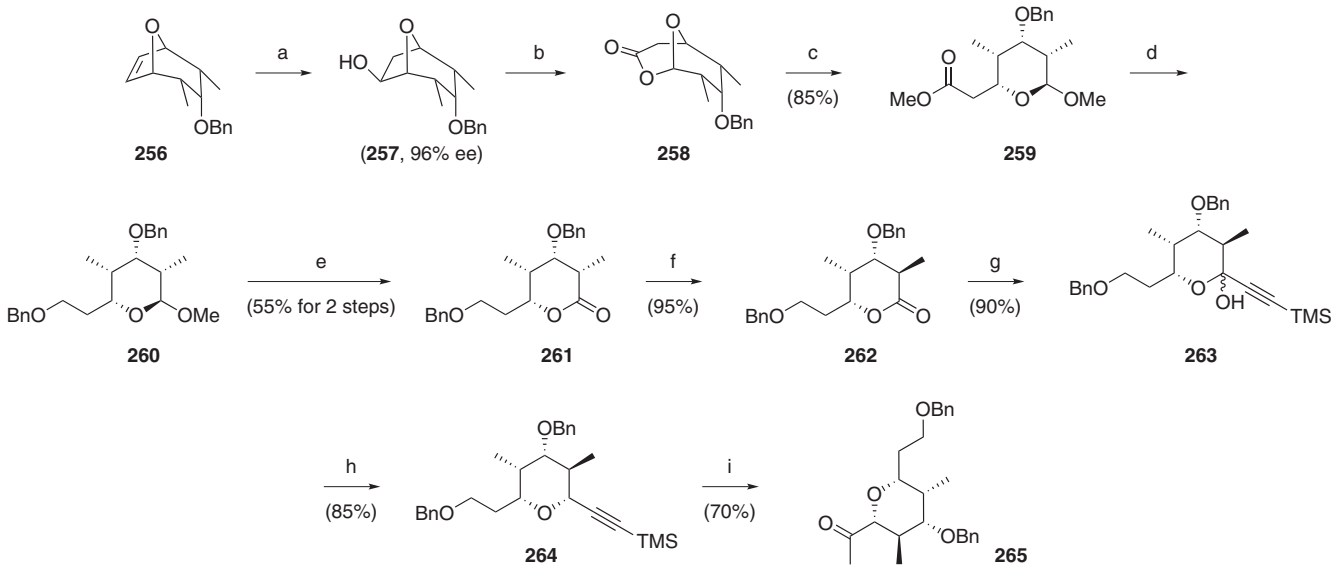


**Scheme 33** (a) (–)-Ipc$_2$BH, THF, –23 °C, 24 h, NaOH (3N), 30% $H_2O_2$, RT, 6 h; (b) (1) PCC, $CH_2Cl_2$, RT, 3 h; (2) m-CPBA, $NaHCO_3$, $CH_2Cl_2$, RT, 10 h; (c) $H_2SO_4$-MeOH, 0 °C to RT, 12 h; (d) (1) $LiAlH_4$, THF, 0 °C to RT, 6 h; (2) BnBr, NaH, THF, RT, 12 h; (e) (1) AcOH-$H_2O$ (3:2), 55 °C, 15 h; (2) PCC, NaOAc, celite, RT, 3 h; (f) DBU, THF, RT, 12 h; (g) *n*-BuLi, TMS-acetylene, THF, –78 °C, 1.5 h; (h) $Et_3SiH$, $BF_3$-$Et_2O$, MeCN/$CH_2Cl_2$ (1:1), –40 °C, 2 h; (i) HgO, $H_2SO_4$, acetone, 50 °C, 1 h.

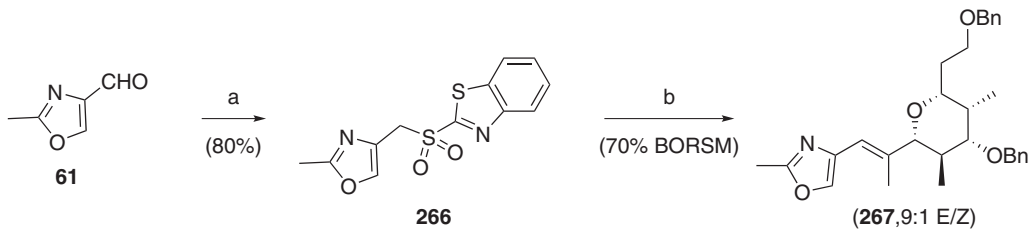


**Scheme 34** (a) (1) **161**, $PPh_3$, DEAD, THF, RT, 12 h; (2) oxone, THF-MeOH-$H_2O$ (2:1:1), 12 h; (b) NaHMDS, THF, –78 °C to RT, 4 h; **265**.

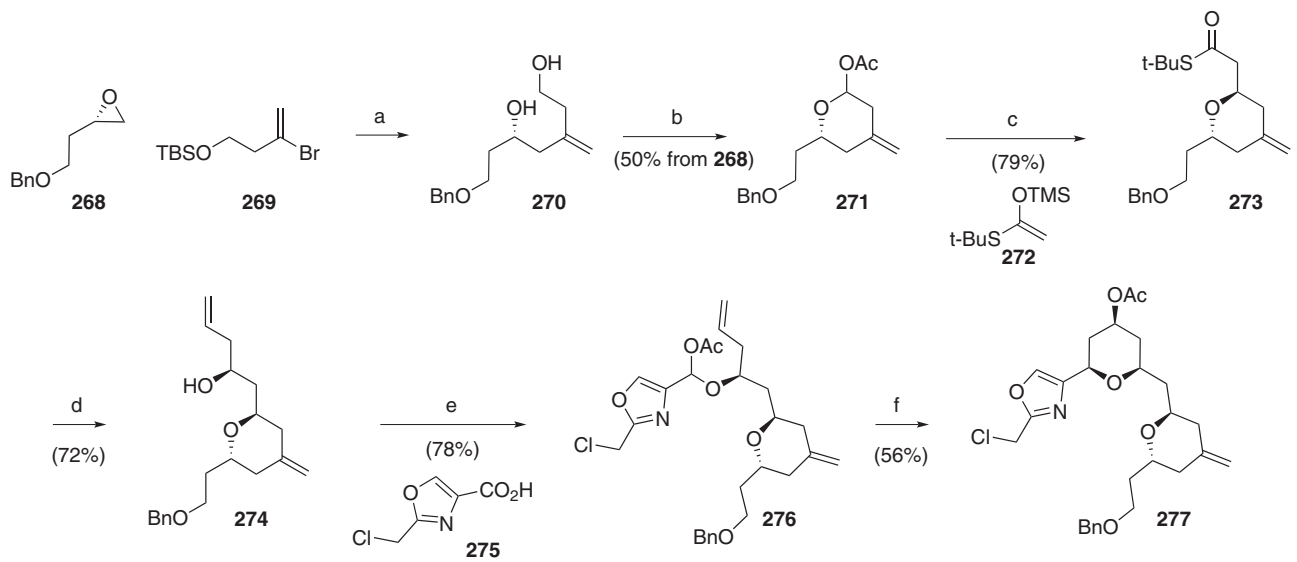


**Scheme 35** (a) (1) *n*-BuLi, $BF_3OEt_2$, THF, –94 °C; (2) TBAF, THF; (b) (1) IBX, DMSO; (2) $Ac_2O$, DMAP, pyridine; (c) TMSOTf, **272**, $CH_2Cl_2$, –78 °C; (d) (1) DIBAL-H; (2) (–)-Ipc$_2$B-allyl, $Et_2O$, –100 °C; (3) NaOH, $H_2O_2$; (e) (1) **275**, DCC, DMAP; (2) DIBAL-H; (3) $Ac_2O$, DMAP, pyridine; (f) (1)TMSBr, $CH_2Cl_2$; (2) CsOAc, 18-c-6, benzene.

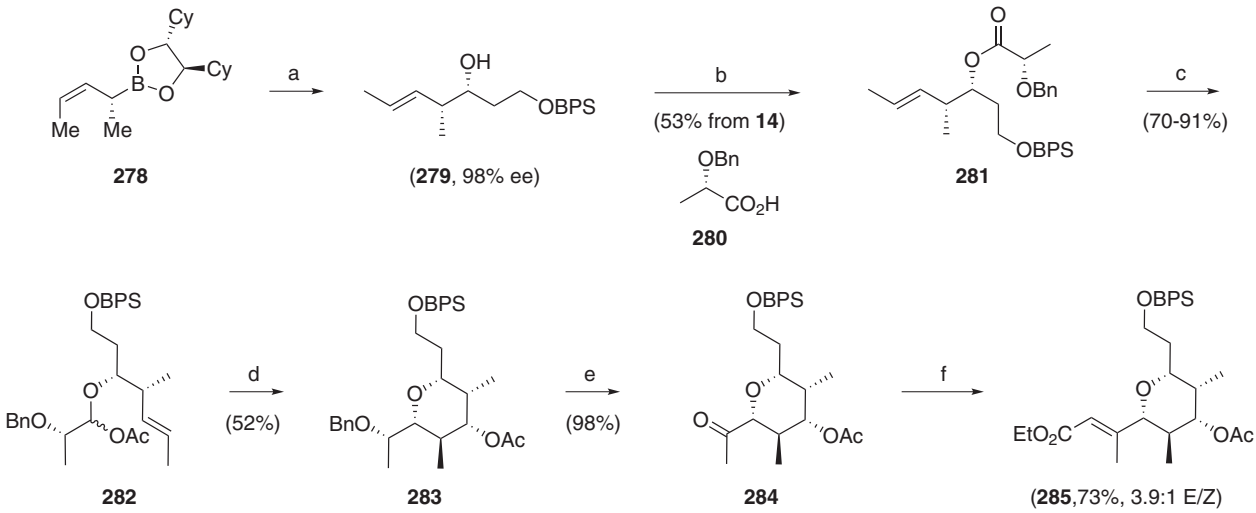


**Scheme 36** (a) **14**, 0 °C 3 d; (b) DCC, $CH_2Cl_2$, **280**, (c) (1) DIBAL-H, −78 °C, (2) $Ac_2O$, pyr, DMAP; (d) 0.1 eq. $BF_3OEt_2$, HOAc, hexanes, 140 min, 0 °C; (e) (1) $H_2$, $Pd(OH)_2/C$; (2) Swern Ox.; (f) KHMDS, $(EtO)_2P(O)CH_2CO_2Et$, THF, 25 °C.

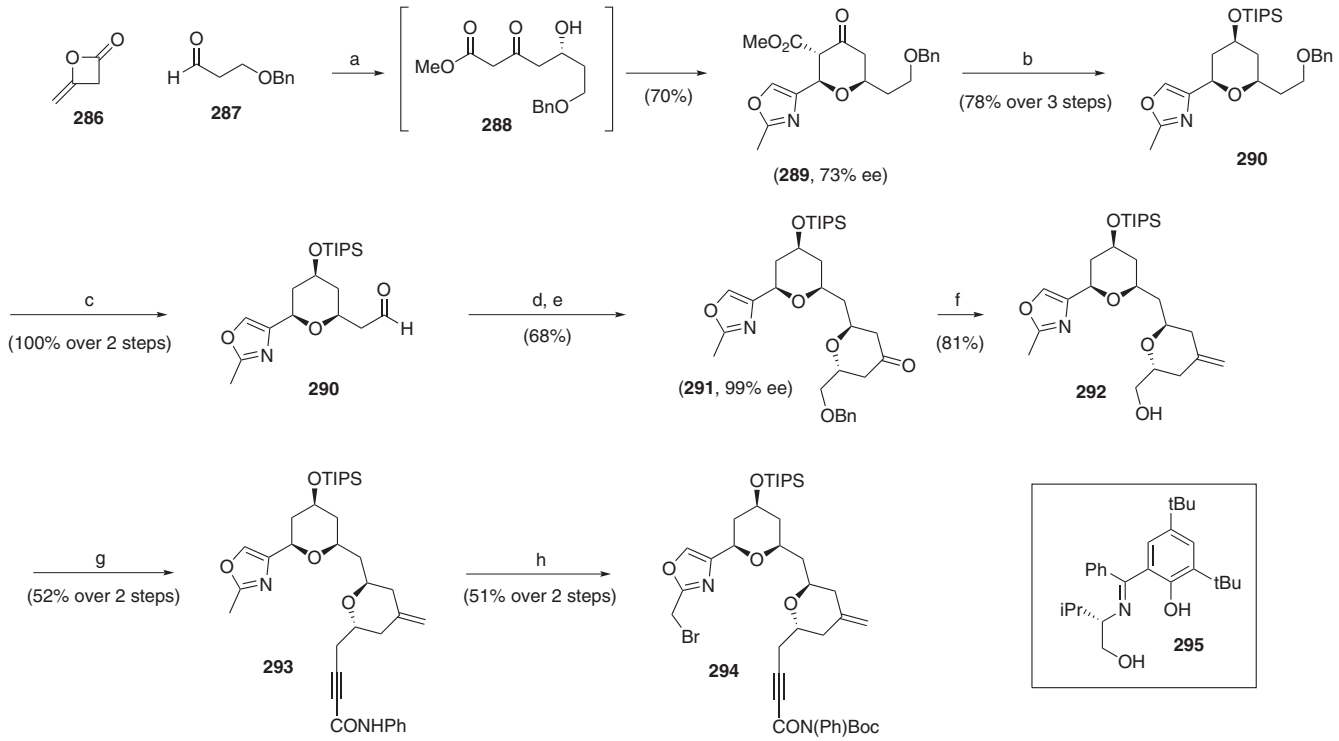


**Scheme 37** (a) $Ti(OiPr)_4$, **295**, MeOH, $CH_2Cl_2$, −78 °C, then **61**, $TiCl_4$, −78 °C to RT; (b) (1) DMF, $H_2O$, mw (300 W), 160 °C, 10 min; (2) $NaBH_4$, MeOH, 0 °C, (3) TIPSCl, imidazole, DMF, 50 °C; (c) (1) 10% Pd-C, $H_2$, MeOH; (2) Dess–Martin, $CH_2Cl_2$; (d) ent-**288**, $TiCl_4$, $CH_2Cl_2$, −20 °C to RT; (e) DMF, $H_2O$, mw (300 W), 160 °C; (f) (1) 10% Pd-C, $H_2$, MeOH (2) $Ph_3PCH_3^+Br^-$, LDA, THF; (g) (1) $Tf_2O$, pyr; (2) PhHNOCCCH, LDA, THF; (h) (1) $Boc_2O$, pyr, DMAP, $CH_2Cl_2$; (2) LDA, NBS, THF, −100 to −78 °C.

Mitsunobu inversion. Ether transfer again selectively introduces the C13 stereocenter of phorboxazole A, and cyclization leads to the C3–C17 fragment **308**.

Donaldson also explored the use of a hetero-Diels–Alder approach to the phorboxazoles (Scheme 40).[36] Allylation of acetal **309** provided the *trans* pyran, and the resulting aldehyde was subjected to asymmetric allylation to create the separable diasteromers **314** and **315**. The initial attempts to elaborate the second pyran via another hetero-Diels–Alder reaction proved possible but ultimately not as productive. Acryloylation of **314** followed by RCM gave the C3–C15 fragment.

The Panek group used their crotylsilane chemistry to approach the phorboxazoles.[37] Treatment of **317** (available in any isomeric form via Sharpless epoxidation) with aldehyde **318** gave *cis*-pyran **319** (Scheme 41) as a single diastereomer. Epoxidation and reduction of the ester set the stage for the selective methylation, which was achieved in excellent

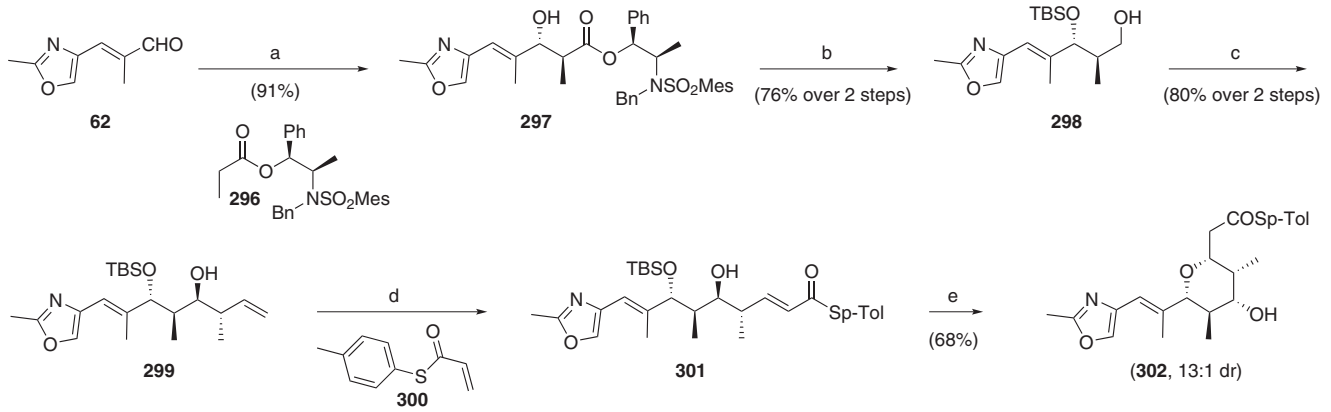


**Scheme 38** (a) **296**, $Et_3N$, (c-hex)$_2$BOTf, $CH_2Cl_2$, −78 °C, 3 h, then **62**; (b) (1) TBSOTf, 2,6-lutidine, $CH_2Cl_2$, 1 h; (2) DIBAL-H, $CH_2Cl_2$, 0 °C, 15 min; (c) Dess–Martin, $CH_2Cl_2$, 0 °C to RT, 1 h; (2) E-crotylboronic pinacol ester, hexane, 0 °C to RT, 17 h; (d) **301**, Grubb's second generation (30 mol%), CuI (20 mol%), $Et_2O$, reflux, 3 h; (e) TFA, $CH_2Cl_2$, $H_2O$, RT.

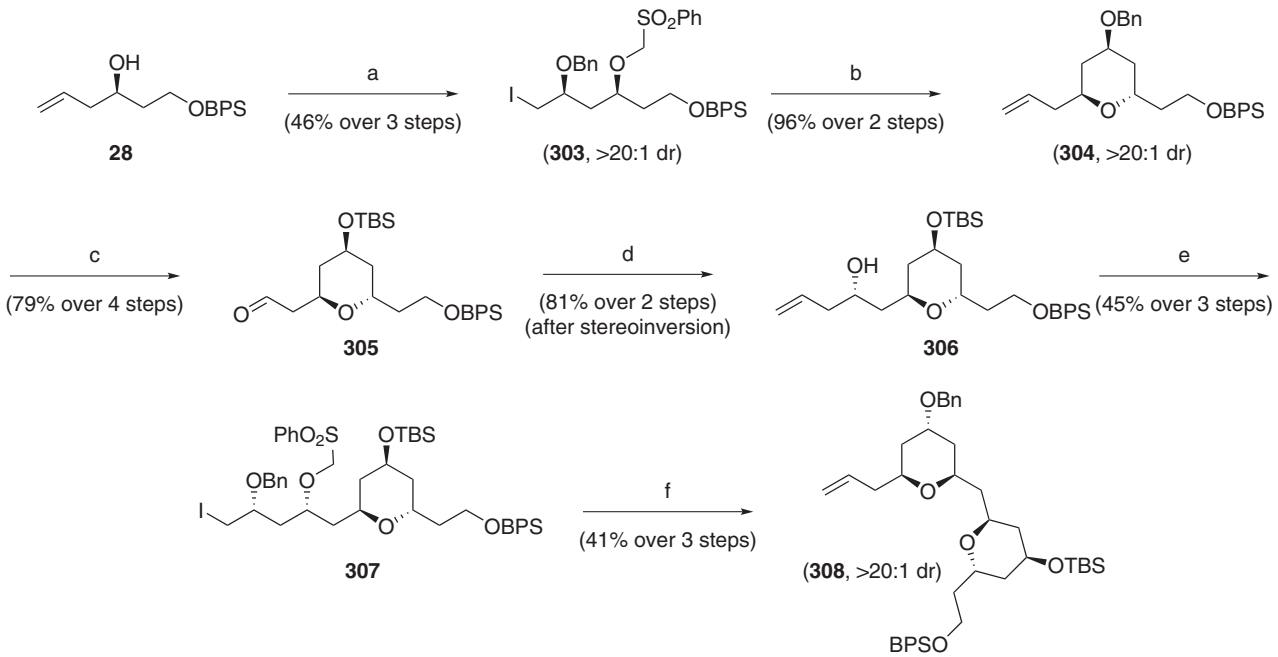


**Scheme 39** (a) (1) BOMCl, DIPEA; (2) ICl, PhSH, $Et_3N$; (3) TPAP, NMO; (b) (1) LiHMDS; (2) $AlCl_3$, AllylTMS; (c) (1) Li/$NH_3$; (2) DDQ; (d) (3) TBSCl, imidazole; (4) $O_3$, $PPh_3$; (d) (1) allylMgBr; (49% of correct diastereomer) (2) DEAD, $PPh_3$, p-NBA, $K_2CO_3$, MeOH (recycled 46% of unwanted diastereomer); (e) (1) BOMCl, DIPEA; (2) ICl, PhSH, $Et_3N$; (3) $(NH_4)_6Mo_7O_{24}$-$4H_2O$, $H_2O_2$; (f) (1) LiHMDS; (2) NaHMDS, allyl iodide, MeOH; (3) TMSOTf, $Et_3SiH$.

yield to give the fully substituted pyran **322** that was subsequently elaborated to C19–C28 fragment **326**. Panek also demonstrated a unique way of installing the exocyclic oxazole to a related fragment via a Stille coupling to triflate **330** (Scheme 42).[38] It is clear that this strategy was also the plan for introducing the other oxazole based on the C19–C20 hydrostannylation.

Chakraborty prepared the pentasubstituted pyran from aldehyde **332** starting with an asymmetric aldol addition (Scheme 43).[39] Sharpless epoxidation installed the C22 stereocenter, but the radical-mediated ring opening gave a considerable amount of olefin **336** in addition to the anticipated **337**. The mixture could be completely converted into the desired **337** via hydrogenation, which could be efficiently converted into alcohol **339**. Upon oxidation to the aldehyde, acetylenation gave a mixture of diastereomeric propargyl alcohols, which could be closed to give **341** as well as the C26 epimer in a 2:1 ratio.

Nagaiah synthesized the pyran from the proline-mediated aldol addition of propionaldehyde to D-mannitol-derived glyceraldehyde **136** (Scheme 44).[40] Wittig elongation and reduction to the allylic alcohol provided the Sharpless epoxidation substrate, which was opened to diol **346**. Selective primary alcohol oxidation and another Wittig elongation allowed for the Michael cyclization and generation of C20–C27 fragment **348**.

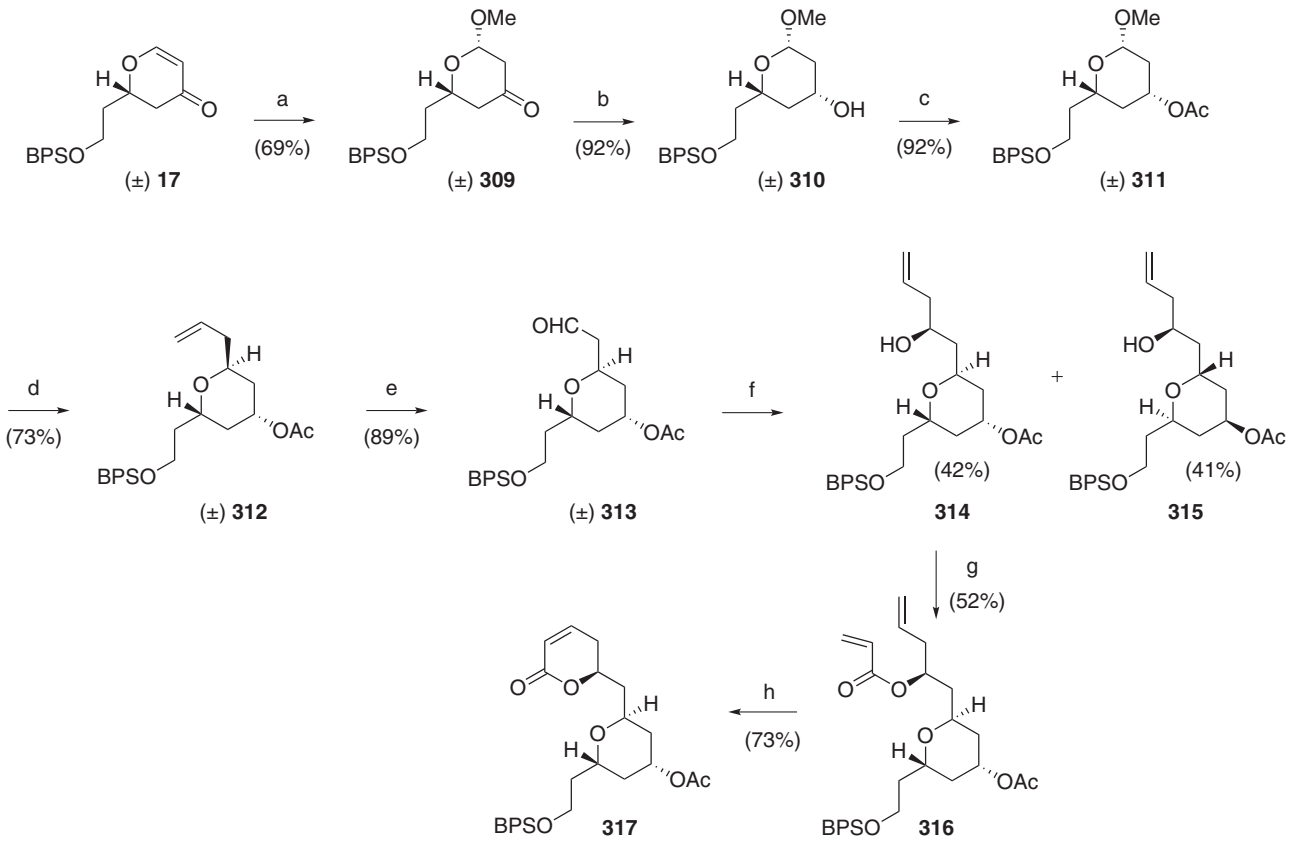


**Scheme 40** (a) $Hg(OAc)_2$, MeOH, $NaBH_3CN$, THF; (b) $LiAl(OtBu)_3$, THF; (c) $Ac_2O$, NaOAc, (d) TMS-allyl, TMSOTf, $CH_3CN$; (e) $O_3$, $CH_2Cl_2$, −78 °C, $PPh_3$; (f) (−)-$(Ipc)_2$B-allyl, toluene, −78 °C, salt-free then $NaBO_3$, toluene, $H_2O$; (g) $H_2C{=}CHCOCl$, $Et_3N$, DMAP; (h) Grubb's cat. (0.2 eq.), $Ti(iPrO)_4$.

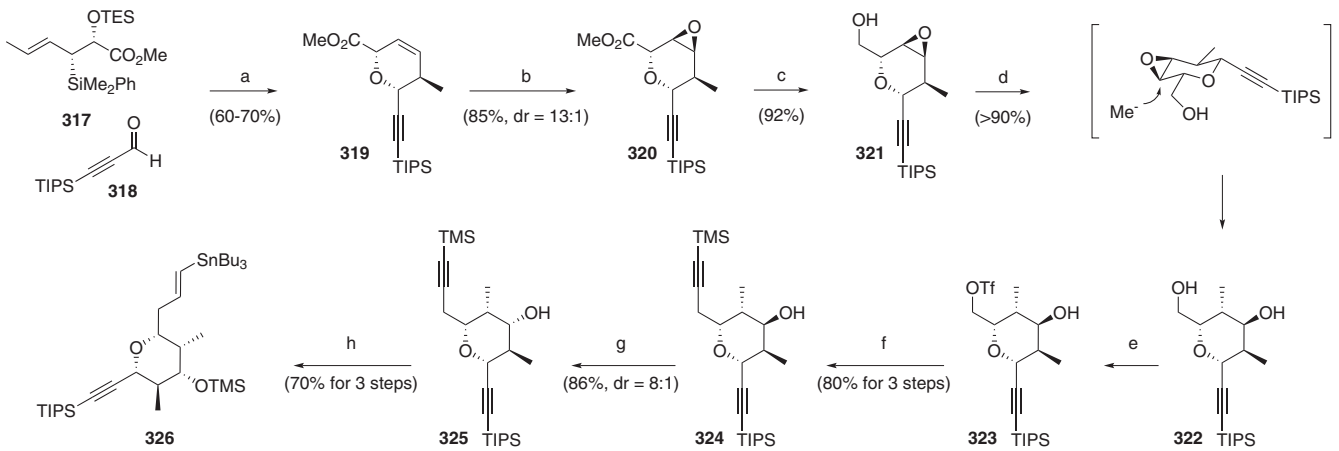


**Scheme 41** (a) TMSOTf (0.5 eq.), $CH_2Cl_2$, 20 °C; (b) m-CPBA, $CCl_4$, RT; (c) $LiAlH_4$, THF, 0 °C; (d) $CH_3MgBr$/CuI, THF, 0 °C; (e) $Tf_2O$, pyr, $CH_2Cl_2$, −15 °C; (f) (1) TMSOTf, 2,6-lutidine; (2) LDA, THF, TMS-acetylene, HMPA, −10 °C; (g) (1) Dess–Martin, $CH_2Cl_2$, RT; (2) $LiAlH_4$, THF, 0 °C; (h) (1) TMSOTf, 2,6-lutidine; (2) NBS, $AgNO_3$; (3)$Bu_3SnH$, $PdCl_2(PPh_3)_2$.

*Exocyclic fragments.* In addition to completing the macrolide, Paterson also completed the entire exocyclic portion of the phorboxazoles.[10] Mukaiyama aldol addition of **101** to **349** using Evans' pybox catalyst installed the C37 stereocenter in >95% ee, and acid-catalyzed lactonization gave β-ketoester **351** (Scheme 45). Hydrogenation of the corresponding vinylogous carbonate simultaneously installed the C35 center and liberated the primary alcohol, which was oxidized to aldehyde **354**. Meanwhile, the triene was formed from asymmetric acetate aldol addition to aldehyde **357** (Scheme 46) in a straightforward manner. The Nozaki–Kishi addition of **362** to **354** proceeded to give the fully elaborated C33–C46 fragment, though the reaction proceeded in disappointing yield and selectivity. The mixture

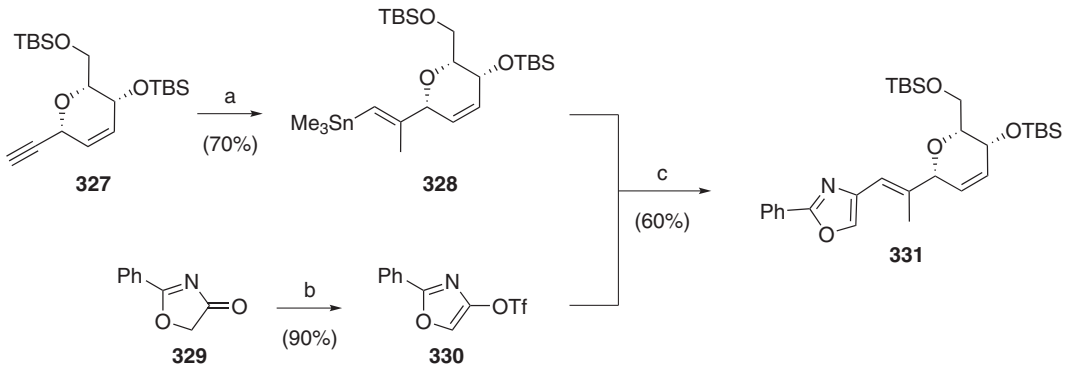


**Scheme 42** (a) $(Me_3Sn)_2CuCNLi_2$, THF, −78 °C; then MeI, DMPU, −78 °C to RT; (b) $Tf_2O$, $Et_3N$, THF, −78 °C; (c) $Pd_2(dba)_3$-$CHCl_3$ (6 mol%), P(*t*-Bu)$_3$ (12 mol%), LiCl, NMP, 60 °C.

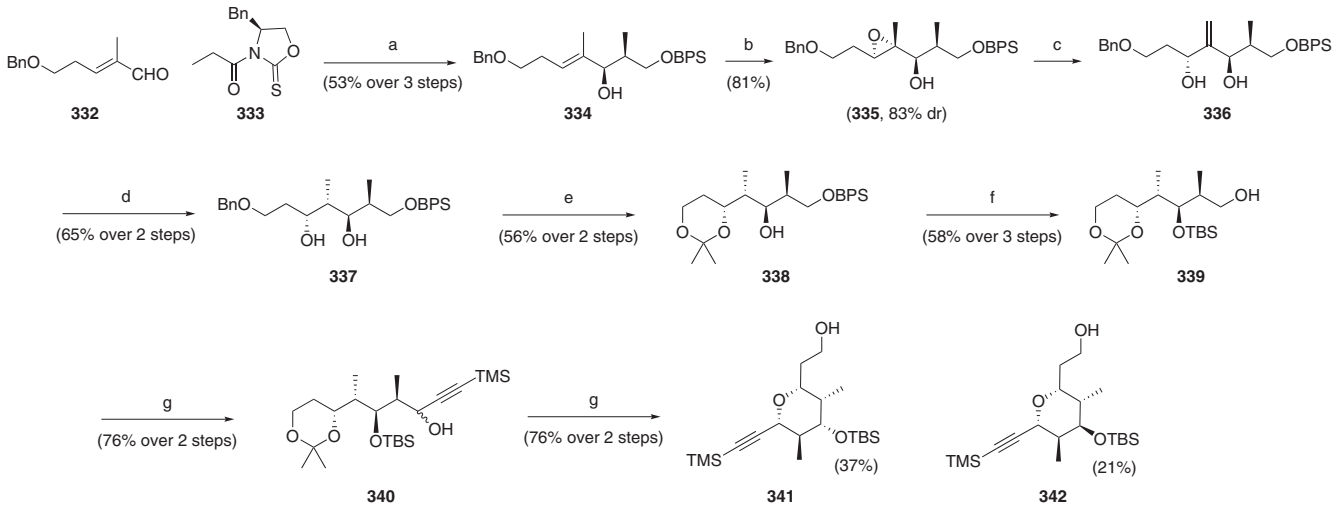


**Scheme 43** (a) (1) **333**, $TiCl_4$, DIPEA, $CH_2Cl_2$, −78 to 0 °C, 0.5 h then **332**, −78 to 0 °C, 1 h; (2) $NaBH_4$, EtOH, 0 °C, 15 min; (3) TBDPSCl, $Et_3N$, DMAP, $CH_2Cl_2$, 0 °C to RT, 4 h; (b) Ti(Oi-Pr)$_4$, (−)-DIPT, TBHP, $CH_2Cl_2$, 4 Å MS, −20 °C, 3 h; (c) $Cp_2TiCl_2$, Zn, $ZnCl_2$, THF, −20 °C to RT, 12 h; (d) $H_2$, 10% Pd-C, $CH_3COONH_4$, MeOH, RT, 0.5 h; (e) (1) $H_2$, Pd-C, MeOH, RT, 24 h; (2) 2,2-dimethoxypropane, CSA, $CH_2Cl_2$, 0 °C, 1 h; (f) (1) TBAF, THF, 0 °C to RT, 4 h; (2) TBS-OTf, 2,6-lutidine, $CH_2Cl_2$, 0 °C, 0.5 h; (3) HF-pyr, THF, 0 °C to RT, 18 h; (g) $SO_3$-pyr, $Et_3N$, DMSO:$CH_2Cl_2$ (2:1.6), 0 °C, 0.5 h; (2) TMS-acetylene, *n*-BuLi, THF, −78 °C to RT, 1 h, then aldehyde, 0 °C, 15 min; (g) (1) MsCl, DMAP, pyridine, 0 °C, 0.5 h; (2) CSA, $CH_2Cl_2$, 0 °C to RT, 3 h.

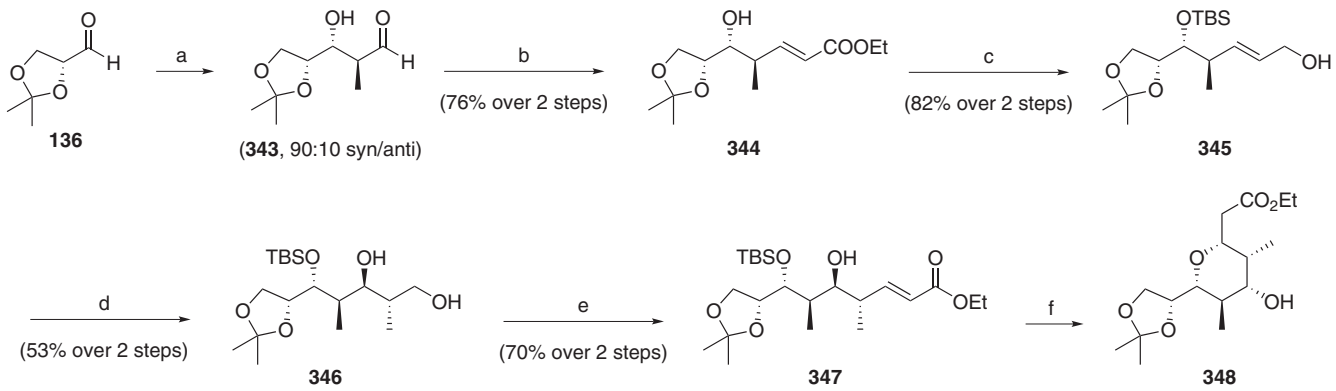


**Scheme 44** (a) L-proline, EtCHO, DMF, 4 °C, 36 h; (b) $Ph_3P$=CHCOOEt, benzene, 80 °C, 12 h; (c) (1) TBSOTf, 2-6,lutidine, $CH_2Cl_2$, 0 °C, 1 h; (2) DIBAL-H, $CH_2Cl_2$, −78 °C to RT, 4 h; (d) (1) (−)-DIPT, Ti(iPrO)$_4$, TBHP, $CH_2Cl_2$, −20 °C, 10 h; (2) MeLi, CuI, $Et_2O$, −20 °C, 6 h; (e) (1) TEMPO, BAIB, $CH_2Cl_2$, RT, 1 h; (2) $Ph_3P$=CHCOOEt, benzene, 80 °C, 12 h; (f) TBAF, THF.

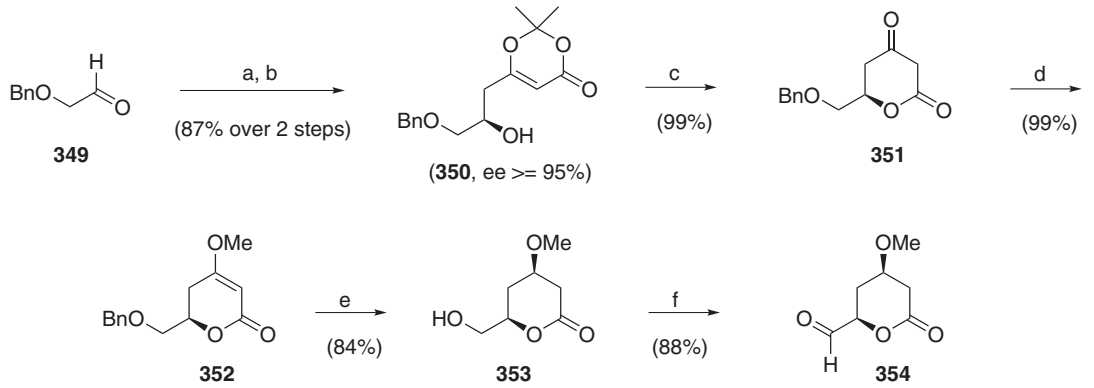


**Scheme 45** (a) **101**, [Cu((R,R)-Ph-pybox)]-$(SbF_6)_2$ (8 mol%), $CH_2Cl_2$, −98 °C to −78 °C; (b) PPTs, MeOH; (c) $K_2CO_3$, MeOH; (d) $(MeO)_2SO_2$, $K_2CO_3$, acetone; (e) $H_2$, Pd-C, EtOAc; (f) Swern oxidation.

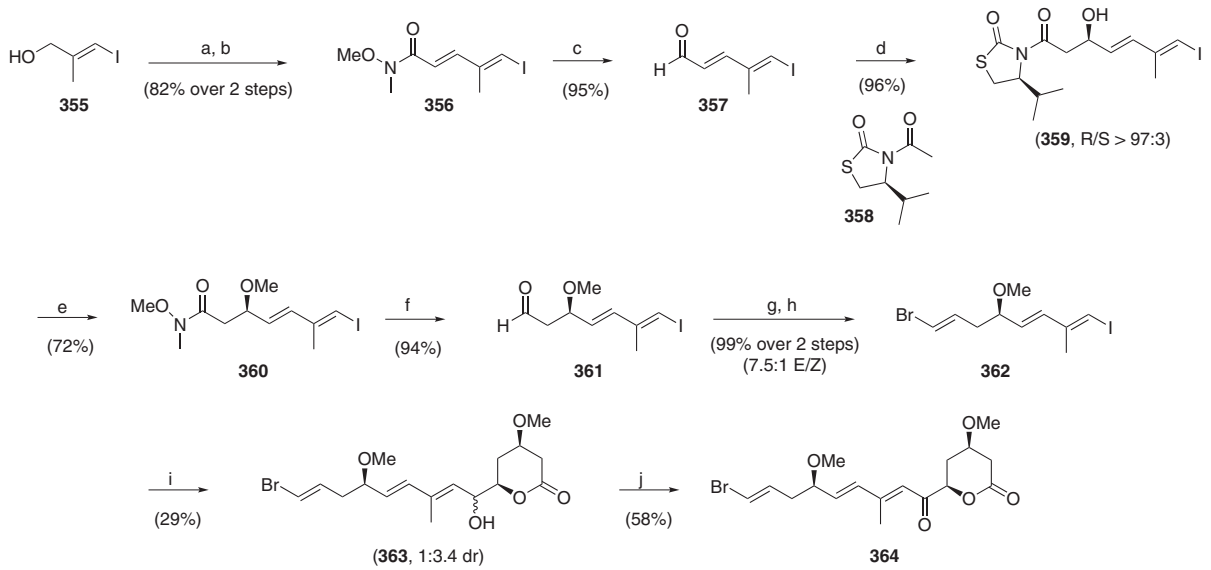


**Scheme 46** (a) $MnO_2$, $CH_2Cl_2$; (b) $MeON(Me)C(O)CH_2P(O)(OEt)_2$, LiCl, DBU, MeCN-$CH_2Cl_2$ (3:1); (c) DIBAL-H, THF, −78 °C; (d) (1) **358**, Sn(OTf), *N*-ethylpiperidine, $CH_2Cl_2$, −40 °C, (2) **357**, −98 to −78 °C; (e) (1) MeNHOMe.HCl, ImH, $CH_2Cl_2$; (2) MeI, $Ag_2O$, $Et_2O$, reflux; (f) DIBAL-H, THF, −78 °C; (g) $nBu_3SnCHI_2$, $CrCl_2$, DMF; (h) NBS, MeCN, 0 °C; (i) $NiCl_2$-$CrCl_2$ (10:1), $tBuC_5H_4N$, THF; **354**; (j) TPAP, 4 Å molecular sieves, $CH_2Cl_2$.

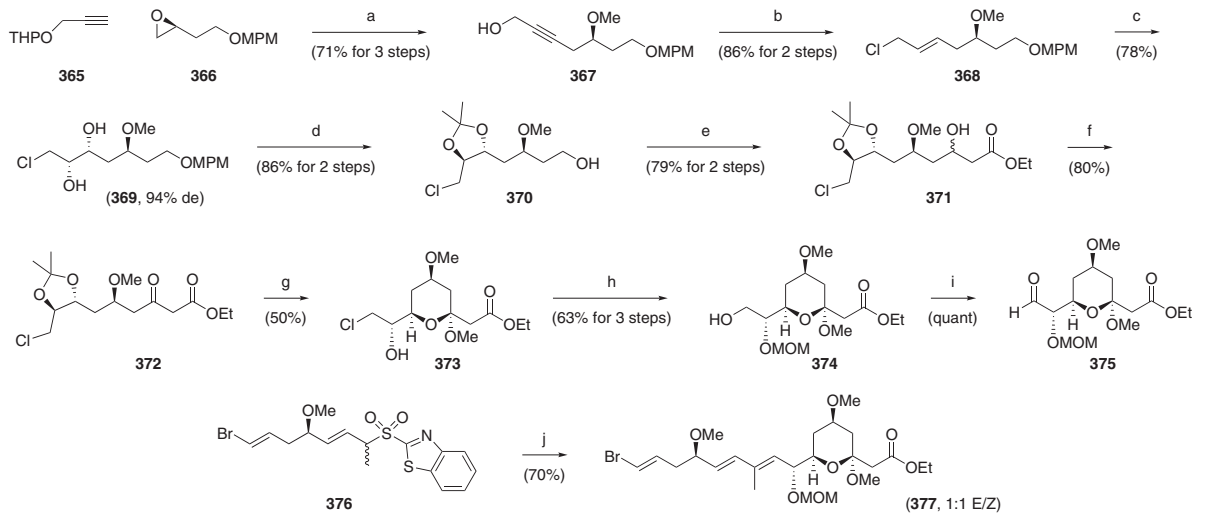


**Scheme 47** (a) (1) *n*-BuLi, $BF_3Et_2O$, −78 °C; (2) NaH, MeI, THF; (3) PTSA, MeOH; (b) (1) $LiAlH_4$, THF, reflux, 2 h; (2) $PPh_3$, $CCl_4$, reflux, 12 h; (c) AD-mix β. 0 °C, 48 h; (d) (1) 2,2-DMP, PTSA, acetone; (2) DDQ, $CH_2Cl_2$-$H_2O$ (7:3); (e) (1) IBX; (2) LiHMDS; $CH_3COOEt$, −78 °C; (f) PDC; (g) PPTS, MeOH, 36 h; (h) (1) MOMCl, DIPEA; (2) HCOONa, NaI, DMF, 80 °C, 3 d; (3) $NaBH_4$, MeOH, 0 °C; (i) Dess–Martin Ox.; (j) **375**, NaHMDS, THF, −78 °C.

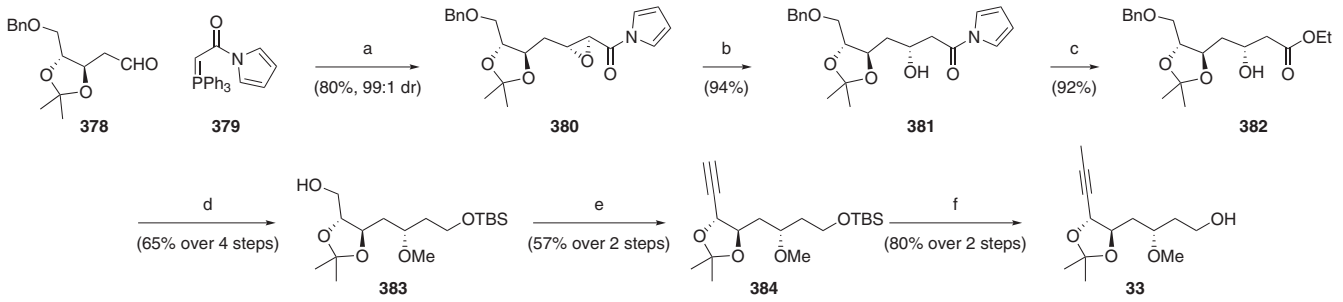


**Scheme 48** (a) **379**, toluene, 65 °C, 36 h, then $H_8$-BINOL (5 mol%), Sm(O-i-Pr)$_3$ (5 mol%), CMHP, THF/toluene 25 °C, 0.7 h; (b) PhSeSePh, $NaBH_4$, EtOH/AcOH, 25 °C, 15 min; (c) EtSLi, EtOH, 25 °C, 40 min; (d) (1) $CH_3I$, $Ag_2O$, MS 3 Å, toluene, 45 °C, 36 h; (2) $LiAlH_4$, $EtO_2$, 25 °C for 30 min then reflux for 40 min; (3) TBSCl imidazole, $CH_2Cl_2$, 25 °C, 50 min, (4) $H_2$ (5 atm), $Pd(OH)_2$, AcOEt/EtOH, $NaHCO_3$, 25 °C, 18 h, (e) (1) PCC, AcONa, MS 3 Å, $CH_2Cl_2$, 25 °C, 20 min then $(CH_3O)_2P(O)C(N_2)COCH_3$, $K_2CO_3$, $CH_3OH$, 25 °C, 80 min.

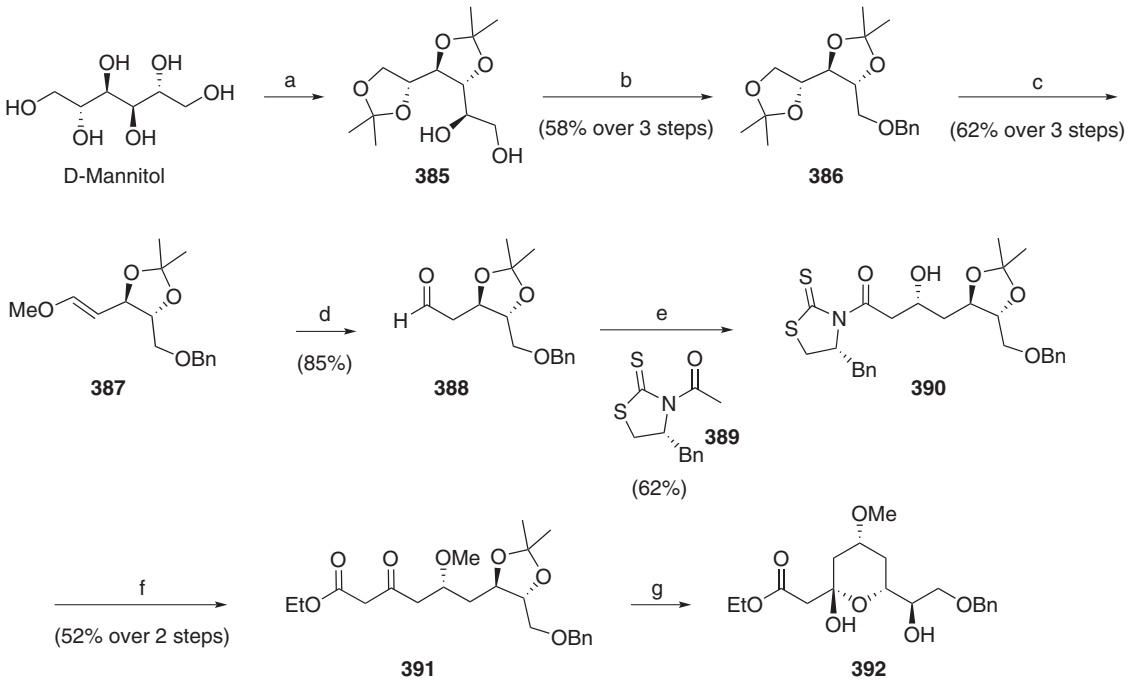


**Scheme 49** (a)[42]; (b) (1) $NaIO_4$, $CH_2Cl_2$, 0 °C, 1 h; (2) $NaBH_4$, MeOH; (3) NaH, THF, BnBr, 0 °C to RT, 12 h; (c) (1) 50% aq. AcOH, RT, overnight; (2) $NaIO_4$, $CH_2Cl_2$, $NaHCO_3$, 0 °C to RT, 4 h; (3) $Ph_3P^+CH_2OMeCl^-$, *t*-BuOK, THF, −78 °C to RT, 4 h; (d) $(AcO)_2Hg$; $NaBH_4$, $CO_2$, 0 °C, THF/$H_2O$ (1:4); (e) **389**, $TiCl_4$, EtN(iPr)$_2$, $CH_2Cl_2$, 0 to −78 °C, 1 h; (f) (1) Proton Sponge, $Me_3OBF_4$, $CH_2Cl_2$, 0 °C, 24 h; (2) $EtOC(O)CH_2COOK$, $MgCl_2$, imidazole, THF, RT, 12 h; (g) PPTS, MeOH/$CH_2Cl_2$, 0 °C to RT, 3 h.

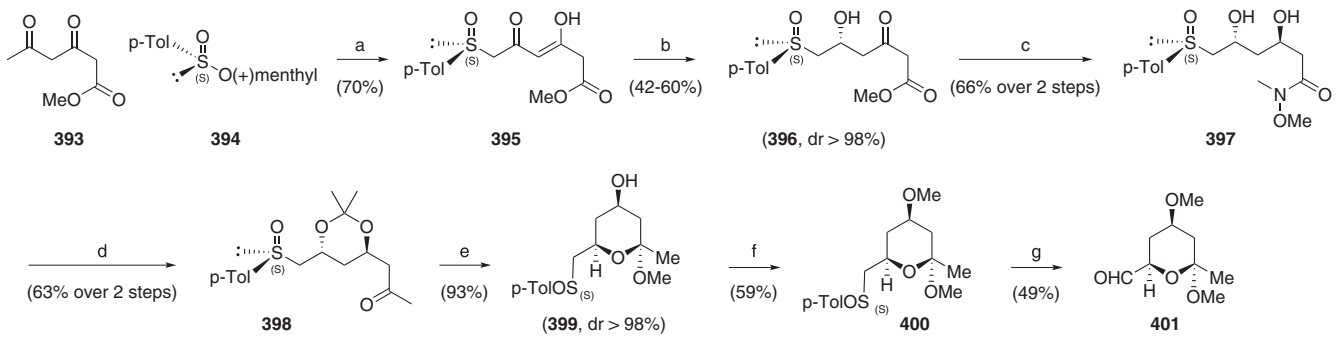


**Scheme 50** (a) NaH (2 eq.), *t*-BuLi (2 eq.), THF, 0 °C; (b) DIBAL-H, THF, −78 °C, 30 min; (c) (1) $Me_4NHB(OAc)_3$, HOAc, RT, 2 h; (2) HCl-N(OMe)Me, $Me_3Al$, $CH_2Cl_2$, heat, 2 h; (d) (1) $(MeO)_2C(CH_3)_2$, acetone, CSA, RT, 24 h; (2) MeMgBr, THF, 0 °C to RT, 1 h; (e) PPTS, MeOH, RT, 24 h; (f) NaH, MeI, THF, 0 °C, 10 h; (g) TFAA, 2,6-lutidine, $CH_3CN$, RT, 10 min.

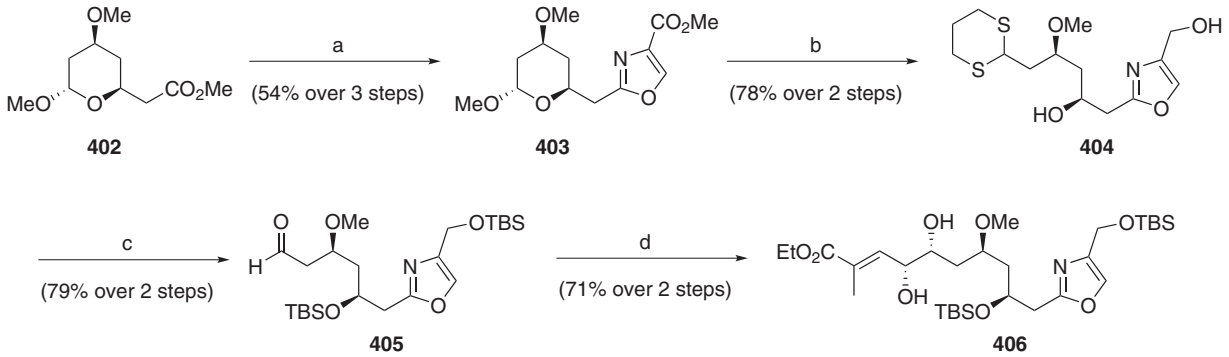


**Scheme 51** (a) (1) IBCF, *N*-methylmorpholine, L-serine methyl ester, $CH_2Cl_2$; (2) Burgess' reagent, THF; (3) $CuBr_2$, HMTA, DBU, $CH_2Cl_2$; (b) (1) DIBAL-H, THF; (2) propane-1,3-dithiol, $BF_3OEt_2$; (c) (1) TBSOTf, 2,6-lutidine, $CH_2Cl_2$; (2) $Hg(ClO_4)_2$, $CaCO_3$, MeCN/$H_2O$; (d) (1) E-$(EtO)_2P(O)CH_2CH=CHCO_2Et$, NaH, $CH_2Cl_2$ 2) AD-Mix β, *t*-BuOH/$H_2O$.

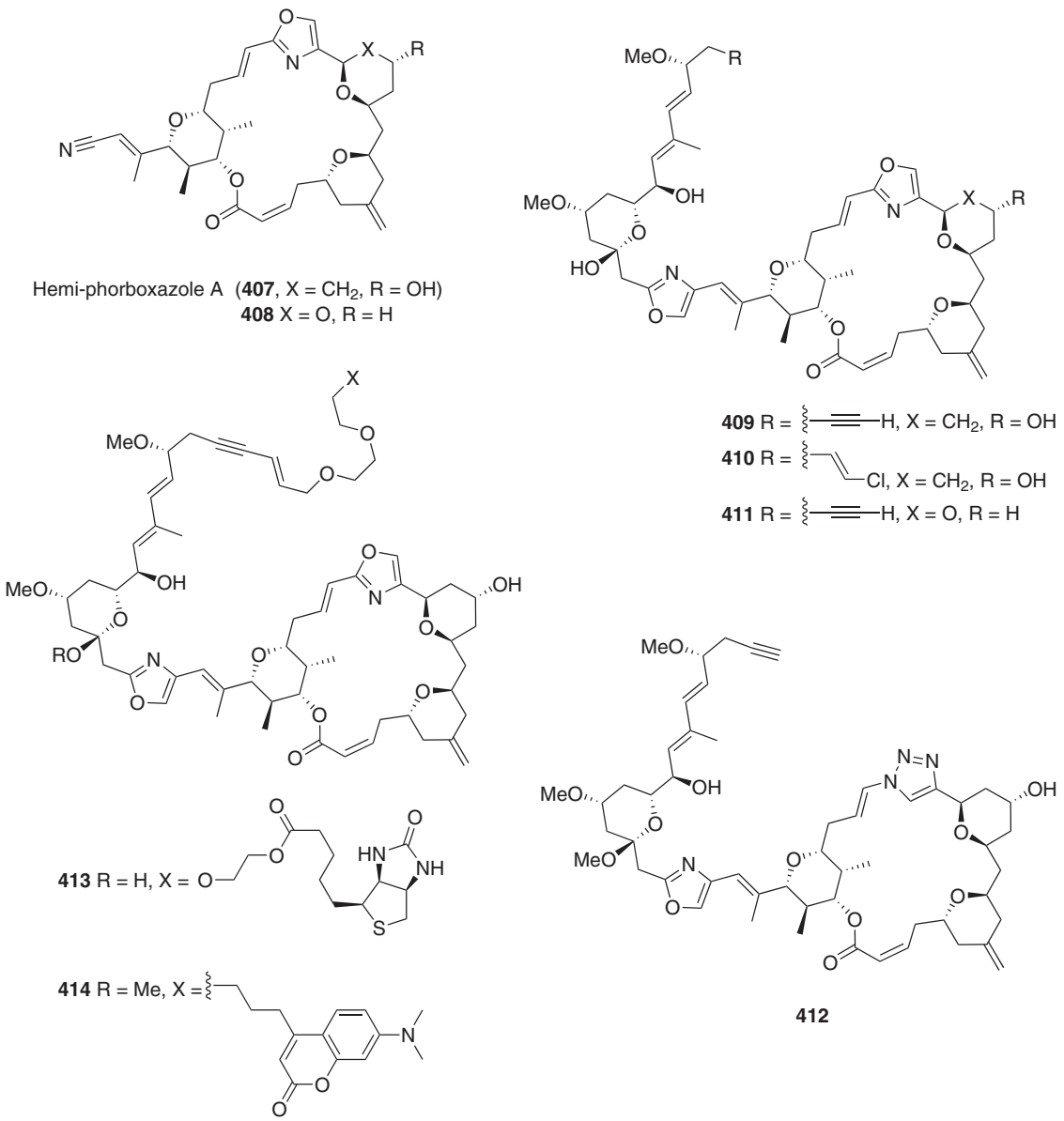


**Figure 12** Examples of synthetic analogs of the phorboxazoles.

could be oxidized for potential controlled reduction, but those results have not been published.

The Yadav group has also completed the entire exocyclic fragment.[41] Acetylenic opening of **366** with **365** set the C35 center, which was converted into allyl chloride **368** (Scheme 47). Sharpless dihydroxylation was then used to install the C37 and C38 stereocenters, and the pyran was elaborated by formation of β-ketoester **372** and ketalization to **373**. Upon formation of aldehyde **375**, Julia olefination with **376** gave the full C31–C46 fragment as a 1:1 mixture of olefin isomers.

Shibasaki synthesized an intermediate from Smith's phorboxazole synthesis to demonstrate the utility of his catalytic asymmetric Michael additions to unsaturated acylpyrroles, installing the C35 stereocenter with >99% control (Scheme 48) and efficiently generating alkyne **33**.[42]

Nagaiah was able to demonstrate that D-mannitol, which is the established synthetic precursor to glyceraldehyde **136**, could also be used for the generation of the exocyclic pyran.[40] Periodate cleavage of diol **385** allowed access to **386**,[43] which could be selectively converted into aldehyde **388** (Scheme 49). An asymmetric acetate aldol was then used to install the C35 stereocenter, which was then extended to β-ketoester **391** and cyclized to the C31–C39 fragment.

Another approach to the exocyclic pyran from chiral sulfoxide **395** was reported from the Carreño and Solladié groups (Scheme 50).[44] Reduction of this diketone proceeded with excellent diastereocontrol to set C37, which was then used to set C35 via a directed reduction. The terminal ester was converted into the methyl ketone, which could then be ketalized to **399**. The sulfoxide could then be converted into aldehyde **401** via the Pummerer reaction.

Hoffmann also completed a synthesis of a ring-opened exocyclic pyran that incorporated the exocyclic oxazole as well (Scheme 51).[45] Addition of serine to **402** and aromatization gave **403**, which could be converted into aldehyde **405**. Extended homologation via vinylogous Horner–Wadsworth–Emmons reaction and installation of the C37 and C38 stereocenters completed the C28–C41 fragment.

### Additional phorboxazoles and analogs

In 2009, Molinski reported the isolation of hemi-phorboxazole A (**407**, Figure 12),[46] which contains the full macrolide but only a nitrile instead of the exocyclic oxazole and hinting at its biosynthetic origin. Smith was able to confirm the structure of **407** via its synthesis from an advanced synthetic intermediate.[47] This synthesis provided sufficient material to allow for the biological evaluation of **407**, which proved to be essentially inactive compared with **1**. Interestingly, synthetic analog **408** showed much greater activity than the natural product.

The extensive synthetic efforts detailed above have also allowed for the generation of phorboxazole analogs and tool compounds useful for understanding its mechanism of action. Both the Forsyth and Smith groups prepared and evaluated alkyne analog **409**,[48,49] demonstrating that it was nearly as active as **1** against several cancerous cell lines. In fact, changes to the terminus are reasonably well tolerated and even could be used to make more active analogs such as vinyl chloride **410**. Although modifications such as ketalization at the C33 position do not destroy activity, the loss of either the macrolide or a significant portion of the exocyclic terminus dramatically reduces activity. Some purely synthetic analogs such as acetal **411** are quite active, while the activity of others such as triazole **412** (formed through a copper catalyzed click 1,3-dipolar cycloaddition) remain unreported.[50]

Forsyth has prepared some phorboxazole-based biological tool compounds such as biotinylated analog **413** and fluorescent analog **414**.[51,52] The latter was shown to be taken up in HeLa cells and to induce extranuclear cytokeratin intermediate filaments to associate with cyclin-dependent kinase 4 (Cdk-4), a kinase that has been explored as a cancer target.[53] The full mechanism of action of the phorboxazoles remains undetermined at this stage.

## CONCLUSIONS

The novel structure and biological properties of the phorboxazoles have clearly attracted the interest of the synthetic community. It has been through these efforts that we have begun to understand some of the structural requirements for their impressive biological activity and gained a glimpse of their biochemical target. Given the impressive strides that have been made in this regard, it is reasonable to think that there remain chapters of the phorboxazole story to be written.

## CONFLICT OF INTEREST

The authors declare no conflict of interest.

1 Searle, P. A. & Molinski, T. F. Phorboxazoles A and B: potent cytostatic macrolides from marine sponge Phorbas species. *J. Am. Chem. Soc.* **117**, 8126–8131 (1995)..
2 Searle, P. A., Molinski, T. F., Brzezinski, L. J. & Leahy, J. W. Absolute configuration of phorboxazoles A and B from the marine sponge Phorbas sp. 1. Macrolide and hemiketal rings. *J. Am. Chem. Soc.* **118**, 9422–9423 (1996).
3 Molinski, T. F. Absolute configuration of phorboxazoles A and B from the marine sponge, Phorbas sp. 2. C43 and complete stereochemistry. *Tetrahedron Lett.* **37**, 7879–7880 (1996).
4 Molinski, T. F., Brzezinski, L. J. & Leahy, J. W. Absolute configuration of phorboxazole A C32-C43 analogs by CD exciton-coupling of allylic 2-naphthoate esters. *Tetrahedron Asymmetry* **13**, 1013–1016 (2002).
5 Capon, R. J. *et al.* Esmodil: an acetylcholine mimetic resurfaces in a southern Australian marine sponge Raspailia (Raspailia) sp. *Nat. Prod. Res.* **18**, 305–309 (2004).
6 Lee, C. S. & Forsyth, C. J. Synthesis of the central C18-C30 core of the phorboxazole natural products. *Tetrahedron Lett.* **37**, 6449–6452 (1996).
7 Seitz, O. Total synthesis of phorboxazole. *Nachr. Chem.* **49**, 1189–1195 (2001).
8 Haustedt, L. O., Hartung, I. V. & Hoffmann, H. M. R. The total syntheses of phorboxazoles–new classics in natural product synthesis. *Angew .Chem. Int. Ed.* **42**, 2711–2716 (2003).
9 Evans, D. A. & Fitch, D. M. Asymmetric synthesis of phorboxazole B. Part II: synthesis of the C1-C19 subunit and fragment assembly. *Angew. Chem. Int. Ed.* **39**, 2536–2540 (2000).
10 Paterson, I., Steven, A. & Luckhurst, C. A. Phorboxazole B synthetic studies: construction of C(1-32) and C(33-46) subtargets. *Org. Biomol. Chem.* **2**, 3026–3038 (2004).
11 Forsyth, C. J., Ahmed, F., Cink, R. D. & Lee, C. S. Total synthesis of phorboxazole A. *J. Am. Chem. Soc.* **120**, 5597–5598 (1998).
12 Smith, A. B. III, Minbiole, K. P., Verhoest, P. R. & Schelhaas, M. Total synthesis of (+)-phorboxazole A exploiting the Petasis-Ferrier rearrangement. *J. Am. Chem. Soc.* **123**, 10942–10953 (2001).
13 Pattenden, G. *et al.* Total synthesis of (+)-phorboxazole A, a potent cytostatic agent from the sponge Phorbas sp. *Org. Biomol. Chem.* **1**, 4173–4208 (2003).
14 Williams, D. R. *et al.* Total synthesis of phorboxazole A. *Angew. Chem., Int. Ed.* **42**, 1258–1262 (2003).
15 Smith, A. B. III *et al.* A second-generation total synthesis of (+)-phorboxazole A. *J. Org. Chem.* **73**, 1192–1200 (2008).
16 Smith, A. B. III *et al.* Evolution of a Gram-scale synthesis of (+)-discodermolide. *J. Am. Chem. Soc.* **122**, 8654–8664 (2000).
17 Smith, A. B. III, Tomioka, T., Risatti, C. A., Sperry, J. B. & Sfouggatakis, C. Gram-scale synthesis of (+)-spongistatin 1: development of an improved, scalable synthesis of the F-ring subunit, fragment union, and final elaboration. *Org. Lett.* **10**, 4359–4362 (2008).
18 White, J. D., Lee, T. H. & Kuntiyong, P. Total synthesis of phorboxazole A. 2. Assembly of subunits and completion of the synthesis. *Org. Lett.* **8**, 6043–6046 (2006).
19 White, J. D., Kuntiyong, P. & Lee, T. H. Total synthesis of phorboxazole A. 1. Preparation of four subunits. *Org. Lett.* **8**, 6039–6042 (2006).
20 Wang, B. *et al.* Total synthesis of phorboxazole A via de Novo oxazole formation: strategy and component assembly. *J. Am. Chem. Soc.* **133**, 1484–1505 (2011).
21 Wang, B. *et al.* Total synthesis of phorboxazole A via de Novo oxazole formation: convergent total synthesis. *J. Am. Chem. Soc.* **133**, 1506–1516 (2011).
22 Li, D.-R. *et al.* Total synthesis of phorboxazole B. *Chemistry* **12**, 1185–1204 (2006).
23 Lucas, B. S., Gopalsamuthiram, V. & Burke, S. D. Total synthesis of phorboxazole B. *Angew. Chem. Int. Ed.* **46**, 769–772 (2007).

24 Wolbers, P. & Hoffmann, H. M. R. trans-C-glycosides from 8-oxabicyclo[3.2.1]oct-6-en-3-one - synthesis of the C3-C13 segment of the phorboxazoles A and B. *Tetrahedron* **55**, 1905–1914 (1999).
25 Dunkel, R. & Hoffmann, H. M. R. Asymmetric synthesis of polyacetate derived building blocks with α-oxyanion functionality. Lewis acid catalyzed opening of 2,9-dioxabicyclo [3.3.1]nonan-3-ones. *Tetrahedron* **55**, 8385–8396 (1999).
26 Wolbers, P., Misske, A. M. & Hoffmann, H. M. R. Synthesis of the enantiopure C15-C26 segment of phorboxazole A and B. *Tetrahedron Lett.* **40**, 4527–4530 (1999).
27 Misske, A. M. & Hoffmann, H. M. R. Asymmetric synthesis of seven-carbon segments of the phorboxazoles and (-)-discodermolide: complementary route from racemic trans-2,4-dimethyl-8-oxabicyclo[3.2.1]oct-6-en-3-one. *Tetrahedron* **55**, 4315–4324 (1999).
28 Ma, P., Martin, V. S., Masamune, S., Sharpless, K. B. & Viti, S. M. Synthesis of saccharides and related polyhydroxylated natural products. 2. Simple deoxyalditols. *J. Org. Chem.* **47**, 1378–1380 (1982).
29 Yadav, J. S., Prakash, S. J. & Gangadhar, Y. General strategy towards chiral methylene bis-pyrans: synthesis of the C2-C16 fragment of phorboxazole A. *Tetrahedron Asymmetry* **16**, 2722–2728 (2005).
30 Yadav, J. S., Satyanarayana, M., Srinivasulu, G. & Kunwar, A. C. A stereoselective synthesis of the C20-C32 fragment of the phorboxazoles. *Synlett* **2007**, 1577–1580 (2007).
31 Vitale, J. P., Wolckenhauer, S. A., Do, N. M. & Rychnovsky, S. D. Synthesis of the C3-C19 segment of phorboxazole B. *Org. Lett.* **7**, 3255–3258 (2005).
32 Rychnovsky, S. D. & Thomas, C. R. Synthesis of the C22-C26 tetrahydropyran segment of phorboxazole by a stereoselective prins cyclization. *Org. Lett.* **2**, 1217–1219 (2000).
33 Clarke, P. A., Santos, S., Mistry, N., Burroughs, L. & Humphries, A. C. The asymmetric Maitland-Japp reaction and its application to the construction of the C1-C19 bis-pyran unit of phorboxazole B. *Org. Lett.* **13**, 624–627 (2011).
34 Clarke, P. A. & Ermanis, K. Synthesis of the C20-C32 tetrahydropyran core of the phorboxazoles and the C22 epimer via a stereodivergent Michael reaction. *Org. Lett.* **14**, 5550–5553 (2012).
35 Kartika, R. & Taylor, R. E. Electrophile-Induced ether transfer: stereoselective synthesis of 2,4,6-trisubstituted tetrahydropyrans. *Angew. Chem. Int. Ed.* **46**, 6874–6877 (2007).
36 Greer, P. B. & Donaldson, W. A. Phorboxazole synthetic studies: the C3-C15 bis-oxane segment. *Tetrahedron Lett.* **41**, 3801–3803 (2000).
37 Huang, H. & Panek, J. S. Formal [4+2]-annulation of chiral crotylsilanes: synthesis of the C19-C28 fragment of phorboxazoles. *Org. Lett.* **3**, 1693–1696 (2001).
38 Schaus, J. V. & Panek, J. S. Palladium-catalyzed cross-coupling of terminal alkynes with 4-trifloyloxazole: studies toward the construction of the C26-C31 subunit of phorboxazole A. *Org. Lett.* **2**, 469–471 (2000).
39 Chakraborty, T. K., Reddy, V. R. & Reddy, T. J. Synthesis of highly substituted tetrahydropyrans: preparation of the C20-C28 moiety of phorboxazoles. *Tetrahedron* **59**, 8613–8622 (2003).
40 Raju, K. B., Kumar, B. N., Kumar, B. S. & Nagaiah, K. Towards stereoselective synthesis of the C(31)-C(39) and C(20)-C(27) fragments of phorboxazole A. *Helv. Chim. Acta* **98**, 386–399 (2015).
41 Yadav, J. S. & Rajaiah, G. A convergent synthesis of the C31-C46 fragment of phorboxazoles. *Synlett* **2004**, 1743–1746 (2004).
42 Matsunaga, S., Kinoshita, T., Okada, S., Harada, S. & Shibasaki, M. Catalytic Asymmetric 1,4-Addition Reactions Using α,β-Unsaturated N-Acylpyrroles as Highly Reactive Monodentate α,β-Unsaturated Ester Surrogates. *J. Am. Chem. Soc.* **126**, 7559–7570 (2004).
43 Wiggins, L. F. The acetone derivatives of hexahydric alcohols; triacetone mannitol and its conversion into d-arabinose. *J. Chem. Soc.* 13 (1946).
44 Brinkmann, Y., Carreno, M. C., Urbano, A., Colobert, F. & Solladie, G. Asymmetric synthesis of the tetrahydropyran ring, C32-C38 fragment, of phorboxazoles. *Org. Lett.* **6**, 4335–4338 (2004).
45 Wolbers, P. & Hoffmann, H. M. R. Asymmetric synthesis of the enantiopure C(28)-C(41) segment of the phorboxazoles A and B. *Synthesis* **1999**, 797–802 (1999).
46 Dalisay, D. S. & Molinski, T. F. Structure elucidation at the nanomole scale. 2. Hemi-phorboxazole A from Phorbas sp. *Org. Lett.* **11**, 1967–1970 (2009).
47 Smith, A. B. III, Liu, Z., Hogan, A.-M. L., Dalisay, D. S. & Molinski, T. F. Hemi-phorboxazole A: structure confirmation, analogue design and biological evaluation. *Org. Lett.* **11**, 3766–3769 (2009).
48 Uckun, F. M. & Forsyth, C. J. Anticancer activity of synthetic analogues of the phorboxazoles. *Bioorg. Med. Chem. Lett.* **11**, 1181–1183 (2001).
49 Smith, A. B. III *et al.* Phorboxazole synthetic studies: design, synthesis and biological evaluation of phorboxazole A and hemi-phorboxazole A related analogues. *Tetrahedron* **67**, 5069–5078 (2011).
50 Ying, L. & Forsyth, C. J. Synthesis of a 16-triazole phorboxazole A analog via intramolecular triazole formation. *Heterocycles* **73**, 841–855 (2007).
51 Hansen, T. M., Engler, M. M. & Forsyth, C. J. Total synthesis of a biotinylated derivative of phorboxazole A via sonogashira coupling. *Bioorg. Med. Chem. Lett.* **13**, 2127–2130 (2003).
52 Chen, J. *et al.* Design and total synthesis of a fluorescent phorboxazole A analog for cellular studies. *Bioorg. Med. Chem. Lett.* **16**, 901–904 (2006).
53 Forsyth, C. J., Lu, Y., Chen, J. & La Clair, J. J. Phorboxazole analogues induce association of cdk4 with extranuclear cytokeratin intermediate filaments. *J. Am. Chem. Soc.* **128**, 3858–3859 (2006).